Programa de doctorado en Biomedicina y Biotecnología
Biotecnología de la Reproducción humana asistida

Analysis of miRNAs in endometrial fluid as a tool for non-invasive diagnosis of endometrial receptivity

Análisis de los miRNAs en el líquido endometrial para el desarrollo de una herramienta no invasiva de la receptividad endometrial

Alessia Grasso

Directores:
Dr. Carlos Antonio Simón Vallés
Dr. Felipe Vilella Mitjana

Valencia, Octubre 2017

VNIVERSITAT DE VALÈNCIA

El Prof. Carlos Antonio Simón Vallés, Catedrático de Pediatría, Obstetricia y Ginecología de la Universidad de Valencia y Profesor asociado de la Universidad de Stanford; y el Dr. Felipe Vilella Mitjana, Doctor en Biología por la Facultad de Medicina en Lleida e Investigador del Instituto de Investigación Sanitaria INCLIVA.

INFORMAN que la doctoranda Alessia Grasso ha realizado bajo su dirección el trabajo de investigación titulado: "*Analysis of miRNAs in endometrial fluid as a tool for non-invasive diagnosis of endometrial receptivity*", y autorizan a su presentación y defensa para optar al título de Doctor en Biomedicina y Biotecnología por la Universidad de Valencia.

Y para que así conste a los efectos oportunos, firman la presente certificación en

Valencia a 20 de Octubre de 2017.

Fdo. Dr. Carlos Antonio Simón Valles

Fdo. Dr. Felipe Vilella Mitjana

Agradecimientos

-Beauty of grace. Thad Fiscella

Quisiera agradecer a mis directores de tesis la posibilidad que me han ofrecido de llevar a cabo este doctorado. Ha sido para mí una gran oportunidad que me ha enriquecido de experiencia, de amigos y de vida. Poder aprender en un entorno lleno de gente con tanta pasión y amor por el trabajo que hace ha sido para mí un honor y un ejemplo que siempre llevaré conmigo.

Gracias a todos los que me habéis enseñado, gracias a todo lo que he aprendido.

A Roser y Jorge por su trabajo, por su paciencia y por entrar en mi vida, sois personas y profesionales especiales.

A todos los besos y los abrazos dados y recibidos. A todos los que siempre habéis estado allí para ayudarme cuando lo he necesitado y para acompañarme en los buenos momentos.

A las “pili”. Esta palabra que un día descubrí casualmente y que con vosotras ha entrado en mi vocabulario como sinónimo de amistad, risas y belleza. Ha sido una suerte encontraros y teneros en mis días.

A “los mellaos”, el lugar donde todo tiene solución y donde siempre se abren posibilidades, y a las “fenomenales” que han compartido esas cervezas de los viernes conmigo. Porque compartir con vosotras, cervezas, viajes, paseos en el monte, noches de viejas, predicciones de Rob, y lo que sea, lo hace todo más dulce.

A los “stranger”, por ser mis amigos, por quererme, por demostrármelo, por estar allí, por esos domingos (y también por dejarme siempre el sillón).

A los tesoros que he encontrado en el master y que sé que nunca perderé.

A voi che purtroppo tengo lontani. Mi mancate ogni giorno, voi e le nostre chiaccherate folli, voi e i nostri caffè. Grazie perchè nonostante la lontanaza non vi siete mai allontanati. Grazie per le canzoni della mattina. Grazie per esserci sempre al mio ritorno.

Alla mia famiglia, ai vostri "Buongiorno" e "Buonanotte" quotidiani. Grazie per gli sforzi, la pazienza e i sacrifi. Grazie per avermi insegnato a saltare.

A mia nonna, e alla dolcezza che mi ha lasciato nel cuore.

A tus ojos que encontré en el camino. Por tu forma de ver. Gracias por mirar conmigo.

Resumen

La implantación embrionaria es el proceso por el que el embrión humano en fase de blastocisto se adhiere al útero materno para comenzar la gestación. El endometrio, la mucosa uterina solo puede aceptar al embrión en un momento determinado del ciclo menstrual que puede variar entre 12 horas y 2 días, identificado como "ventana de implantación". Desde siempre se ha buscado la forma de identificar de forma fiable dicha ventana utilizando técnicas histológicas, como los criterios de Noyes, a través de la observación morfológica vía ecográfica, o estudiando los cambios en los perfiles transcriptómicos, proteómicos o metabolómicos. No obstante, en reproducción asistida, se está abriendo el camino a un nuevo tipo de diagnóstico que ve como protagonista el líquido endometrial, en el cual están presentes moléculas secretadas por el epitelio luminal y glandular. El objetivo es encontrar entre ellas potenciales biomarcadores que permitan el desarrollo de nuevas herramientas diagnósticas más rápidas y menos invasivas. Confrontado con la toma de la biopsia, la aspiración del líquido endometrial tiene la ventaja de ser una técnica mínimamente invasiva que no comporta riesgo para la paciente ni afecta a la tasa de implantación embrionaria. En esta dirección han sido enfocados estudios que trataban de caracterizar proteínas, lípidos y desde la pasada década ha ganado importancia el estudio de miRNAs. Los miRNAs son pequeños RNAs que no codifican para proteínas y que son potenciales reguladores epigenéticos de la función y de la expresión de miles de genes. Se unen a la extremidad 3’ del RNA mensajero diana y dependiendo del grado de complementariedad pueden, o bien mediar la inhibición de la traducción, o degradar el mRNA. En el endometrio los miRNAs están expresados de forma célula-específica y están regulados por esteroides, hecho que se denota por los cambios de expresión desde la fase pre-receptiva hasta la fase receptiva. Un estudio previo de nuestro laboratorio ha detectado 20 miRNAs secretados en el líquido endometrial, diferencialmente expresados a lo largo del ciclo natural. Gracias a este estudio hemos caracterizado el miRNA hsa-miR-30d-5p, cuyos niveles de expresión eran los más elevados, comparado con los otros, en la ventana de implantación, y hemos conseguido ver como el miRNA, libre o embebido en vesículas, se internaliza en las células del trofectodermo. Además, en un modelo *in vitro* con embriones de ratón tuvimos la evidencia de que los embriones tratados con este miRNA,

tenían una mayor tasa de adhesión. Esto nos llevó a pensar que los miRNAs secretados en el líquido endometrial tenían una función de relevancia en la comunicación con el embrión y en el proceso de receptividad endometrial. Este estudio fue la base de esta tesis doctoral que está dirigida a la determinación de los perfiles de los miRNAs a lo largo de la fase lútea de mujeres en ciclo natural y sucesivamente tratadas con los métodos que se utilizan en las prácticas de reproducción asistida para la estimulación ovárica controlada (COS, del inglés *Controlled ovarian stimulation*) y terapia de reemplazo hormonal (HRT, del inglés *Hormone replacement therapy*).

Este trabajo de tesis doctoral está enfocado en la caracterización y en la búsqueda de miRNAs como posibles biomarcadores en el líquido endometrial que pudieran, en un futuro, servir para el desarrollo de una nueva herramienta de diagnóstico no invasiva para predecir el momento de receptividad endometrial.

Hipótesis

La aspiración del líquido endometrial es considerada una técnica mínimamente invasiva. Esta propiedad le confiere la característica de ser un método ideal para el diagnóstico de la receptividad endometrial.

Previamente, hemos demostrado que el endometrio secreta miRNAs en el líquido endometrial durante la ventana de implantación que son recibidos por el embrión y que potencialmente podrían regular el proceso de implantación.

Nuestra hipótesis es demostrar la existencia de un perfil de expresión diferencial de miRNAs en el líquido endometrial que permitiría el reconocimiento de la ventana de implantación.

Objetivos

Objetivos generales

- Caracterizar el perfil de miRNAs en el líquido endometrial a lo largo de la fase lútea del ciclo natural, ciclo de terapia de reemplazo hormonal (HRT), ciclo de estimulación ovárica controlada (COS) con gonadotropina coriónica humana (hCG) (COS +hCG) y con agonista de la hormona liberadora de gonadotropina (GnRH) (COS +GnRH-a).
- Describir los miRNAs diferencialmente expresados en las mismas pacientes en ciclo natural y ciclo HRT.

- Caracterizar las diferencias en la expresión de los miRNAs que existen entre COS +hCG y COS +GnRH-a en las mismas pacientes**.**

Objetivos específicos

- Comparar los perfiles de miRNAs en el líquido endometrial entre fase pre-receptiva y receptiva en cada tratamiento para identificar posibles biomarcadores de receptividad endometrial.
- Validar los miRNAs diferencialmente expresados obtenidos gracias al análisis bioinformático.
- Basándonos en los perfiles de los 238 genes de ERA, identificar *in silico*, las posibles dianas de los miRNAs.
- Demonstrar *in vitro* la relación inversa entre miRNA/mRNA diana.

Métodos

Recolección de muestras

Se obtuvieron 125 muestras de líquido endometrial reclutadas en la clínica IVI Valencia a partir de 47 voluntarias donantes de óvulos según los criterios de inclusión establecidos para este estudio. El estudio ha sido aprobado por el Comité ético de investigación clínica (CEIC): 1304-C-117-FV. Las muestras han sido tomada a lo largo de la fase lútea en ciclos natural en día LH +0, LH +3, LH +5 y LH +7; En HRT, específicamente en día P +0, P +1, P +3, P +5 y P +7; en COS +HCG en día hCG +0, hCG +3, hCG +5, hCG +7 y hCG +9 y finalmente en COS +GnRH-a en día GnRH-a +0, GnRH-a +3, GnRH-a +5, GnRH-a +7 y GnRH-a +9. Una vez obtenidas, las muestras se guardaron congeladas a -80ºC hasta su procesamiento.

Extracción de RNA total y secuenciación

De cada muestra se obtuvo RNA total utilizando el kit comercial miRNeasy mini kit (Qiagen). Para identificar los miRNAs diferencialmente o exclusivamente expresados en la ventana de implantación de los cuatro ciclos hemos utilizado secuenciación masiva. Para la construcción de las librerías se ha utilizado TruSeq Small RNA Sample Pre Kit, Illumina. Las librerías cualificadas y amplificadas han sido secuenciadas en la plataforma Illumina HiSeq2000/1000.

Análisis bioinformático

El análisis bioinformático se ha llevado a cabo con el objetivo de determinar los miRNAs que se expresan de manera diferencial, entre fases correspondientes de diferentes ciclos y entre diferentes fases dentro del mismo ciclo. El análisis de expresión diferencial se llevó a cabo utilizando los paquetes de Biocondcutor edgeR_3.10.0 y DESeq2_1.8.1 EdgeR y DESeq2. Los miRNAs que no expresaban más de 1 lectura por millón (CPM) en al menos 3 muestras han sido excluidos del análisis. Sólo los miRNAs diferencialmente expresados en los dos métodos con un valor de "fold change" superior a 2 y con FDR (del inglés *False discovery rate*) <0.05 fueron considerados para los análisis.

Validación datos de secuenciación

Por cada comparativa entre fase pre-receptiva y receptiva de cada ciclo, se seleccionaron unos miRNAs para su validación mediante técnica de RT-qPCR.

Análisis funcional

El análisis funcional ha sido focalizado hacia los genes incluidos en el predictor del ERA. De esta forma, hemos utilizado los perfiles de los miRNAs diferencialmente expresados durante el ciclo sustituido y los hemos comparado con los perfiles transcriptómicos de las dianas. Solo aquellas interacciones que tenían tendencia opuesta fueron seleccionadas. Partiendo de nuestros previos resultados en que hemos demostrado la importancia de hsa-miR-30d-5p durante el proceso de la implantación embrionaria y su importante papel durante la comunicación materno-fetal, nos dirigimos a la validación de su interacción con KIF11 en un modelo *in vitro* con células Ishikawa, línea celular comúnmente usada como modelo de epitelio endometrial luminal. Las células han sido transfectadas con un análogo (*mimic*) de hsa-miR-30d-5p y con un inhibidor que inhibe la expresión del miRNA endógeno.

Resultados

La caracterización de los miRNAs en el líquido endometrial procedente de los distintos días de la fase lútea en ciclo natural ha permitido caracterizar el perfil fisiológico de los miRNAs. De esta forma, hemos identificado 72 miRNAs diferencialmente expresados que son secretados en el líquido endometrial a lo largo de la fase lútea de mujeres que no han recibido ningún tratamiento hormonal. Profundizando en la búsqueda de

potenciales biomarcadores de la receptividad endometrial, la comparativa entre la fase pre-receptiva tardía (LH +5) vs. receptiva (LH +7) no se ha encontrado ningún miRNA diferencialmente expresado. Sin embargo, 5 miRNAs se han encontrado diferencialmente expresados (reprimidos) entre LH +3 vs LH +7. Entre ellos se ha validado la expresión para hsa-miR-30d-5p, hsa-miR-345-5p, hsa-miR-873-3p, y hsa-miR-141-3p.

La sincronización endometrial con el estado de desarrollo embrionario puede llevarse a cabo en ciclo natural, monitorizando el momento de la ovulación o se puede llevar a través de HRT. Debido a que la fase lútea de las mujeres en ciclo natural no siempre es constante, el transfer en HRT representa la mejor opción. Por esta razón hemos caracterizado los perfiles de miRNAs secretados en el líquido endometrial de mujeres en HRT, en la cual, hemos encontrado 154 miRNAs diferencialmente expresados como resultado de todas las comparativas dentro del ciclo. Específicamente, en la comparativa entre P +3 vs. P +5 hemos obtenido 15 miRNAs diferencialmente expresados. Entre ellos se ha validado la expresión de hsa-miR-223-3p y hsa-miR-582-5p, dos miRNAs cuyos niveles están muy altos en la fase receptiva. Gracias a la comparativa de los perfiles de miRNAs secretados en las mismas fases de los dos ciclos hemos revelado que no hay diferencias significativas entre los perfiles de miRNAs secretados. El análisis funcional ha mostrado 62 interacciones validadas con los genes del ERA y 81 interacciones predichas que concuerdan con nuestros parámetros de selección. La interacción miR-30d-KIF11 se ha validado en nuestro modelo *in vitro* de epitelio luminal. Los resultados demuestran que los niveles de mRNA de KIF11 bajan de forma consistente después de 48h de transfectar con el mimic de hsa-miR-30d-5p. Consistentemente, los niveles de KIF11 no bajan, sino que ligeramente se incrementan en la condición en la que las células habían sido transfectadas con un inhibidor del hsa-miR-30d-5p.

En las técnicas de reproducción asistida otro aspecto importante es la obtención de ovocitos que se lleva a cabo mediante los ciclos de estimulación ovárica controlada. En nuestro estudio hemos llevado a cabo la caracterización de la fase lútea de ciclos estimulados con hCG y con GnRH-a. En el ciclo COS +hCG se han encontrado un total de 351 miRNAs diferencialmente expresados, y representa el ciclo con el mayor número de miRNAs diferencialmente expresados. No obstante, las diferencias entre hCG +5 y hCG

+7 se reducen a 3 miRNAs diferencialmente expresados (sobreexpresados). Estos son hsa-miR-410-3p, hsa-miR-431-3p y hsa-miR-127-5p y su mayor expresión ha sido validada en hCG +5. Con referencia al ciclo con GnRH-a, hemos caracterizado 322 miRNAs diferencialmente expresados. También en este caso encontramos 3 miRNAs entre GnRH-a +5 y GnRH-a +7. De estos hemos validado la expresión en dos miRNAs, hsa-miR-181a-3p y hsa-miR-224-5p. Los resultados de la comparativa entre las mismas fases de los ciclos estimulados que difieren en el desencadenante de la ovulación han mostrado que, en las comparativas entre fases pre-receptivas obteníamos muy pocas diferencias significativas. Interesantemente, el número de miRNAs diferencialmente secretados se incrementa significativamente en la comparativa entre las fases receptivas hCG +7 y GnRH-a +7. En esta comparativa encontramos 47 miRNAs diferencialmente expresados. Entre los miRNAs menos expresados en el ciclo con GnRH-a hemos validado la expresión de 4 miRNAs (hsa-miR-4772-5p, hsa-miR-193a-5p, hsa-miR-30d-5p, hsa-miR184 y hsa-miR146b-5p).

Conclusiones

1. La aspiración del líquido endometrial representa una técnica mínimamente invasiva para el estudio de miRNAs durante la fase lútea del ciclo menstrual y para el desarrollo de herramientas de diagnóstico para evaluar la función endometrial.

2. Considerando los diferentes miRNAs diferencialmente expresados durante el ciclo natural, los ciclos de estimulación ovárica y el ciclo sustituido, podemos confirmar que los tratamientos hormonales influyen en la secreción de los miRNAs al líquido endometrial.

3. En cada tratamiento hemos sido capaces de encontrar potenciales miRNAs biomarcadores de receptividad endometrial. En LH +3 vs. LH +7 (hsa-miR-30d-5p, hsa-miR-345-5p, hsa-miR-873-3p, y hsa-miR-141-3p), en P +3 vs. P +5 (hsa-miR-223-3p y hsa-miR-582), en COS +hCG en hCG +5 vs. hCG +7 (hsa-miR-410-3p, hsa-miR-431-3p y hsa-miR-127-5p) y finalmente en COS +GnRH-a en GnRH-a +5 vs. GnRH-a +7 (hsa-miR-181a-3p y hsa-miR-224-5p).

4. No se han encontrado diferencias significativas en la expresión de los miRNAs entre ciclo natural y ciclo sustituido. Esta conclusión apoya la similitud del estado del endometrio en los dos ciclos.

5. Hemos identificado, con los genes del ERA, 62 interacciones validadas y 81 interacciones predichas de los miRNAs diferencialmente expresado en ciclo de HRT.

6. Basado en el perfil de expresión de los miRNAs en los cuatro ciclos podemos concluir que el endometrio alcanza la receptividad de manera diferente en ciclo natural/HRT comparado con los ciclos estimulados.

7. Las diferencias encontradas en la comparativa entre la fase receptiva de ambos ciclos estimulados, y sobre todo, la evidencia de que miRNAs como el hsa-miR-30d-5p, considerado fundamental en la ventana de implantación, esté menos secretado en COS +GnRH-a sugiere una investigación adicional para entender el efecto de la GnRH-a en el endometrio.

LIST OF ABBREVIATIONS

2D-DiGE	2D-differential in gel electrophoresis
AGO	Argonaute
ART	Assisted reproduction techniques
ATP	Adenosine triphosphate
BMI	Body mass index
CAM	Cell adhesion molecule
cAMP	Cyclic adenosine monophosphate
COS	Controlled ovarian stimulation
CPM	Count per million
dNTP	Deoxynucleotide
E2	Estradiol
ECM	Extracellular matrix
ED	Egg donation
EECs	Endometrial epithelial cells
EF	Endometrial fluid
EGF	Epidermal growth factor
EMT	Epithelial mesenchymal transition
ERA	Endometrial receptivity analysis
ERs	Estrogen receptors
ET	Embryo transfer
FC	Fold change
FDR	False discovery rate
FET	Frozen-thawed embryo transfer
FSH	Follicle-stimulating hormone
FSH-r	Recombinant follicle-stimulating hormone
GE	Glandular Epithelium
GnRH-a	Gonadotropin-releasing hormone agonist
GnRH	Gonadotropin releasing hormone
hCG	Human chorionic gonadotrophin

HRT	Hormone replacement therapy
ICSI	Intracytoplasmic sperm injection
IVF	In vitro fertilization
IL	Interleukin
KID	KEGG identifier
KIF11	Kinesin Family Member 11
LE	Luminal epithelium
LH	Luteinizing hormone
LIF	Leukemia inhibitory factor
mRNA	Messenger RNA
miRNAs	MicroRNAs
NGS	Next generation sequencing
NK	Natural killer
OHSS	Ovarian hyperstimulation syndrome
P/P4	Progesterone
PAGE	Polyacrylamide gel electrophoresis
PCA	Principal component analysis
pET	Personalized embryo transfer
PGE2	Prostaglandin E2
PGF2α	Prostaglandin F2α
PlGF	Placental growth factor
PRs	Progesterone receptors
RT-qPCR	Quantitative reverse transcription polymerase chain reaction
RT	Retrotranscription
RA3	RNA 3' adapter
RA5	RNA 5' Adapter
RISC	RNA-induced silencing complex
RIF	Repeated implantation failure
RNA	Ribonucleic acid
RNA-seq	RNA sequencing
scRNA-seq	Single-cell RNA-seq

uNK	Uterine natural killer
VEGF	Vascular endothelial growth factor
WHO	World health organization
WOI	Window of implantation

Summary

1. Introduction 3

1.1. Infertility 3

1.2. Assisted reproduction techniques (ART) 3

1.2.1. Hormone replacement therapy (HRT) 4

1.2.2. Controlled ovarian stimulation (COS) protocols 5

1.3. The endometrium 5

1.4. Menstrual cycle 8

1.5. Endometrial receptivity: Window of implantation 10

1.6. Diagnostic evaluation of endometrial receptivity based on endometrial biopsy 11

1.6.1. Noyes criteria 12

1.6.2. Pinopods 13

1.6.3. Omic sciences 14

1.6.3.1. Transcriptomics 14

1.6.3.2. Endometrial receptivity Analysis (ERA) 15

1.6.3.3. Proteome 17

1.7. Non-invasive tool for endometrial receptivity assessment 18

1.7.1. Ultrasound evaluation 18

1.7.2. Diagnostic of endometrial receptivity based on EF and future prospective 18

1.7.2.1. Proteome 19

1.7.2.2. Lipidomic 20

1.8. miRNAs 21

1.8.1. miRNA in endometrial fluid as potential biomarker of endometrial receptivity ... 22

1.9. High throughput tools 23

1.9.1. Sequencing 23

1.9.2. NGS data analysis 25

2. Hypothesis 30

3. Objetives 34

4. Methods 38

4.1. Study design 38

4.2. Inclusion and exclusion criteria 39

4.2.1. Natural cycle protocol 39

4.2.2. HRT protocol 40

4.2.3. COS protocol triggered by hCG 40
4.2.4. COS protocol triggered by GnRH-a 41
4.3. Sample collection and processing 41
4.3.1. Aspiration of EF samples 41
4.3.2. RNA extraction from EF 41
4.4. RNA sequencing: Experimental procedures 42
4.4.1. Library construction and sequencing 42
4.5. Bioinformatic analysis 44
4.5.1. Pre-processing data 44
4.5.2. Normalization 45
4.5.3. Differential expression analysis 46
4.6. Sequencing results validation 46
4.6.1. Retrotranscription 46
4.6.2. RT-qPCR 47
4.6.3. Functional analysis based on ERA genes 48
4.6.4. *In vitro* target validation 49
4.6.5. RNA extraction from cultured cells 50
4.6.6. RT-qPCR 50
4.6.7. Primer design 51
4.6.8. Protein extraction and analysis 51
4.6.9. Western blot 51
5. Results and discussion 56
5.1. miRNAs signature identified in EF in natural cycle 56
5.2. miRNAs signature identified in EF in HRT cycle 63
5.3. miRNA signature comparison between natural vs. HRT cycle 69
5.3.1. Integrated miRNAs and gene expression analysis bases on ERA genes 70
5.3.2. miRNA-mRNA interaction validation 77
5.4. miRNA signature identified in EF in COS + hCG cycle 79
5.5. miRNA signature identified in EF in COS + GnRH-a cycle 83
5.6. Comparison of COS + hCG vs. COS + GnRH-a cycle 87
6. Conclusions 96
7. References 100

List of Figures

Figure 1. Representation of the uterus and the endometrial anatomy 6
Figure 2. Endometrial and ovarian cycle phases.....9
Figure 3. Embryo adhesion into endometrial wall.....11
Figure 4. Noyes criteria. Descriptive table of the normal phases of the endometrium during a menstrual cycle 13
Figure 5. Pinopod expression across the luteal phase.....14
Figure 6. Schematic view of personalized embryo transfer workflow validation.....16
Figure 7. miRNAs biogenesis and mechanism of action 22
Figure 8. Study design 38
Figure 9. Sample processing. TruSeq Small RNA Sample Library Construction, Sequencing and bioinformatic data analysis workflow 45
Figure 10. Filtering method based on negative regulation of miRNAs.....48
Figure 11. Pre-processing data in natural cycle 57
Figure 12. miRNAs behaviour in natural cycle 60
Figure 13. Potential biomarkers miRNAs in natural cycle.....61
Figure 14. RT-qPCR validation of potential biomarker in natural cycle 63
Figure 15. Pre- processing data in HRT cycle 64
Figure 16. miRNAs behaviour in HRT cycle 66
Figure 17. Potential biomarker miRNAs in HRT cycle 67
Figure 18. RT-qPCR validation of potential biomarker in HRT cycle 69
Figure 19. Differential expressed miRNAs between correspondent phases in natural and HRT cycle.....69
Figure 20. miR-200 family members trend and their target RASSF2 trend 74
Figure 21. Expression profile of Kif11 and hsa-mir-30d-5p during luteal phase 77
Figure 22. Kif11 mRNA fold change after mimic and inhibitor transfection experiment 78
Figure 23. Pre-processing data in COS +hCG cycle.....79
Figure 24. miRNAs behaviour in COS +hCG cycle.....81
Figure 25. Potential biomarker in COS +hCG cycle 82
Figure 26. RT-qPCR validation of potential biomarker in COS +hCG samples 83
Figure 27. Pre-processing data in COS +GnRH-a cycle.....84
Figure 28. miRNAs behaviour in COS +GnRH-a cycle.....85
Figure 29. Potential biomarkers miRNAs in COS +GnRH-a cycle 86
Figure 30. RT-qPCR validation of potential biomarkers in COS +GnRH-a samples.....87
Figure 31. Number of miRNAs with a statistically significant differential expression between corresponding phases of the two COS cycles 88
Figure 32. RT-qPCR validation in hGC+7 vs GnRH-a +7 samples.....92

List of Tables

Table 1. mRNA/microRNA-seq analysis pipelines in common use 25
Table 2. Final sample size obtained 39
Table 3. Number of samples remained for the analysis after the outlier exclusion.....46
Table 4. Primers used for validation of sequencing results 47
Table 5. Kif11 primers used for miRNA/mRNA validation 51
Table 6. Number of differential expressed miRNAs along natural cycle 59
Table 7. Differential expressed miRNA in LH +3 vs LH +7 62
Table 8. Differentially expressed miRNAs in a HRT cycle (p-value <0,05; FC>2) 65
Table 9. Differentially expressed miRNAs, between P +3 and P +5 68
Table 10. ERA genes target of differentially expressed miRNAs in HRT cycle 71
Table 11. Kegg pathways associated with 28 ERA genes. Each pathway is showed with its KID.....75
Table 12. Differentially expressed miRNAs during the luteal phase of COS + hCG cycle 80
Table 13. Potential biomarkers from COS + hCG cycle 82
Table 14. Number of differentially expressed miRNAs between GnRH-a phases comparison 84
Table 15. Differentially expressed miRNAs in pre-receptive vs receptive phases of GnRH-a cycle 87
Table 16. Differentially expressed miRNAs between receptive phases of the two COS cycles 88
Table 17. Kegg pathway regulated by downregulated miRNAs in GnRH-a +7 vs hCG +7. Each pathway is showed with its KID 90
Table 18. Kegg pathway regulated by upregulated miRNAs in GnRH-a +7 vs hCG +7. Each pathway is showed with its KID.....91

1. Introduction

-Baleen morning. Balmorhea

1. Introduction

1.1. Infertility

The term <Infertility> is defined by the World health organization (WHO) as the inability to conceive after a year or more of unprotected sexual intercourse (1-3). It is estimated that 48.5 million couples worldwide have suffered this condition (4). Within the definition, it is possible to distinguish "primary infertility", indicating the absence of any gestation, and "secondary infertility", indicating the condition in which, after having had a previous gestation, another pregnancy cannot be achieved (4). Through a demographic health survey (1994-2000), the WHO estimated, that 186 million women in developing countries take 5 years to achieve a pregnancy or a live birth. The first global report by the WHO on disability of 35 million women with primary infertility has shown that it is prevalent in developing countries and represents the fifth largest overall cause of all disabilities assessed among women in reproductive age (4). The infertility state in women, can be due to several causes being the most common ovulatory dysfunctions (5) which could be caused by polycystic ovary syndrome (6), obesity (7), thyroid dysfunction (8), and hyperprolactinemia (5). Finally, the displacement of the window of implantation (WOI), represents one of the major causes of implantation failure in ART. Clinically, a condition of repeated implantation failure (RIF) is identified when, a patient who has undergone three treatments of in vitro fertilization (IVF) in which one or two embryos of good quality have been transferred unsuccessfully (9). It is estimated that 60% of conceptions in the natural cycle ends with a pre-clinical loss of pregnancy (10). For all these reasons, the phenomenon of implantation and trophoblast invasion are the major limiting factor in the establishment of pregnancy (11).

1.2. Assisted reproduction techniques (ART)

ART help to overcome the infertility problems, IVF is a technique which involves the management of the gametes or embryos outside the body. The fertilized oocyte can then be transferred to the woman's uterus. Since the past years the freeze-all strategy has emerged as an alternative to fresh embryo transfer during IVF cycles (12).

The first successful pregnancy using frozen-thawed embryo transfer (FET) was reported in 1984 (13). Nowadays, the 16th annual publication of the European IVF monitoring Consortium under the European Society of Human Reproduction and Embryology (ESHRE) on European data on ART, using data recovered from 34 European countries between 1st January 2012 and 31st December 2012, shows a continuing moderate expansion in the number of treatment cycles. With a total of 640.144 cycles reported in 2012 in the 34 countries included. Among that, it was calculated that 452.578 were fresh cycles, 139.558 were frozen embryo replacement, and 33.605 from egg donation (ED). The advantage of performing FET is that it allows to select and transfer the best embryos in a later cycle into a more physiologic endometrial environment (14). This process involves the hormonal control of the ovulatory process, extracting one or more oocytes from the maternal ovaries. Also, at the time of embryo transfer (ET), is fundamental that the development of both, embryo and endometrium, must be synchronized in order to maximize the pregnancy rate. The synchronization can be achieved using a method for endometrium preparation which consists of the exogenous administration of estrogen and progesterone (with or without a GnRH agonist), also called hormonal replacement therapy (HRT) cycle (15).

1.2.1. Hormone replacement therapy (HRT)

Women undergoing ET with frozen embryos or from ED require the appropriate endometrial preparation. It consists in the suppression of the natural menstrual cycle and its regulation with exogenous Estrogen and Progesterone (16). Recent studies demonstrated that no significant differences exist in live birth rates in embryo transfers between natural cycles and HRT (17), moreover, the costs of the two methods is comparable (18). The HRT protocol consists in the estrogen administration at the beginning of the cycle until the endometrial thickness reaches 6 to 7 mm with the typical trilaminar pattern, that occurs in one-week time approximately. Then, micronized vaginal progesterone is administered. The day on which progesterone administration begins is considered P +0 and ET is generally programmed on day P +3 or P +5, with excellent pregnancy rates of up to 40.5% (19). The exogenous administration of estrogen and progesterone does not guarantee the complete suppression of the pituitary gland, for this reason, endogenous progesterone should be assessed before the

administration of exogenous progesterone, and in case of escape intramuscular dose of a GnRH analogue, or GnRH antagonist should be added in order to downregulate the pituitary, thus preventing ovulation (15).

1.2.2. Controlled ovarian stimulation (COS) protocols

In a natural cycle, the surge of LH from the pituitary, induces the resumption of the meiosis in the oocyte and the follicular rupture (20). Since the endogenous LH surge is usually absent in patients undergoing COS cycle, exogenous hCG is used to obtain final oocyte maturation (21). Different drugs for the induction of ovulation can be used instead of hCG, including GnRH agonist. Currently, one of the standard COS protocols used for patients undergoing IVF is the pituitary suppression with GnRH agonist, followed by hCG to induce oocyte maturation. With the introduction of GnRH antagonists, an immediate dose-dependent inhibition of LH release is induced by a competitive binding of the GnRH receptor to the pituitary gland in a reversible manner (22). It has been demonstrated that the administration of a GnRH agonist to induce the final oocyte maturation may result in avoidance of the risk of ovarian hyperstimulation syndrome (OHSS) (23). Accumulated evidence suggests that this type of treatment, is associated with a reduction in the probability of obtaining a pregnancy compared with the use of hCG as a trigger (24-26).

1.3. The endometrium

Reproductive organs work together and independently with the common aim of obtaining a successful pregnancy. The uterus is the organ that harbors embryonic implantation, fetal development and delivery. This is a pyriform shaped organ originated from the mesoderm composed by three different layers: the outermost layer is the serosa, a membrane of connective tissue; the myometrium, formed by smooth muscle tissue; and the innermost mucosa named as the endometrium (27). The endometrium is organized into a basal and a functional layer. In the basal layer reside stem cells in their niche and are responsible for the regenerative properties of the organ (28). Physically, it is attached to the myometrium and is comprise by the endometrial glands surrounded by stroma **(Figure 1)**. Every month the functional layer is shed and expulsed with menstruation.

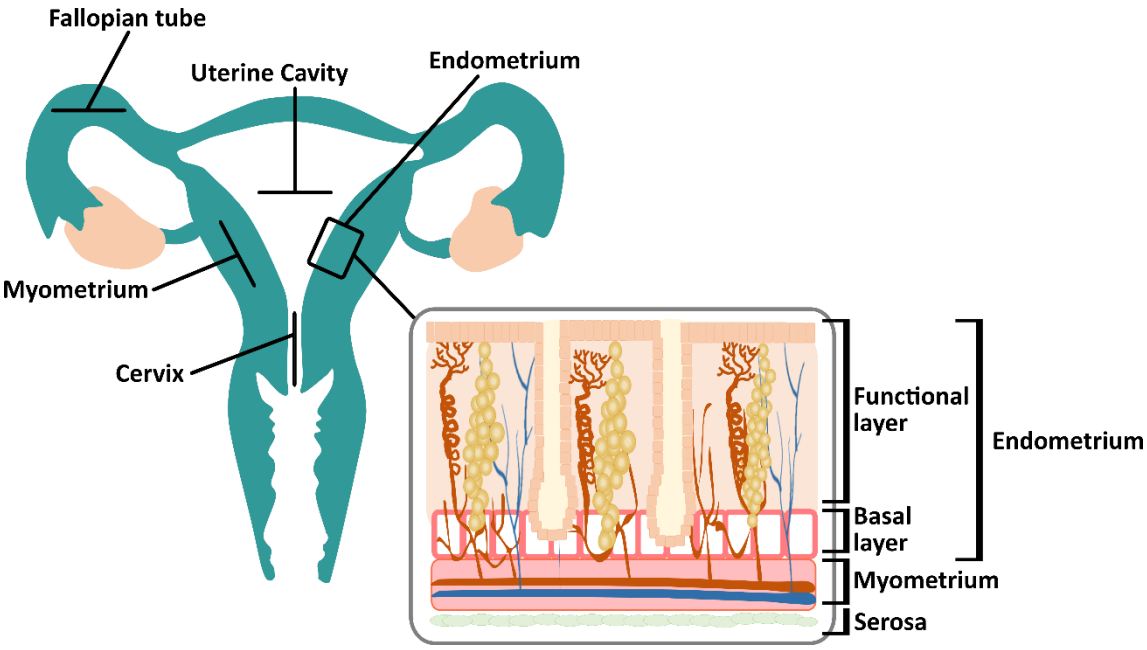

Figure 1. Representation of the uterus and the endometrial anatomy.

The endometrium consists of different cell types:

- Luminal epithelium (LE): It represents the first surface which the embryonic trophectoderm reaches during implantation. A dialogue occurs between the LE and trophectoderm using secreted substances that act in synergy for successful implantation (29). Alterations in the luminal epithelial plasma membrane are suggested to be the main factor for receptivity. Specifically, at the apical surface, these features include a decrease of the number of microvilli and an increase of cytoplasmic prominences. At the same time, on the lateral surface, the number of microvilli of the plasma membrane increases; also, due to vacuolization, the intracellular distances rises, connection complexes decrease, and the tight connections between neighbouring cells disappear (30).
- Glandular epithelium (GE): The glandular epithelium develops as invaginations of LE that progressively invade the stroma, ultimately resulting in an extensive network of epithelial glands that extend to the myometrium (31). Uterine glands are essential for pregnancy, they secrete or transport bioactive substances such as amino acids, ions, glucose, lipids, cytokines, enzymes, hormones, growth factors, proteases and their inhibitors, and transporters (32) that regulate endometrial receptivity for blastocyst implantation. Deficient glandular activity is usually described as a secretory phase defect, and is hypothesized to be a cause of early pregnancy failure

in women (33). Mouse models demonstrated that a condition of reduced or absent uterine glands as well as leukemia inhibitory factor (*Lif*)-null mice, exhibit a subfertile or infertile phenotype due to defects in blastocyst implantation. This defect could be attributed to inadequate uterine receptivity, because the LE failed to undergo changes associated with development of receptivity showing a persistent expression of mucin 1 (MUC1) protein and microvilli (34). Thus, the blastocyst trophectoderm is unable to attach to the uterine luminal epithelium. In this way, a recent *in vivo* study demonstrates the biological roles of Forkhead box A2 (FOXA2) as a critical regulator of uterine gland development in the neonate as well as of differentiated gland function in the adult uterus. It acts by regulating the uterine expression of Lif which also play active roles in stromal cell decidualization and placental development (35).

- Endometrial Stroma: It is a connective tissue formed by fibroblasts and extracellular matrix. It plays an important role in endometrial morphological changes throughout the cycle, and above all, it is involved in a process called decidualization (36), which determine the success of the implantation and the correct placentation. Decidualization of stromal cells starts near the terminal spiral arteries and under the glands around day 23 of a 28-day cycle in response to the postovulatory rise in progesterone and increasing endometrial cAMP levels (37). During this process, the superficial spiral arteries dilate and micro-vessel density grows. Natural killer (NK) cells are also recruited to the spiral arteries area. Endometrial stromal cells transform from spindle shaped cells into epithelioid cells and get in touch with vessels and immunocytes (38). Paracrine crosstalk between the glandular epithelium and stroma is indispensable to establish a receptive endometrium and stromal cell decidualization. Stromal cells, also, establish an important communication with immune cells. The uterine leukocyte population consist mainly of uterine natural killer (uNK) cells. After ovulation, uNK cell numbers increase dramatically in the stromal compartment. The uNK cell population remains prominent in early decidua and in the absence of pregnancy, vanishes before menses (39). Decidual cells are *a priori* programmed to select against embryos that are perceived to lack fitness due to insufficient hCG production (40).

- Vascular component: During decidualization, the maternal uterine vasculature undergoes great changes in response to hypoxia. Under the regulation of estradiol (E2) and progesterone (P4), stromal cells secrete vascular endothelial growth factor (VEGF), tissue factor and Interleukin-8 (IL-8), all of which participate in the modulation of vascular reconstruction (38). VEGF play an important role inducing angiogenesis and increasing the permeabilization of blood vessels (41, 42). The last stage of embryo implantation consists of the invasion process during which the trophoblasts get in a direct contact with the maternal blood establishing the uteroplacental circulation (43).

1.4. Menstrual cycle

The menstrual cycle is under control of hormones secreted by both the hypothalamus, pituitary and the ovaries that impact the uterus inducing the cyclic changes identified as proliferative, secretory, and menstrual phases **(Figure 2)**. The initial signals for a menstrual cycle are initiated from the central nervous system, specifically in the hypothalamus. The arcuate nucleus of hypothalamus produces the gonadotropin releasing hormone (GnRH), described for the first time in the 1970s (44), which is secreted into the portal pituitary circulation in a pulsatile manner (45, 46). GnRH act on the anterior lobe of the pituitary to stimulate the secretion of follicle-stimulating hormone (FSH). FSH travels in the bloodstream to the ovaries where it is responsible for the recruitment of a cohort of ovarian follicles as well as a selection of the dominant follicle that secretes estrogens (47) which stimulates the growth of the endometrium to a thickness of 6-8 mm. The increasing level of estrogen also feed-backs to decrease FSH and increase the luteinizing hormone (LH). A surge of LH promotes the cumulus maturation and the rupture of the pre-ovulatory follicle, releasing the mature oocyte. Ovulation occurs after 36 hours of the LH surge on day 14-15 of the cycle. Following ovulation, luteinization of the granulosa cells increases progesterone production. Regulated by these ovarian hormones, in the endometrium take place also cyclic changes which constitute the endometrial cycle. From the first to the 14^{th} day, in response to increasing circulating levels of E2, the endometrium is in its proliferative phase, this phase could be subdivided into: early proliferative phase (days 4–7), the mid proliferative phase (days 8–10), and the late proliferative phase (days 11–14) (57).

Physiologically, the proliferative phase is characterized by a progressive mitotic growth of the functional endometrium (48).

After the LH surge, circulating E2 begins to decrease, and P4 increases. The latter inhibit cellular proliferation and induce the secretory activity of the glands and differentiation (decidualization) of the stromal fibroblasts (57).

During the secretory phase, the secretory glands increase their size and become sinuous. The stromal cells swell up into decidual round cells through a process called decidualization allowing the placentation. At the same time, the empty follicle become a corpus luteum which secretes progesterone, necessary to maintain the decidua (49). In the absence of implantation, the corpus luteum atrophies and estrogen and progesterone level falls together with a vasoconstriction of the spiral arteries (50). The Funtional layer of endometrium is flushed with menstruation and the cycle restarts with the regeneration of the epithelium.

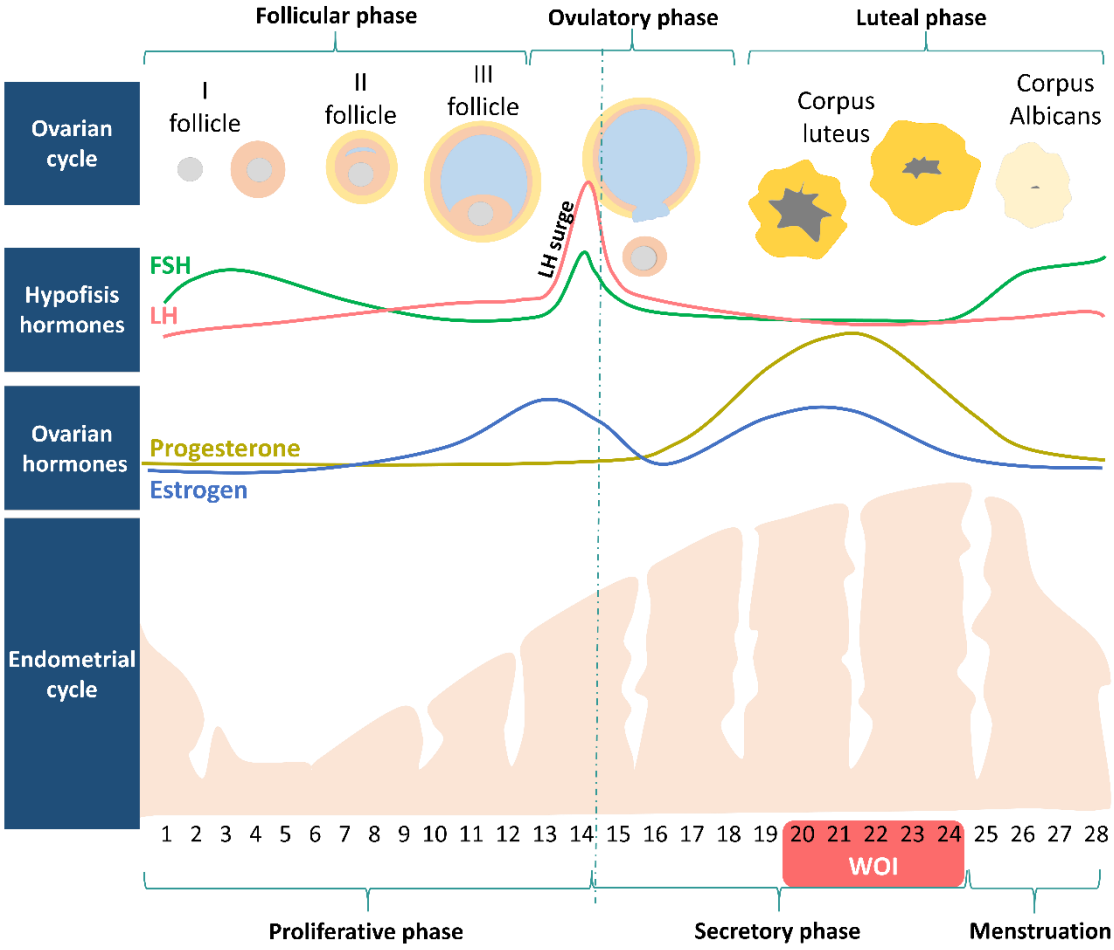

Figure 2. Endometrial and ovarian cycle phases. The menstrual cycle and ovarian cycle are regulated by the cyclic action of steroid hormones.

1.5. Endometrial receptivity: Window of implantation

The embryo is able to attach at the endometrium only during a short period of time within the luteal phase, identified between days 20-24 of a regular menstrual cycle of 28 days, this period called the window of implantation (WOI) **(Figure 2)** lasts between 12 h and 2 days and varies among women (51, 52). In this brief period, the LE acquires a receptive phenotype through structural, morphological and functional changes. Epithelial cells contact neighboring cells laterally with tight junctions, adherens junctions, gap junctions, and desmosomes. In particular, epithelial cells connect to neighboring cells at adherens junctions using the adhesion molecule E-cadherin (epithelial type cadherin). During endometrial preparation for implantation, epithelial cells lose cell polarity, change characteristic cytoskeleton structures, and acquire mesenchymal properties. This phenomenon is called epithelial mesenchymal transition (EMT). During EMT, the major adhesion molecule at adherens junctions is changed from E-cadherin to N-cadherin (neuron type cadherin), through a mechanism called 'cadherin switch'. As a result epithelial cells lose cell polarity determining a redistribution of adhesion molecules at the cell surface and makes adhesion between endometrial epithelial cells (EECs) and the embryo possible (53).

The implantation process consists on the arrival of the embryo at the morula stage, in the uterine cavity. There, the embryo develops into the blastocyst and releases the *zona pellucida* by a mechanism called "hatching". This occurs in a closed period between 72 and 96 hours (32). In this microenvironment cross-talk between the embryo and the endometrium which is crucial for successful pregnancy occurs.

The process of implantation consists in the **apposition** of the trophoblast on the receptive endometrial luminal epithelium, followed by the **attachment** to endometrial basal lamina and stromal extracellular matrix (ECM), and the final **invasion** of the blastocyst trophectoderm through the LE into the stroma **(Figure 3)**. Here the implanting embryo is rapidly surrounded and encapsulated by migrating decidualizing stromal cells until gradually a vascular relationship with the mother is established (54). Growing evidence indicates that decidual cells are responsive for embryonic signals and play a critical role in embryo biosensoring and rejection of developmentally abnormal embryos that have breached the LE (55, 56). Animal studies demonstrate an apoptotic

mechanism of endometrial epithelial cells at the embryo–EEC interface (57). Apoptotic cells release nucleotides, which interacts with Toll like receptors which in turns activate the immune system (58). Implantation is dependent on ovarian production of estrogen and progesterone. These hormones regulate the expression of their receptors in the uterus and their roles during implantation are executed by juxtacrine, paracrine, and autocrine factors. These factors are orchestrated by various growth factors, cytokines, lipid mediators, homeobox transcription factors, and morphogens (59).

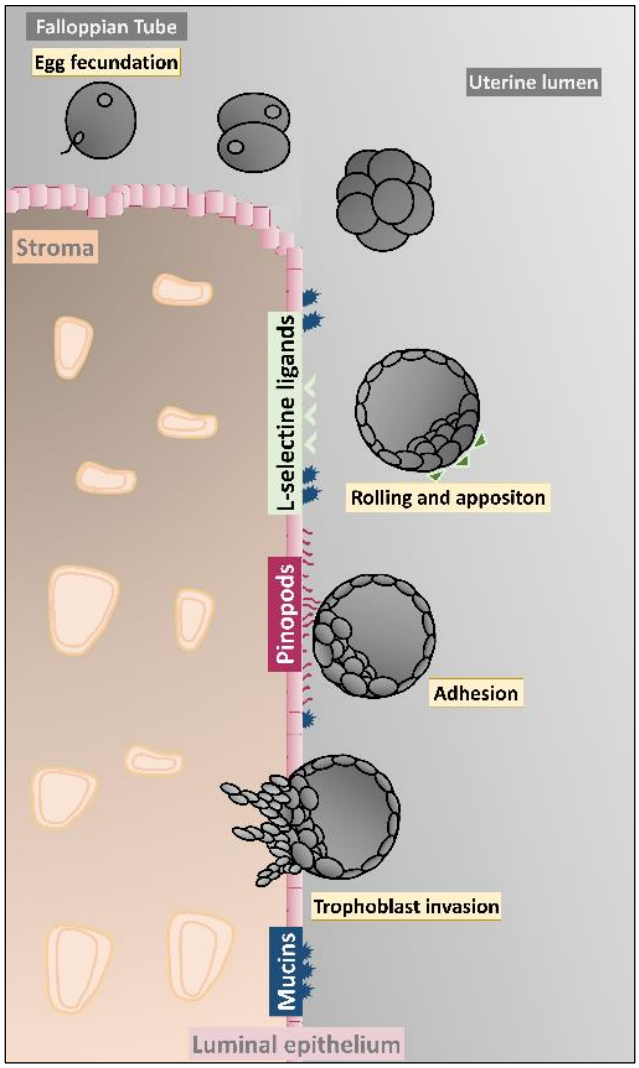

Figure 3. Embryo adhesion into endometrial wall.

1.6. Diagnostic evaluation of endometrial receptivity based on endometrial biopsy

The correct timing of the endometrium is fundamental in ART. For this reason, it is necessary to identify new biomarkers which could help in achieving this objective. An ideal marker should be safe and easy to measure, cost efficient, modifiable with

treatment, and consistent across gender and ethnic groups (57). The different methods used to study endometrial receptivity are the following:

1.6.1. Noyes criteria

In the last 6 decades, the identification of endometrial status has been evaluated based on the Noyes criteria established in 1953. Noyes with his collaborators, observed 8,000 histological sections of endometrial biopsies of patients and were able to create a description of stages of the endometrial cycle (60) **(Figure 4).**

They described the following phases of the endometrium:

- Early proliferative phase: extending from day 4 to 7 of a normal 28-day cycle. In this phase, the endometrium presents tubular and narrow glands, mitotic activity and nuclei predominantly positioned at the basal endometrium. The epithelial layer, lost with menstruation is regenerated at this time (60).
- Mid proliferative phase: the endometrium presents a columnar epithelium, slightly larger glands and the stroma begins to retreat (60).
- Late proliferative phase: the endometrium presents tortuous glands with moderate activity and the epithelium appears wavy (60).
- The secretory phase begins on the day in which the LH peak occurs, indicated as LH +0 and lasts until the day of the menstruation. It represents the phase in which the most consistent changes occur. Morphologically, from day LH +0 until the day indicated as LH +5, the endometrium presents vacuoles in the sub-nuclear position, there is no mitotic activity, and also, the glands become thick and start to secrete.

However, this technique cannot be considered accurate and reliable due to the subjectivity of the observer (61), which does not allow the distinction between fertile and infertile women. This method, also, does not consider the differences between women and the differences between cycles in the same woman (62) and the variability in the endometrial maturation that exists in the cycles of assisted reproduction compared with natural cycle (63).

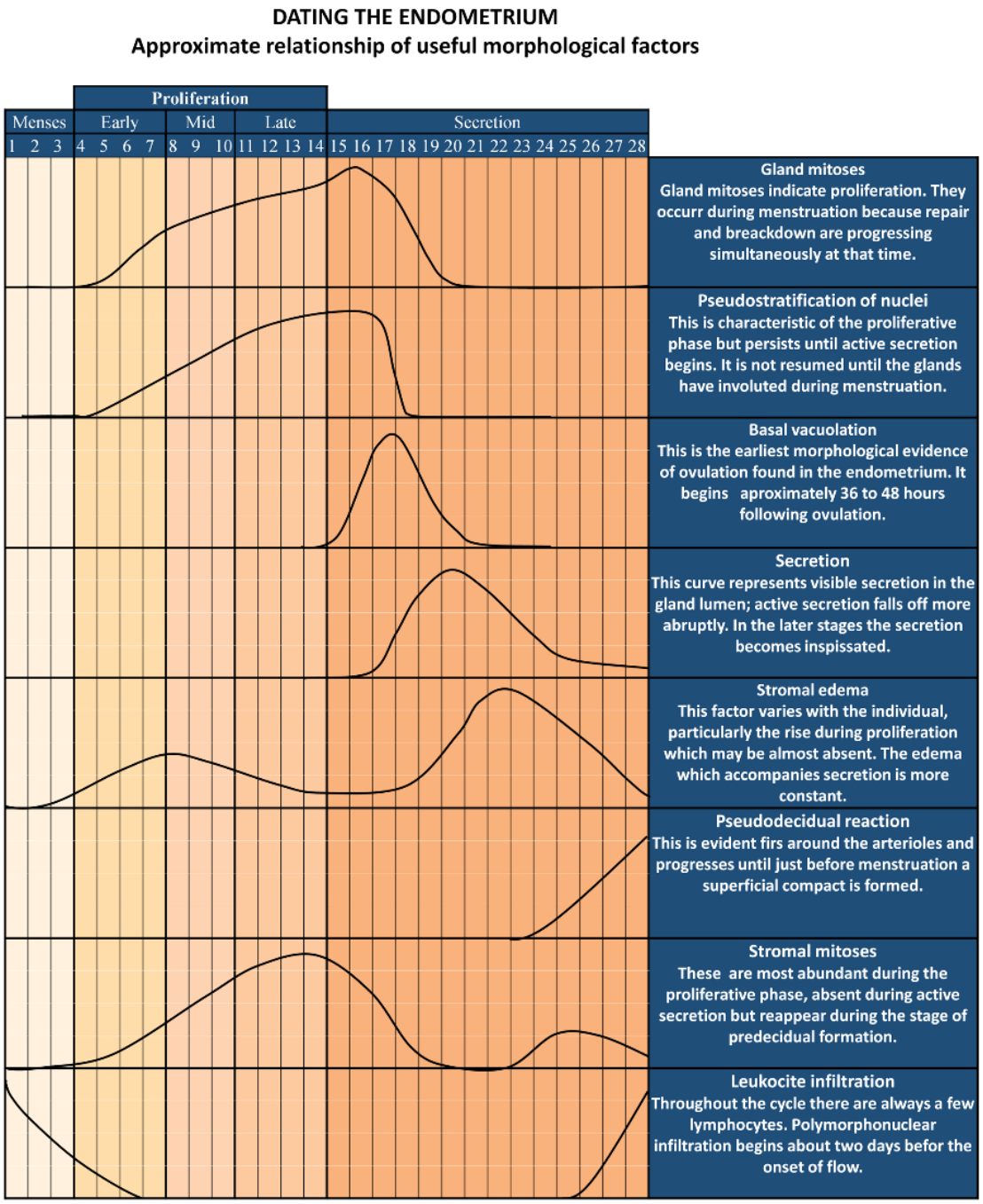

Figure 4. Noyes criteria. Descriptive table of the normal phases of the endometrium during a menstrual cycle.

1.6.2. Pinopods

Pinopods are protrusions on the apical surface of the endometrial epithelium (64) and appear to be progesterone dependent **(Figure 5)**. They were observed for the first time in mice in 1958 (65). A strong temporal correlation between theirs appearance and the expression of LIF in human endometrium was reported (66). They were seriously

considered as potential markers of receptivity, with a putative expression pattern within the 4 to 5-day period of receptivity. Even if their role remains unknown, it seems that they are the preferred sites of embryo–endometrial interactions *in vitro* (67). They have been detected by electron microscopy and are specific markers for uterine receptivity (68).

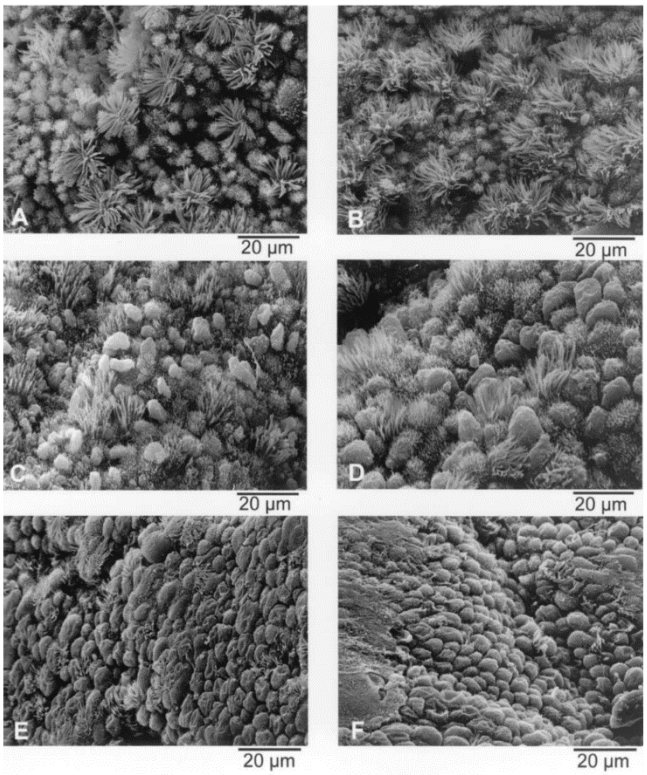

Figure 5. Pinopod expression across the luteal phase. (A) Luteal day 2. (B) Luteal day 5. (C) Luteal day 8. (D) Luteal day 10. (E) Luteal day 11. (F) Luteal day 14 (64).

1.6.3. Omic sciences

The sufix "-*omics*" refer to the application of high-throughput techniques which simultaneously examine changes in the gene expression, epigenetic modification, transcripts, proteins or metabolites in a biological sample. Also, the "omics" sciences are ever expanding with new fields in biological data, such as exomics, lipidomics, secretomics, interactomics (interactome, or "systems biology") and others (69).

1.6.3.1. Transcriptomic

Technologies such as microarray and RNA sequencing (RNA-seq) have allowed the study of the expression of thousands of genes simultaneously, providing great deal of

information, as well as in the field of human reproduction, describing the gene expression profile of the WOI (70, 71) or the whole-genome of the endometrium in normo-ovulatory women during a menstrual cycle (72) as well as comparing different treatments or gynecological conditions (73). A recent study also identified a transcriptomic signature containing 303 genes predictive of RIF (74). Another study was based on comparing stroma and glands in both receptive and non-receptive endometrium isolated first by laser capture microdissection, excluding the possible global gene expression of different genes seen when using the whole endometrium. Based on their study, they propose Ectonucleotide pyrophosphatase/phosphodiesterase family member 3 (ENPP3) as a molecular marker for progesterone action at the endometrial level in women (75).

1.6.3.2. Endometrial receptivity analysis (ERA)

An important diagnostic tool for endometrial receptivity, definitively much more accurate and reproducible than the histological evaluation, is the ERA, a customized assay based on the transcriptomic profile of endometrial receptivity. It has been developed to identify endometrial receptivity by comparing the genetic profile of samples in the receptive phase of natural cycle, LH +7, or in P +5 of an HRT cycle (76). For this purpose, the gene expression profile of the human endometrium in the receptive phase vs. the pre-receptive stage was compared. Those genes, differentially expressed between the receptive phase vs. the pre-receptive and receptive vs. post-receptive, were selected to build initially a customized Agilent microarray based on gene expression (77). It consists of 238 differentially expressed genes, which are coupled to a computational predictor that can diagnose the WOI for a personalized embryo transfer (pET), regardless of endometrial histology (78). To verify the clinical efficacy of this tool, a prospective interventional, multicenter, clinical trial was carried out with 85 patients who suffered RIF and 25 women from ovum-donation program (79) **(Figure 6)**.

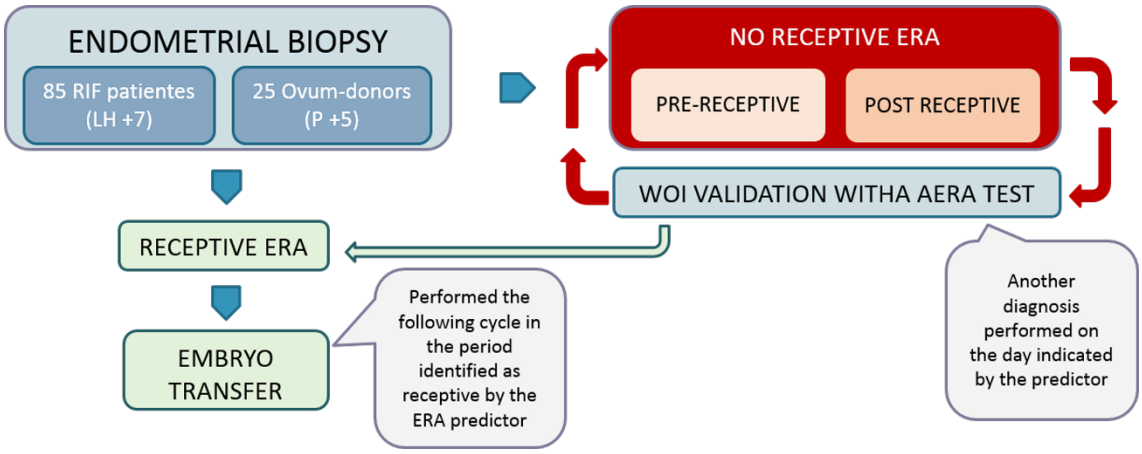

Figure 6. Schematic view of personalized embryo transfer workflow validation.

The results showed that among the patients included in ovum donation program, 81.8% achieved a successful pregnancy; in 55.0% only the embryo implantation took place. Among the patients with repeated implantation failure, 51.7% achieved a successful pregnancy while in 33.9% only the embryo implantation took place. The doubt that arose after that study was if the damage caused by the biopsy could have influenced the embryo implantation. To solve the doubt, the efficiency of the test was tested after six months from the endometrial biopsy. The pregnancy and implantation rates were still high, 50.0% in the first case and 33.3% in the second. Demonstrating that biopsy does not affect implantation (79). Although this tool is very powerful and reliable, with a high specificity (0.8857) and sensitivity (0.9976) (78), it has the disadvantage to rely on an endometrial biopsy. The damage on the endometrium prevent the ET in the same cycle in which the test is performed. The technological advances of the last years have moved toward a change in technology for the ERA test. In this way, the routine diagnosis by microarray has been supplanted by the new generation sequencing technologies. This allows the expression analysis of 236 genes related to endometrial receptivity, and increase the number of samples processed at the same time. In addition, the large amount of data obtained through this analysis allows a more detailed characterization of the WOI. The development of the new predictor, has been based on the information obtained after the analysis with ERA of more than 12,000 patient samples. Thus, to date, the ERA test has become the most reliable predictor of endometrial receptivity in the market. In fact, a prospective and randomized study has shown that ET in a personalized way is associated with a significant increase in pregnancy rates. In addition, implantation

rates as well as pregnancy success have been favored with respect to ET performed with fresh or frozen embryos (73). For these reasons, ERA-NGS was implemented for routine clinical diagnosis.

1.6.3.3. Proteome

The human endometrial proteome has been also widely studied throughout the menstrual cycle to find biomarkers of endometrial receptivity. The literature has extensively described the presence and regulation of cell adhesion molecules (CAM) such as integrins (80, 81), selectins (82, 83), cadherins and immunoglobulins. These surface ligands, usually glycoproteins, mediate cell-to-cell adhesion. Integrin proteins are the major class of ECM, and participate in cell–to-cell and cell-substratum interactions, members of integrins play key roles in the signaling maintenance of epithelial polarity (84), and in developmental progression of placental cytotrophoblast to an invasive phenotype (54). Also, mucins, cytokines such as LIF, IL-6, IL-1, VEGF, HOX, EGF, TGFα, HB-EGF, and hCG are found in several compartments of the endometrium during the receptive phase (85). Studies of proteomics have been conducted to compare the proteomic profiles of receptive vs. non-receptive women according to ERA. The results showed that seven proteins were upregulated and fifteen downregulated in non-receptive vs. receptive women; among these the expression of Annexin A6 and Progesterone Receptor Membrane Component 1 were further studied to confirm their importance in the WOI (86). Another study identified 31 proteins supposedly involved in the embryo implantation process, comparing LH +2 proteomic profile with LH +7 proteomic profile (87). Proteomics is a rather complex field because changes in gene expression do not necessarily reflect in the abundance of proteins. There is a very low correlation between the percentage of the mRNA expression and the abundance of their protein product, in addition the great majority of the structural proteins could mask the minority proteins at the time of the analysis (70). Another unfavorable aspect is that, mainly, endometrial studies are based on endometrial biopsies, composed of a mixture of the different cell types of which the endometrium is composed. To implement and resolve this problem, recent studies have analyzed the specific transcriptomic profile of the different cell types composing the endometrium (88). For all this, the research in

this field moves towards the development of minimally invasive diagnostic techniques opening a new field of research that is the secretomics.

1.7. Non-invasive tool for endometrial receptivity assessment

1.7.1. Ultrasound evaluation.

The ultrasound evaluation of the endometrium is considered as a non-invasive method to assess the timing of endometrium development based on its thickness and pattern (89). In addition, another predictor for endometrial receptivity, could be the endometrial volume, which can be measured through 3D Ultrasound (90). Eventually, 3D-DOPPLER can be added which, takes into account endometrial perfusion and vascularization (91). Imaging techniques allow the non-invasive observation of the endometrium, despite the evaluation of endometrial receptivity based on these parameters is subject to conflicting opinions. For this reason, it is necessary to complement the traditional methods with others diagnostic tools.

1.7.2. Diagnostic of endometrial receptivity based on EF and future perspectives

Other option for a less invasive method of endometrial receptivity assessment would be blood sampling and analysis of a biomarker or a panel of biomarkers predictive of optimal endometrial receptivity such as miRNAs or differences in DNA sequence, which could be detected by sequencing the exome of DNA obtained from extracted blood (92). Examination of cervical mucus was also considered a non–invasive method to study the cytokines and growth factors produced by a receptive endometrium (93). Analysis of endometrial secretions is considered a less invasive technique to determine the receptive status of endometrium. Secretomic is the study of those factors secreted by cells or tissues at a given moment, under particular physiological, pathological or experimental conditions (94). Endometrial fluid (EF) is a complex fluid which contains secretions from the LE and glands, proteins selectively transferred from blood, a cellular fraction consisting of endometrial cells and blood cells (95) and microvesicles (96). It acts as a lubricant, serve as defense against pathogens and helps sperm migration (97). EF was used in studies of endometriosis for biomarker discovery, in which a new panel of candidate biomarkers were described (98). The study of secretions in EF offers the possibility to find biomarkers involved in endometrial receptivity to develop less-

invasive clinical tools, which can produce an accurate and quick diagnosis while reducing the number of invasive techniques required. It has also been demonstrated that it does not affect pregnancy rates within the same cycle (99).

1.7.2.1. Proteome

Glandular secretions consist of glycoproteins that feed the embryo in the pre-implantation period. With this base, several studies identified the protein profile of the EF. The EF protein profile was described for the first time in 1988 (100). Great advances have been done, and several studies had described several useful proteomic factors to identify WOI or predict the outcome of pregnancy (85). In a study conducted by Boomsma et al., in 2009, they describe the endometrial secreted cytokine profile and proposed it as a non-disruptive approach to study the role of the endometrium in human embryo implantation. They identified in this manner a profile which appears to be conducive to clinical pregnancy (87, 101); in another study, they compared the endometrial and cervical mucus cytokine profile concluding that they differ significantly (101).

Concerning the chemokine profile, an increase in CX3CL1, CCL14, and CCL4 chemokines favoring trophoblast migration during the WOI was observed (102). Another study demonstrated, using 2D-differential in gel electrophoresis (2D-DiGE), that several proteins were present at altered levels depending on cycle stage or fertility status (103). In that study, it was described that many of these proteins were protease inhibitors, more commonly associated with serum. However, they demonstrated by immunohistochemical analysis that they were expressed in the luminal and glandular epithelium, suggesting that their presence in uterine fluid was due to secretion from the endometrial epithelium instead of transudation from blood. Scotchie et al. in 2009 used the2D-DiGE technique to determine which proteins were most represented in the secretory phase. Specifically, they found a total of 82 differentially expressed proteins, which were mainly related to the regulation of apoptotic processes, immune response, molecular transport and ionic homeostasis (104). In the mid secretory phase, the number of proteins secreted by endometrial cells increase. A list of 803 proteins identified in EF (105) is also available in the public data repository PRIDE

(http://www.ebi.ac.uk/pride/). Analysis of uterine fluid using quantitative Luminex assays revealed the presence of over 30 cytokines and growth factors, of which eight were previously unknown in human uterine fluid (106). In another important study developed by Boomsma and colleagues it was demonstrated that ovarian stimulation for IVF causes significant changes in endometrial secretory profiles. Specifically, significantly higher concentrations of IL-1b, IL-5, IL-10, IL-12, IL-17, TNF-a, heparin-binding EGF, Dkk-1, and eotaxin were observed in the endometrial secretions of the stimulated cycle vs. the natural cycle (107). Proteomic analysis of human uterine lavage fluid identified the presence of placental growth factor (PlGF) a homolog of VEGF, that binds the VEGF receptor 1. PlGF is a member of the VEGF subfamily, playing key roles in both angiogenesis and vasculogenesis, as well as important roles during embryogenesis (105).

1.7.2.2. Lipidomic

Besides the protein fraction, several factors have already been identified in the EF; endometria possess an important lipid component which plays an essential role in reproduction. Triglycerides and eicosanoids can be mentioned among the lipid mediators secreted from the endometrium. The objective of lipidomics is the characterization of lipid species and their biological role in the expression of proteins involved in lipid metabolism and its functions. A recent Liquid chromatography-tandem mass spectrometry (LC-MS/MS) based on lipidomics study evaluated possible changes in the EF of patients with ovarian endometriosis at the time of embryonic implantation for the first time (108). The importance of lipids at the time of embryo implantation and their possible use as biomarkers of endometrial receptivity have been studied. These include endocannabinoids with lysophosphatidic acid and prostaglandins (109, 110). Prostaglandins are bioactive lipids synthesized from arachidonic acid by phospholipase A2. They exert their action through union with specific receptors coupled to G proteins. It has been proposed to have important roles in reproductive processes like ovulation, menstruation and implantation (111). Our laboratory has studied the changes in prostaglandins, PGE2 and PGF2α throughout the menstrual cycle, concluding that the levels of these increase significantly during the WOI with respect to the other phases of the menstrual cycle. Reduced levels of prostaglandins synthesis in the human

endometrium has been identified as one of the major cause of RIF in patients undergoing IVF (112).

1.8. miRNAs

Since their discovery, 20 years ago with lin-4 in *Caenorhabditis elegans* (113), microRNAs (miRNAs) have been thoroughly studied, displaying great potential as novel diagnostic biomarkers with high specificity and sensitivity. One of the advantages, to study miRNAs is that they are stable and can be easily isolated and measured from tissues and body fluids (113). miRNAs are small RNAs that do not encode proteins and are potential epigenetic regulators of gene expression; They are composed of about 19-22 evolutionarily conserved nucleotides (114) and control gene expression at the post-transcriptional level through the degradation or the repression of their target messenger RNA.

Nowadays, there are more than 1,500 miRNAs known in miRBase and it is estimated that more than 60% of proteins could be regulated by miRNAs (115). In the nucleus the DNA is transcribed by RNA polymerase II into a primary miRNA (pri-miRNAs) of > 100 nucleotides that has a hairpin structure and which contains one or more miRNA sequences (116). Here the complex formed by RNAse III Drosha and its cofactor DGCR8 (DiGeorge syndrome critical region gene 8) cuts the handle of the primary miRNA to form the pre-miRNA of ≈70-100 nucleotides. Exportin 5 transports the latter to the cytoplasm. Here the RNAse III endonuclease, DICER, binds the pre-miRNA and process it into miRNA duplexes. Subsequently, the miRNA duplex is unwound leaving single strands, one of which will function as a mature miRNA loading it into the RNA-induced silencing complex (RISC), a ribonucleoprotein complex containing the Argonaute (AGO) protein, miRNA, the protein DICER and TNRC6A (70). The RISC complex binds to the miRNA target and either inhibits its translation or silences it **(Figure 7)**. The degradation or translational repression of mRNA occurs when the miRNA–RNA-induced silencing complex binds to specific sites in the untranslated region of target mRNA. Depending on the degree of complementarity they may either mediate translation inhibition or degrade the mRNA (117). The miRNAs are expressed in the endometrium in a cell-specific manner and are regulated by steroids, a fact that is denoted in the endometrium by changes in expression from the pre-receptive to the receptive phase (116, 118). In

addition, a different expression profile of miRNAs has been identified by comparing endometrial tissues in the receptive phase of subfertile women for various causes, such as RIF or endometriosis, with samples of fertile women (118). Also, main molecular targets of the miRNAs identified in the endometrium are members of the family Transforming growth factor beta (TGFβ), estrogen receptors (ERs) and progesterone receptors (PRs) and aromatase (119).

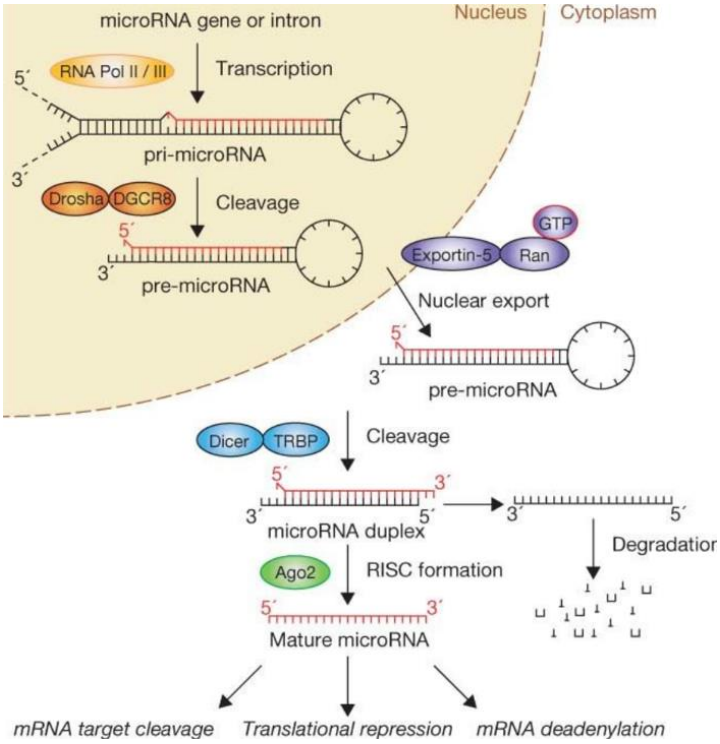

Figure 7. miRNAs biogenesis and mechanism of action (120).

1.8.1. miRNAs in endometrial fluid as potential biomarker of endometrial receptivity

Our previous study focused on the detection of differentially expressed miRNA in EF throughout the natural cycle, we demonstrate the presence of twenty differential expressed miRNAs detected by microarray throughout the natural cycle in endometrial fluid (EF). Also, EF samples were separated in principal component analysis (PCA) graph in relation to the expression profiles of miRNAs during the cycle (121). In this study, hsa-miR-30d was found to be the most differentially expressed miRNA during the WOI and also, demonstrated through labeling experiments with miR-30d that this miRNA is internalized in vesicles and secreted in exosomes which will be received by embryonic trophoblast cells. The presence of relatively stable, extracellular miRNAs in serum and

plasma has generated great interest in the potential use of changes in these miRNA levels as non-invasive biomarkers for a variety of diseases. Using RNA purified from serum or plasma, unique expression of several miRNAs has been shown for some cancers. The best way to understand the function of a miRNA is to identify the genes which regulates. Direct molecular identification of miRNA-mRNA interactions is usually employed to compare expression profiles of miRNAs and their potential target mRNAs (122). Normally, an opposite trend in expression would be expected for a true miRNA-mRNA pair (123-125). The functional mechanism through which miRNAs interact with their mRNA target, and the consequence resulting from their interaction, have been highly investigated and remain a subject of hot debate. At first, it was thought that miRNAs repress the protein output of a small number of target genes without significantly affect in their mRNA levels, but after the contribution of some genetic studies in *C. elegans* and zebrafish it was demonstrated that miRNAs promote the degradation of their target mRNAs (126, 127). A recent study from Guo et al. based on *in vitro* cultured mammalian cell lines which were transiently transfected with chemically synthesized miRNA mimics demonstrated that over 80% of the decreased protein production was assigned to a decrease in mRNA levels (128). Likewise, re-analysis of the previous datasets from cultured cell lines transiently transfected with synthetic miRNA mimics also found that translation repression precedes mRNA degradation (129).

1.9. High throughput tools

1.9.1. Sequencing

The methods for the detection and measurement of miRNAs derive from the methods used for mRNA expression analysis, and they routinely have a clinical use; however, these techniques are already being challenged by NGS methods as the emerging standard method. Furthermore, it has been recently reported that NGS analysis of miRNA is useful in the prediction of clinical outcomes**.** Sanger and colleagues were the first in developing a method for DNA sequencing (130) and Maxam and Gilbert (131) in 1977. By 2004, the Sanger technique had enabled the completion of the first human genome sequence (132). In this scenario, the commercialization of NGS technologies began to grow quickly, leading in 2015, to the reconstruction of the genome of 2,504

people from 26 different population by the 1,000 genomes project (133). Among the existing platforms for sequencing, Illumina, Inc allows a variety of applications, such as genome sequencing through whole-genome sequencing, exome sequencing, Chip-seq for epigenomics, Dna-metilation sequencing and RNA-seq. RNA-seq is nowadays used for the study of biological problems and for the quantification of the expression of mRNA transcripts. It has managed to overcome the limitations of microarrays enabling the identification and quantification of transcripts without prior knowledge of a specific gene and allowing the discovery of new transcripts of miRNA and novel sequences (134). It offers high reproducibility, and better data quality compared with microarray data, representing for this reason, the platform of choice in the search and quantification of miRNAs (135, 136) in the field of human reproduction among others. The first human endometrial transcriptome expression profile using RNA-seq was obtained by sequencing 12 biopsies from women with normal cycle (137). Also, recently single-cell RNA-seq (scRNA-seq) has become a viable alternative option to bulk-RNA analysis. It was demonstrated that scRNA-seq can be performed on single stromal cells from endometrial biopsy samples (138). Concerning the field of human reproduction, the sequencing potential was demonstrated in a study which allowed the characterization of the small RNA transcriptome, comparing expression signatures of known miRNAs in leiomyoma vs. matched normal myometrium and the discovery of novel miRNAs. They were able to identify more than 50 miRNAs exhibiting altered expression and 25 genomic *loci* that encode putative novel miRNA genes, thus expanding the list of miRNAs representing the unique signature of uterine leiomyoma (139). NGS technology has emerged as the preferred platform for studying miRNA expression. A basic step in NGS workflow is the conversion of the nucleic acid into a sequencing library. A large variety of NGS library preparation protocols exist, but they share the fact that DNA or RNA molecules are fused with platform-specific adapters. Adapters are oligos complementary to the oligos attached on the surface of sequencing flow cells. First step of miRNA library construction is to capture miRNAs using specific adapters (140) which are ligated at the 3' and 5' of the miRNAs, followed by reverse transcription to generate cDNA libraries which are then amplified by PCR and purified by gel extraction and quality-checked prior to sequencing (141). Sequencing allows multiplexing of samples

by tagging libraries with barcodes (unique nucleotide tag sequences incorporated into the index or during library construction) during library preparation (142).

1.9.2. NGS Data analysis

Due to the large amount of data generated by NGS experiments, several efficient and robust analysis tools have been developed over the years to allow researchers and clinicians to interpret the data (**Table 1**). First, the images captured by the sequencer are analyzed and converted into reads using the manufacturer's base-calling system. The output of this procedure is a standard text-based format called FASTQ, which stores both the nucleotide sequence and its corresponding quality scores. Quality assessment of the reads should be done to trim or remove bad quality or too short sequences and to eliminate adaptors, contaminating the sequences. FastQC, NGSToolkit, Cutadapt are some examples of bioinformatic packages commonly used for this goal. The second stage is the alignment of the reads, which depending on the availability of a reference sequence, is based on a *de novo* assembly or on a mapping strategy. This has allowed for the development of many studies at the level of DNA, RNA, miRNAs, etc. in humans. The knowledge generated from all these projects has given rise to databases specialized in genetic variants, gene expression and regulation. An example is miRBase, one of the most widely used databases in the study of miRNAs.

Table 1. mRNA/microRNA-seq analysis pipelines in common use (143).

Tool	Alignment engine	Reference sequence	Limited species	Local computer	Open source	Citation
miRExpress	Smith-Waterman	miRbase	All miRbase	Yes	Yes	Wang et al. 2009
DSAP	Smith-Waterman	miRbase	All miRbase	Web-server only	NA	Huang et al. 2010
MIReNA	MEGABLAST	Whole genome	Any	Yes	Yes	Mathelier and Carbone 2010
miRDeep	MEGABLAST	Whole genome	Any	Yes	Yes	Friedländer et al. 2008
miRDeep2	Bowtie1	Whole genome	Any	Yes	Yes	Friedländer et al. 2012
miRanalyzer	Bowtie1	miRbase and whole genome	34 species	Web-server only	No	Hackenberg et al. 2011
Shortran	Bowtie1	Whole genome	Any	Yes	Yes	Gupta et al. 2012
mirTools2	SOAP2	Whole genome	32 species	Yes, and web-server		Wu et al. 2013b
MiRNAkey	BWA	miRbase	All miRbase	Yes	Yes	Ronen et al. 2010
UEA sRNA workbench	PatMaN	Whole genome	Any	Yes	Yes	Stocks et al. 2012
ShortStack	Any	Whole genome	Any	Yes	Yes	Axtell 2013

The number of sequence reads of a miRNA compared to the total reads in the sample gives us the relative abundance of the miRNA (144). The resulting count data are normalized to remove variations of the data that are of non-biological origins and can affect the measured abundance levels. Besides the miRNAs profiles generated,

sequencing allows the comparison of miRNA expression between different conditions (145) and the detection of differentially expressed miRNAs. One of the most used tool for this analysis is DEseq2 which provides methods to test for differential expression by use of negative binomial generalized linear models (146).

2. Hypothesis

-Mountains. Message to bears

2. Hypothesis

Aspiration of endometrial fluid (EF) is considered to be a minimal-invasive intervention making it an ideal method for endometrial diagnosis.

We previously demonstrated that the human endometrium releases specific miRNAs at the EF during the WOI which are received by the embryo and could potentially regulate the process of implantation.

We hypothesize the existence of a differential endometrial miRNAs signature during the WOI that might help us diagnose the endometrial receptivity status.

3. Objectives

-A la folie. Michael Nyman

3. Objectives

General Objectives

- To characterize and compare the miRNA signature in EF during the pre-receptive and receptive phases in natural cycles, hormonal replacement therapy (HRT) cycles, and controlled ovarian stimulated (COS) cycles which final maturation was triggered with hCG or GnRH-a.
- To describe the differences in the miRNA signature between the natural and HRT cycles in the same patients.
- To characterize the differences in miRNA expression existing between COS +hCG and COS +GnRH-a cycle in the same patients.

Specific Objectives

- To compare miRNA profiles in EF among pre-receptive and receptive phases of each treatment modality in order to identify possible biomarkers for endometrial receptivity.
- To validate the differences in miRNA expression obtained from bioinformatic analysis.
- To identify, by *in silico* analysis, the putative gene targets of miRNAs based within ERA gene database.
- To demonstrate *in vitro* the inverse correlation between miRNA and mRNA of ERA targets.

4. Methods

-Aria. Giovanni Allevi

4. Methods

4.1. Study design

To investigate the expression profiles of secreted miRNAs in EF during luteal phase, EF were obtained from healthy ovum donor volunteers (n=47) as outlined in **Figure 8A**. Each woman underwent a natural cycle, an HRT cycle, a COS cycle in which final oocyte maturation was induced either with hCG and GnRH-a. To identify the miRNA expression pattern, total RNA extraction was performed and shipped to BGI (Beijing Genomics Institute) for sequencing. Bioinformatic analisis was performed by the bioinformatic department in Igenomix. Functional analysis was performed using as reference the ERA genes trends **(Figure 8B)**.

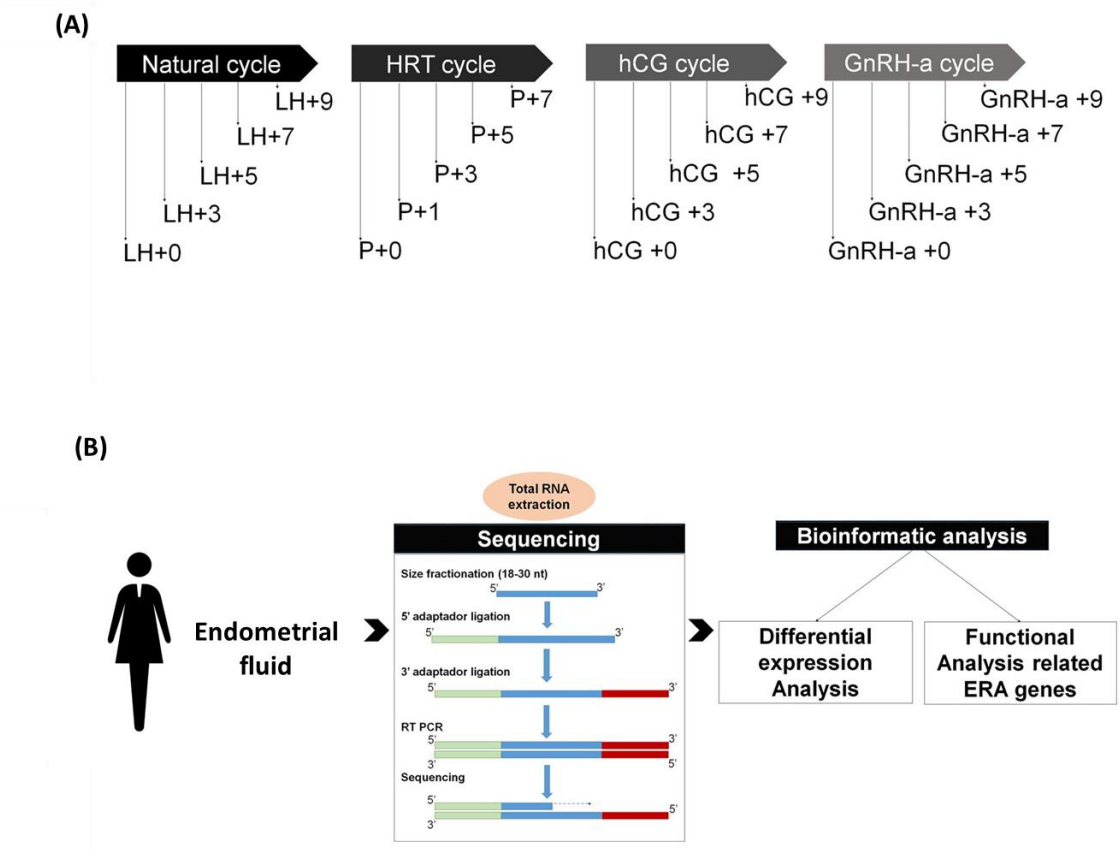

Figure 8. Study design. (A) Ovum donor volunteers underwent 4 consecutive treatments (n=10 for each time-point). Time-points for sample collection were in natural cycles LH +0, LH +3, LH +5, LH +7; in HRT cycle: P +0, +1, +3 and +5; in COS +hCG: +0, +3, +5, +7 and +9; and finally, in COS +GnRH-a: +0, +3, +5, +7, and +9; (B) Total RNA extraction was performed for sequencing. Data resulting from sequencing were bioinformatically analysed.

4.2. Inclusion and exclusion criteria

Recruitment of the patients was based on the following inclusion/exclusion criteria. The inclusion criteria were women between 18 and 34 years old, with normal karyotype, negative serological tests for human immunodeficiency virus (HIV), Hepatitis B virus (HBV), Hepatitis C virus (HCV), rapid plasma reagin (RPR), with a body mass index (BMI) in a range of 19-29 kg/m2 (both inclusive) and regular menstrual cycle (3-4/28-30 days). Exclusion criteria included women who had carried an intrauterine device (IUD) in the previous 3 months, or who had taken hormonal contraceptives in the previous 2 months, or that suffered uterine pathologies. The existence of serious or uncontrolled bacterial, fungal or viral infections, which, in the opinion of the principal investigator, could have interfered with the patient's participation in the study or in the evaluation of the study results, was considered as another exclusion criteria.

Patient recruitment and sample collection

EF aspirates (n=125) were obtained from healthy ovum donor volunteers n=47 in IVI Valencia. The Clinical Research Ethics Committees (CEIC) of IVI approved this study with number 1304-C-117-FV. All participants who met the study criteria signed an informed consent before the EF samples were obtained. The number of samples included in each phase of the four treatments is shown in the **table 2**.

Table 2. Final samples size obtained.

Natural cycle	**LH +0**	**LH +3**	**LH +5**	**LH +7**	**LH +9**
n=	9	9	7	2	0
HRT cycle	**P +0**	**P +1**	**P +3**	**P +5**	**P +7**
n=	9	8	8	6	2
COS +GnRH-a	**GnRH-a +0**	**GnRH-a +3**	**GnRH-a +5**	**GnRH-a +7**	**GnRH-a +9**
n=	10	9	9	8	3
COS +hCG	**hCG +0**	**hCG +3**	**hCG +5**	**hCG +7**	**hCG +9**
n=	10	3	3	4	6

4.2.1. Natural cycle protocol

The ovaries were assessed by ultrasound during the first three days of menstruation to ensure that they were in the quiescent state. Once that was verified, a second check was performed on day 8-11 of the menstrual cycle to monitor the ovarian cycle. When a

dominant follicle with 16-mm of diameter was observed, the patients carried out the urine reagent strip test every 12h, and they were screened by ultrasound regularly every day, until a positive LH result was obtained. Then EF aspiration was performed as previously described, considering as LH +0 the day of LH surge.

4.2.2. HRT protocol

A baseline transvaginal scan was performed to ensure that the endometrium and ovaries were in basal conditions. Endometrial preparation was initiated using a daily dose of 0.25mg of Cetrorelix (Cetrotide®, 0, 25 mg Merck-Serono) during 5 days of the previous cycle an oral administration doses of 6 mg of estradiol valerate (Progynova; Schering) was given. After 10-12 days from treatment started, an ultrasound was performed to evaluate endometrial (Utrogestan® 200mg, Besins Healthcare) growth and when endometrial lining reached 7 mm with a typical triple layer pattern 400 mg/day (Utrogestan® 200mg, Besins Healthcare) was administered. The day of the initiation of P4 administration was considered as P +0.

4.2.3. COS protocol triggered by hCG

Ovarian stimulation started on the third day of menstrual cycle with 225 IU/day dose of FSH-r (Gonal-F®; Merck-Serono). When one or more follicles achieved more than 12 mm of diameter, 0.25 of Cetrorelix (Cetrotide®, 0.25 mg Merck-Serono) were provided to prevent the premature LH surges and ovulation. Thereafter, it was injected daily until hCG administration. Doses were adjusted according to the ovarian response as determined by serum estradiol concentrations and ultrasound scans every three days. Follicle puncture for retrieval of oocyte was programmed when follicles were between 17.5 mm and 20.5 mm. Then, 6500 UI hCG (Ovitrelle®, Merck-Serono) was administered to trigger ovulation. About 36 hours later, oocyte aspiration was performed with woman under general sedation. The day after aspiration, a vaginal dose of progesterone (Utrogestan® 200mg, Besins Healthcare) 200 mg/12h was administered until EF aspiration depending on the time point selected considering as hCG +0 the day of initial dose of hCG.

4.2.4. COS protocol triggered by GnRH-a

Ovarian stimulation was performed as previously indicated. When follicular maturation criteria were achieved, 0.2 mg of triptorelin acetate (Decapeptyl® IPSEN PHARMA) was administered to triggered ovulation. About 36 hours later, oocyte aspiration was performed. The day after aspiration, vaginal dose of progesterone 200 mg/12h (Utrogestan® 200mg, Besins Healthcare) were administered until EF aspiration depending on the group membership considering as GnRH-a +0 the day of initial dose of GnRH-a.

4.3. Sample collection and processing

4.3.1. Aspiration of EF samples

Aspiration of EF was performed with the woman lying in the lithotomy position. The cervix was cleansed after insertion of a speculum. A flexible catheter (Wallace, Smith Medical International), was gently introduced transcervically into the uterine cavity. When the catheter was correctly positioned, a 10-ml syringe was connected to the catheter and suction was gradually applied. To prevent contamination by cervical mucus during catheter removal, the outer sheath of the embryo transfer catheter was advanced to a depth of 4 cm from the external cervical os, following the application of suction. Thereby, approximately 10-50 µl of EF was obtained from each woman**.**

4.3.2. RNA extraction from EF

RNA extraction was performed using miRNeasy Mini Kit (Qiagen) which enables the purification of total RNAs from EF including miRNA. This protocol consists of adding 1 ml of qiazol and 200 µl cloroform to the EF. After a centrifugation at 12,000 x g at 4°C for 15 minutes the watery phase was transferred to a tube containing 700 µl ethanol 100% and was well mixed. Successively, 700 µl of this mix was passed through a column and centrifuged at 8,000 rpm for 15 seconds at room temperature. Overturn to empty the 2-ml tube. Treatment with DNase was carried out on the samples by mixing 10 µl DNase I and 70 µl Buffer RDD (Kit RNase DNase Set I) and adding the 80 µl DNase mixture onto the membrane for 15 minutes at room temperature. After repeated washing with RWT buffer and RPE buffer the RNA extracted was eluted using 30 µl of RNase-free water on

the membrane and centrifuged at 8,000 rpm for 1 minute to elute the RNA. The concentration of RNA was determined by measuring the absorbance at 260 nm (A260) using a Nanodrop™ photometer (Thermo Scientific) for yield and sample quality. The ratio of the readings at 260 nm and 280 nm (A260/A280) provides an estimate of the purity of RNA with respect to contaminants that absorb UV light, such as protein.

4.4. RNA sequencing: Experimental Procedures

NGS was performed using Illumina HiSeq2000/100 to analyse microRNA species. Agilent 2100 Bioanalyzer (Agilent RNA 6000 Nano Kit) was used to test sample integrity and concentration, and NanoDrop to estimate inorganic ions or polycarbonate contamination. These steps aim to provide a reference for library construction and later analysis.

4.4.1. Library Construction and sequencing

The libraries for the TruSeq Small RNA Sample Prep Kit (Illumina), was prepared as follow: Small RNAs were filtered using 200ng-1µg of RNA sample, then RNA segments of different sizes were separated by polyacrylamide gel electrophoresis (PAGE). Segments between 18-30nt (14-30 ssRNA Ladder Marker, TAKARA) were selected, striped and recycled. For the 3’ adapter ligation steps, in a 200 µL PCR tube on ice was used to combined 1 µL of RNA 3' adapter (RA3), with 1 µg total RNA in 5 µL of nuclease-free water. That mixture was incubated at 70°C for 2 minutes. Then, samples were stored on ice and the thermal cycler was preheated to 28°C. In in a new 200 µL PCR tube on ice, 2 µL of Ligation Buffer was combined with 1 µL of RNase Inhibitor and 1 µL of T4 RNA Ligase 2, Deletion Mutant. After a brief centrifugation, this solution was added to the tube containing RA3/total RNA. The final mixture, with a total volume of 10 µL, was incubated at 28°C for 1 hour. Next, 1 µL of Stop Solution was added and samples were re-incubated at 28°C for 15 minutes. For the 5’ adapter ligation, thermal cycler was preheated to 70°C; 1,1×N µl RNA 5' Adapter (RA5) was added to a new 200 µl PCR tube and incubated on the thermal cycler at 70°C for 2 minutes. The thermal cycler was then preheated to 28°C and 1.1 × N µl 10mM ATP were added to the tube of RA5 and mixed. Then, 1.1 × N µl T4 RNA Ligase was added to the RA5/ATP mixture and mixed. Finally, 3

µl of this mixture was added to the tube of RA3 mixture, in order to obtain a total volume of 14 µl. That solution was incubated at 28°C for 1 hour.

T4 RNA Ligase catalyses the ATP-dependent ligation of single-stranded RNA or DNA onto the 5´-phosphoryl termini of single-stranded RNA or DNA (147). After the adapter ligation, reverse transcription followed by amplification promoted the creation of cDNA constructs based on the small RNA ligated with 3' and 5' adapters. Indeed, this step selectively enriches RNA fragments with adapter molecules on both ends. The amplification was performed with 2 primers that anneal to the adapter ends. For this purpose, for each sample, 0.5 µl of 25 mM deoxynucleotide (dNTP) mix and 0.5 µl of ultrapure water were combined with 12.5 mM dNTP Mix, and briefly centrifuged. 6 µl of each adapter-ligated RNA library was dispensed in a new 200 µl PCR tube. To that, 1 µl of RNA RT primer was added and the mixture was briefly centrifuged and then incubated at 70º C for 2 minutes in a preheated thermal cycler. In a new 200 µl PCR tube on ice the following was combined for each library: 2 µl of 5X first strand buffer; 0.5 µl of 12.5 mM dNTP mix; 1 µl of 100 mM dithiothreitol (DTT); 1 µl of RNase Inhibitor; and 1 µl of SuperScript II Reverse Transcriptase. From that, 5.5 µl were added to the tube of adapter-ligated RNA/primer mix, in order to obtain a total volume of 12.5 µl, which was incubated in the thermal cycler at 50°C for 1 hour. In a new tube were combined for each library: 8.5 µl of ultrapure water; 25 µl of PML; 2 µl of RNA PCR Primer (RP1); and 2 µl of PCR Primer index (RPIX). That solution was added to the adapter-ligated RNA mixture after a brief centrifugation, since a total volume of 50 µl was obtained.

Several rounds of PCR amplification with PCR Primer Cocktail and PCR Master Mix were performed to enrich the cDNA fragments. In detail, samples were incubated at 98°C for 30 seconds; followed by 11 cycles of: 98°C for 10 seconds; 60°C for 30 seconds; 72°C for 15 seconds; 72°Cfor 10 minutes and 4°C hold. Each library was run on a High Sensitivity DNA chip. PCR products were then purified using PAGE gel; this gel purifies the amplified cDNA construct in preparation for subsequent cluster generation. For this purpose, 2 µl of Custom RNA Ladder (CRL) and 2 µl DNA loading dye were combined in a 1.5 ml microcentrifuge tube and 1 µl High Resolution Ladder (HRL) and 1 µl DNA loading dye were combined in a new 1.5 ml microcentrifuge tube. Also, 10 µl of DNA Loading Dye were combined with all the amplified cDNA constructs (typically 48–50 µl) in a new 1.5

ml microcentrifuge tube. On the gel, 2 gel lanes were loaded with 2 µl CRL/loading dye mixture; 1 gel lane with 2 µl HRL/loading dye mixture and other 2 gel lanes with 25 µl each of amplified cDNA construct/loading dye mixture. The total loaded volume was 50 µl. The gel was run for 60 minutes at 145 V or until the blue front dye left the gel. Purified constructs were then recovered. The gel was stained with ethidium bromide in a clean container for 2–3 minutes and viewed on a Dark Reader transilluminator or a UV transilluminator: the 147 nt band primarily contains mature miRNA generated from ~22 nt small RNA fragments, the 157 nt band contains piwi-interacting RNAs, some miRNAs, and other regulatory small RNA moleculesgenerated from ~30 nt RNA fragments. The bands from the 2 lanes that correspond approximately to the adapter-ligated constructs derived from the 22 nt and 30 nt small RNA fragments were cut using a razor blade. The band of interest was placed into the 0.5 ml gel breaker tube. And centrifuged at 20,000 × g for 2 minutes to move the gel through the holes into the 2 ml tube. 200 µl ultrapure water was added to the gel debris in the 2 ml tube. The tube was shaken for at least 2 hours to elute the DNA, and then, the eluted and gel debris were transferred to the top of a 5 µm filter and centrifuged at 600 × g for 10 seconds. In order to validate the library, 1 µl of the re-suspended construct was quantified using the Agilent 2100 bioanalyzer instrument (Agilent DNA 1000 Reagents), and by real-time quantitative PCR (TaqMan Probe). In this way, the size, purity, and concentration of the library was checked. The qualified libraries were amplified on cBot system (Illumina) to generate the cluster on the flow cell. Finally, the amplified flow cell was sequenced single end on the HiSeq 2000 System (Illumina).

4.5. Bioinformatic analysis

4.5.1. Pre-processing data

A schematic workflow of samples processing and data analysis is showed in **Figure 9**. Delving into the data analysis section, miRNAs counts were obtained using miRDeep2 (version 2.0.07) following the default work-flow described by the authors (148). The miRDeep package allows discovery of known or novel miRNAs from deep sequencing data, processing it through a series of steps. Briefly, at first, the reads were aligned to the genome using *Homo sapiens* genome (GRCh37) as reference; reads shorter than 18

nucleotides were eliminated. Mature and immature miRNA sequences from 21st release of miRbase (149) were used for quantification of reads per miRNA to generate an expression profile per sample; genomic DNAs, bracketing the alignment, were extracted to calculate their secondary structure. Secondly, potential precursors which were inconsistent with miRNA biogenesis were discarded. Then, it uses a probabilistic model of miRNA biogenesis to score each potential miRNA precursor for the combined compatibility of energy stability, positions, and frequencies of reads with Dicer processing (148).

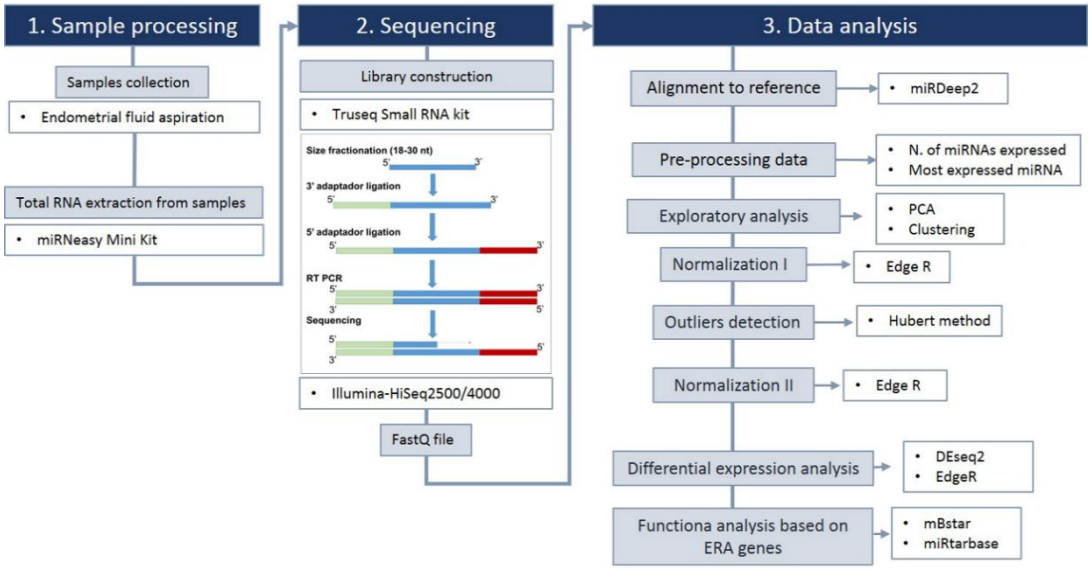

Figure 9. Sample processing. TruSeq Small RNA Sample Library Construction, Sequencing and bioinformatic data analysis workflow.

4.5.2. Normalization

Normalization was done using Trimmed mean of M (TMM) method from edgeR package (150). That normalization method takes into account the composition of the RNA population being sampled, which is neglected in total count scaling (135). miRNAs that did not express more than 1 count per million (CPM) in at least 3 samples were removed from the analysis (considered as not expressed). In order to detect and remove the outliers in the study, Hubert method was applied (151). Downstream analysis was performed using the number of samples as shown in **table 3**.

4.5.3. Differential expression analysis

Differential expression analysis (DEA) was done using both edgeR and DESeq2 following the guidelines of the packages. Comparisons were performed among time points within each treatment as a time series study and among treatments within related clinical phases (Natural cycle vs. HRT and COS +hCG vs. COS +GnRH-a) as a treatment effect study. Those miRNAs which false discovery rate (FDR) value was smaller than 0.05 and with a fold change (FC) higher than 2 in both methods, were considered as significantly differentially expressed and were used to do clustering, principal components and heatmap analysis.

Table 3. Number of samples remained for the analysis after the outlier exclusion.

Natural cycle	**LH +0**	**LH +3**	**LH +5**	**LH +7**	**LH +9**
n=	7	8	6	2	0
HRT cycle	**P +0**	**P +1**	**P +3**	**P +5**	**P +7**
n=	6	8	5	4	
COS + GnRH-a	**GnRH-a +0**	**GnRH-a +3**	**GnRH-a +5**	**GnRH-a +7**	**GnRH-a +9**
n=	8	6	6	6	2
COS + hCG	**hCG +0**	**hCG +3**	**hCG +5**	**hCG +7**	**hCG +9**
n=	8	2	2	3	3

4.6. Sequencing results validation

From each comparison between pre-receptive vs. receptive phase, we selected some miRNAs detected as differentially expressed to validate the accuracy of sequencing data results using quantitative reverse RT-PCR (RT-qPCR). In detail, four differentially expressed miRNAs were selected from natural cycle, three miRNAs were selected from hCG treatment, two miRNAs were also selected from GnRH-a-a treatment, and two from HRT treatment. Also, five miRNAs were validated in hCG +7 vs. GnRH-a +7 samples. Independent samples were used for validation analysis. In detail (n=2) for Natural cycle, (n=2) for hCG cycle, (n=3) for GnRH-a cycle and for HRT cycle (n=5).

4.6.1. Retrotranscription

For reverse transcription of total RNA containing miRNA we used the miScript PCR Kit (QIAGEN) which enables single-step cDNA synthesis and allow quantification of miRNA

and mRNA from the same cDNA. We employed the HiFlex Buffer protocol according to the manufacturer's recommendations.

4.6.2. RT-qPCR

A total of 2 µL of cDNA generated with the miScript II RT Kit was used as a template for RT-qPCR using the miScript SYBR Green PCR Kit (Qiagen) and LightCycler FastStart DNA Master SYBR green I in a LightCycler 480 (Roche AppliedScience, USA) and the fold-change was estimated using the $2^{-\Delta\Delta Ct}$ formula. The miRNAs primers from miScript Primer Assay Qiagen used, were detailed in **table 4.** The Mann-Whitney U test and nonparametric Spearman's rank correlation coefficient were used for statistical analysis.

Table 4. Primers used for validation of sequencing results.

Product name	Sequence
Hs_miR-4772-5p_1 miScript Primer Assay	5'UGAUCAGGCAAAAUUGCAGACU
Hs_miR-193a-5p_1 miScript Primer Assay	5'UGGGUCUUUGCGGGCGAGAUGA
Hs_miR-146b_1 miScript Primer Assay	5'UGAGAACUGAAUUCCAUAGGCU
Hs_miR-184_1 miScript Primer Assay	5'UGGACGGAGAACUGAUAAGGGU
Hs_miR-345_3 miScript Primer Assay	5'GCUGACUCCUAGUCCAGGGCUC
Hs_miR-141_1 miScript Primer Assay	5'UAACACUGUCUGGUAAAGAUGG
Hs_miR-582-3p_1 miScript Primer Assay	5'UAACUGGUUGAACAACUGAACC
Hs_miR-181a*_1 miScript Primer Assay	5'ACCAUCGACCGUUGAUUGUACC
Hs_miR-431*_1 miScript Primer Assay	5'CAGGUCGUCUUGCAGGGCUUCU
Hs_miR-410_1 miScript Primer Assay	5'AAUAUAACACAGAUGGCCUGU
Hs_miR-127-5p_1 miScript Primer Assay	5'CUGAAGCUCAGAGGGCUCUGAU
Hs_miR-223_1 miScript Primer Assay	5'UGUCAGUUUGUCAAAUACCCCA
Hs_miR-224_1 miScript Primer Assay	5'CAAGUCACUAGUGGUUCCGUU
Hs_miR-30d_2 miScript Primer Assay	5'UGUAAACAUCCCCGACUGGAAG
Hs_miR-873-3p_1 miScript Primer Assay	5'GGAGACUGAUGAGUUCCCGGGA
Hs_SNORD96A_11 miScript Primer Assay	Cat. No. MS00033733 (Qiagen)

4.6.3. Functional analysis

Functional analysis was done using the genes expression profiles from ERA samples as reference with the objective to understand which miRNAs could identify a receptive phenotype. Data from gene expression profile from 60 ERA patients who underwent HRT treatment was used. Target genes were defined for each differentially expressed miRNAs resulting from progesterone treatment, using miRTarBase database (release 6.0) (152) and MBStar (multiple instance learning of binding sites of miRNA TARgets) software for accurate prediction of true or functional miRNA binding sites (153). To filter mRNA target, miRNAs expression profiles were merged with ERA genes target expression profiles. Based on miRNAs mechanism of action, interaction in which miRNAs profiles and mRNAs profile were opposite along the luteal phase (P +0, P +1, P +3, P +5) were elected. Conversely, all the interactions that did not show the opposite trend were discarded **(Figure 10).** Also, those interactions in which miRNAs showed opposite trend with their mRNA target but, with small count number across the cycle were discarded.

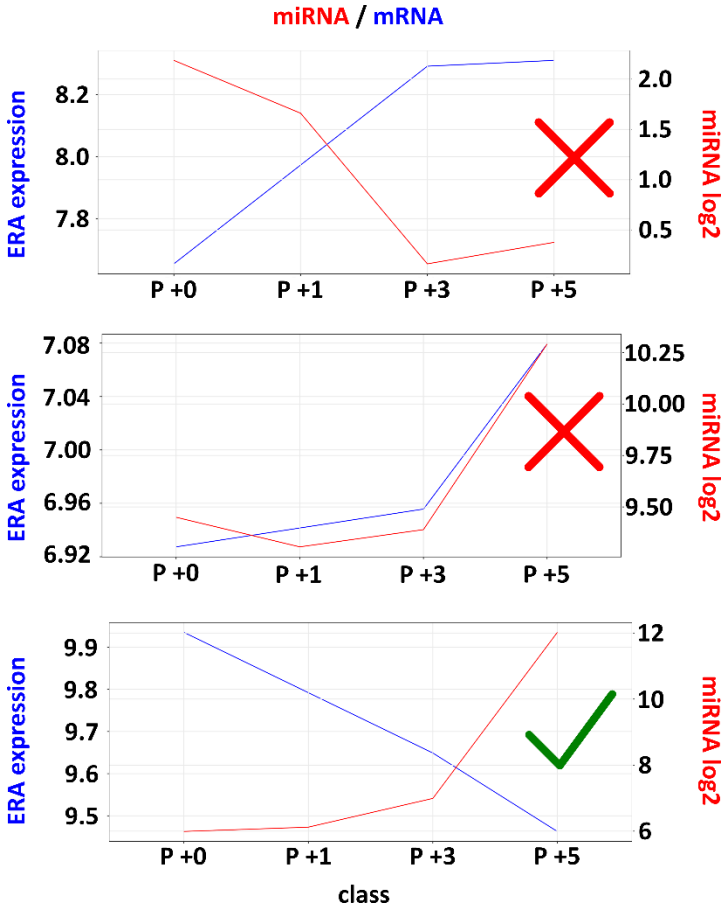

Figure 10. Filtering method based on negative regulation of miRNAs.

These genes were annotated using KEGG database (154) in order to find functions in which miRNAs could be potentially involved. It is important to know that the method used does not include regulation by translation inhibition, in that case, protein levels should be also measured.

Regarding COS cycle, functional analysis was focused on differentially expressed miRNAs between receptive phase of hCG cycle vs. GnRH-a cycle. Due to the big amount of predicted target for each miRNA, only those miRNAs with a FC greater than 4 were chosen.

DIANA miRPath v.2.0 web server was used to perform enrichment analysis of KEGG pathways for Homo sapiens. The *in silico* target prediction was performed using DIANA-microTCDS. The default algorithm utilized was the one-tailed Fisher's exact test and multiple hypothesis testing was corrected using the FDR method. P-value threshold was fixed at 0.05, and MicroT threshold at 0.08. Multiple miRNA effect analysis was performed using pathways union, in this mode, the server identified all the significantly targeted pathways by the selected microRNAs.

4.6.4. *In vitro* target validation

Based on bioinformatic results from the functional analysis, we selected hsa-mir-30d-5p/KIF11 interaction in order to validate the miRNA-ERA genes interaction. This choice was due, mainly, to the high expression of hsa-miR-30d-5p in hCG +7 in comparison with GnRH-a +7. KIF11 was the only gene, target of hsa-miR-30d-5p, which accomplished our selection criteria. With this aim, we used Ishikawa cell line ((155), Sigma Aldrich), an epithelial-like cell line derived from human endometrial adenocarcinoma, as a model for receptive endometrium. For the experiments (n=3) Ishikawa cells from three different passage (P8, P11 and P12) were cultured in MEM + 2mM Glutamine + 1% Non-Essential Amino Acids + 5% Foetal Bovine Serum. Cell cultures were maintained in a humidified atmosphere containing 5% CO2 at 37°C. Ishikawa cells were seeded in 24-well culture plates for 72 hours. When Ishikawa cultures reached 50% confluency the cells were transiently transfected with 5 nM of Syn-hsa-miR-30d-5p miScript miRNA Mimic (Qiagen, cat No. MSY0000245) 5'UGUAAACAUCCCCGACUGGAAG or 50nM of Anti-hsa-miR-30d-5p miScript miRNA Inhibitor, (Qiagen, cat No. MIN0000245) 5'UGUAAACAUCCCCGACUGGAAG.

Transfection was performed using HiPerfect (Qiagen), which allows the encapsulation of miRNAs within charged lipid complexes that are able to merge with cellular membranes to release their contents. Total RNA and proteins were extracted from cells at 48 and 72 hours after the transfection.

4.6.5. RNA extraction from cultured cells.

Plated cells were washed in 500 µL of PBS and 500 µL of trypsin were added for dissociation of the monolayer. After centrifugation at 2,000 x g for 5 minutes, the pellet was resuspended in a mixture solution of 900µL of bovine serum albumin and 100 µL EDTA 0.1 M. Another centrifugation was performed at 3,000 x g for 5 minutes. 100 µL of extraction buffer were added to the pellet which was warmed at 42º for 30 minutes. Total RNA was extracted using the Arcturus PicoPure RNA isolation Kit (Applied Biosystems). After a centrifugation at 3,000 x g for 2 minutes, the supernatant was transferred into a new microcentrifuge tube with 100 µL of absolute ethanol. The mixture solution was filtered in the purification column which was previously treated with 250 µl of condition buffer for 5 minutes at room temperature. After several washes, the RNA was eluted in 20 µL of RNAse-free water.

4.6.6. RT-qPCR

With the aim of estimating *KIF11* expression under different conditions we used the PrimeScript™ RT Reagent Kit (Perfect Real Time) (Takara) for the conversion of RNA into cDNA. Once RNA has been converted to cDNA, relative quantitative PCR was performed using LightCycler FastStart DNA Master SYBR green I in a LightCycler 480 (Roche Applied Science) and the fold-change was estimated using the $2^{-\Delta\Delta Ct}$ formula. T-test was used for the statistical analysis.

4.6.7. Primer design

Primer3 (v.0.4.0) was used to design appropriate PCR primers for *KIF11*, the primer melting temperature (tm) was calculated. Primers were constructed based on the optimal length (20-22 bases) **(Table 5)** and a melting temperature in the range of 60ºC. To avoid regions of homology all primers were tested using NCBI Primer Blast software.

Table 5. Kif11 primer used for miRNA/mRNA validation

Forward primer	5'-GGC AGT TGA CCA ACA CAA TG-3'
Reverse primer	5'-TCT AGC ATG GCC TTT TGC TT-3'

4.6.8. Protein extraction and analysis

For total protein extraction, cell pellets were lysed in liquid N_2; after one night at -80 the pellet and was resuspended in ice-cold RIPA buffer containing 300 mM NaCl, 20 mM Tris-HCL, 10 mM EDTA, 2% (v/v) Triton X-100, pH = 7.3 supplemented with a protease inhibitor cocktail (Roche Applied Science), and 10 mM PMSF (Sigma-Aldrich). Protein quantification was performed using the colorimetric protein assay called the Bradford assay. The Bradford assay is a protein determination method based on the observation of the absorbance shift from 465 nm to 595 nm, that depends on the binding of Coomassie Brilliant Blue G-250 dye to proteins (156). The dye is predominantly in the protonated red form but when it binds to proteins, it is converted to a stable unprotonated blue form, detected at 595 nm in the assay using a spectrophotometer. A purified preparation of different concentration of BSA protein (0-2 ng) was used as standard for the protein assayed.

In a 96 well plate, 5 µL of standard and 5 µL of samples per well were added in duplicate. A total of 200 µL of colour reagent mix, composed of 50 µL of Bradford reagent (Bio-Rad) diluted in 150 µL of deionized water, was added to each well, incubated for 5 minutes and read on Multiscan Go (Thermofisher). Then, the concentration of the unknown sample was calculated based on the linear equation of the calibration curve.

4.6.9. Western Blot

For immunoblotting, 30 µg/lane of protein extracts from the cell lysates were separated on 8% SDS-polyacrylamide gels. The gels ran for 1 to 2 hours at 120 V and transferred to

polyvinylidene difluoride membrane (Biorad) using Tris/Glycine Transfer Buffer (Biorad). After one hour, the membranes were blocked with 5% fat-free milk in PBS-Tween at room temperature for 1 hour, and then incubated overnight at 4˚ C with antibodies specific to human KIF11 (MEM-259, Abcam) diluted 1:500 in 3% BSA, and β-ACTIN as a loading control (ab8227, Abcam) diluted 1:1000 in 3% BSA. After washing three times, the blots were incubated with an anti-rabbit secondary antibody (Santa Cruz Biotechnology) at a concentration of 1:10,000, for 1 hour at room temperature. Blots were then washed extensively and proteins were revealed using SuperSignal West Femto Chemiluminescent kit (Thermo Fisher Scientific).

5. Results and discussion

-Al di là del vetro- Ludovico Einaudi

5. Results and Discussion

To date, several reports have confirmed the existence of miRNAs secreted by the human endometrium and differential miRNAs present in EF during the window of implantation (125, 127). Related to this, our group evidenced that it was possible to assess the receptivity status (early proliferative, late proliferative, early secretory, WOI and late secretory phases) according to the miRNA profile detected in the EF collected from patients. Moreover, we demonstrated that those miRNAs secreted from epithelial cells into the EF during the WOI could be acquired by early embryos resulting in a modification of their transcriptome. More specifically, we discovered that the acquisition of hsa-miR-30d through exosome-like vesicles promoted an overexpression of cell adhesion molecules, thus improving the implantation rates achieved in the early stages of development (130)

In view of this, we aim to investigate the miRNAs signature present in the EF in the same patients during the WOI that underwent consecutively different hormonal treatments commonly used in ART.

5.1. miRNAs signature identified in EF in natural cycles

FastQ obtained from sequencing, containing sequence and quality data, were aligned to the reference genome (*H. sapiens*) and counted into annotated terms, using mirdeep2 package. This first step is important to remove read duplicates, low quality reads, contaminating sequences, and adaptor or barcode sequences (157). Then, an exploratory analysis of the raw data was performed in order to describe features such as the number of covered miRNA **(Figure 11.A)** and miRNA with the highest percentage of reads per sample **(Figure 11.B)**.

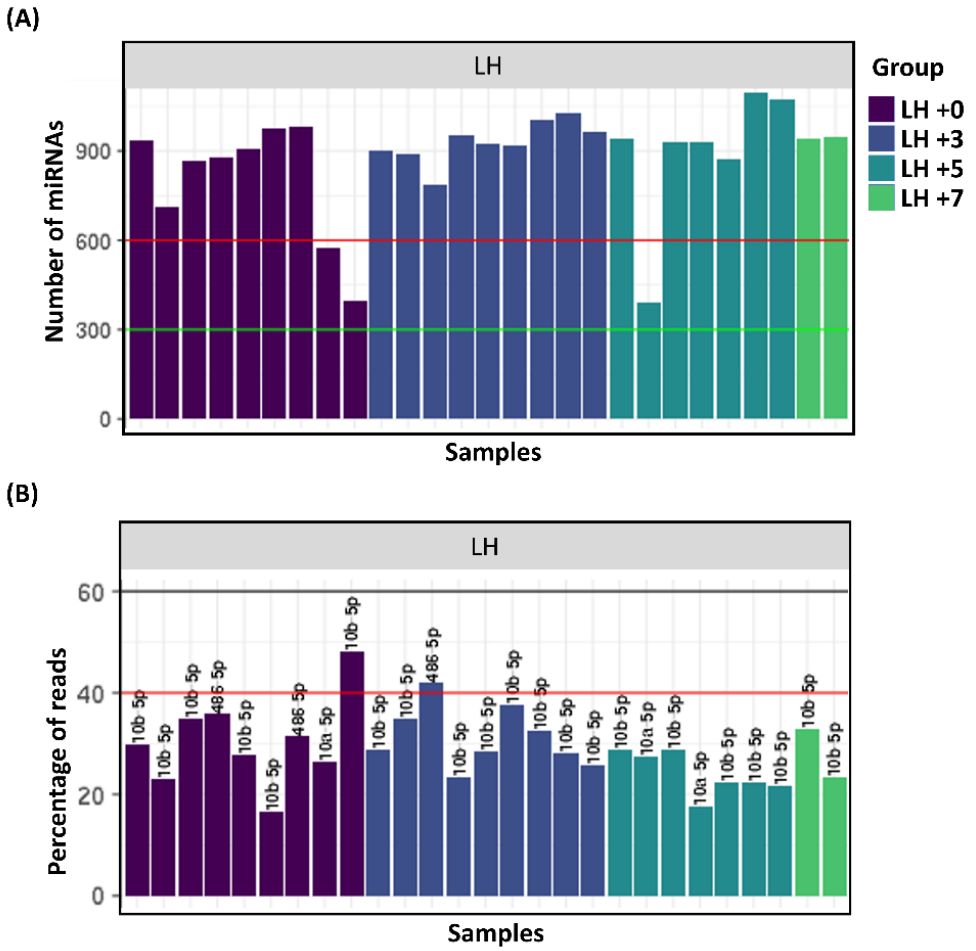

Figure 11. Pre-processing data in natural cycle. (A) Each bar in the graph represents a different sample of natural cycle. In purple are represented LH +0 samples, in blue LH +3 samples, in dark green LH +5 samples and in light green LH +7 samples. The red and the green lines mark 600 and 300 miRNAs expressed, respectively. (B) The graph shows the percentage of the highest miRNA per sample.

Since no NGS studies aimed to characterize miRNAs in EF exist, we referred to those studies investigating miRNAs in other body fluids in order to understand what could be normal in our data. These studies observed that the total number of miRNAs mapped to miRbase amount to 548 miRNAs detected in 18 plasma samples (158). Also, on average, serum and cerebrospinal fluid had 532 and 486 miRNAs (159). Moreover, 269 miRNAs were described in follicular fluid vesicles (160). With these basis, we considered that the number of miRNAs in our samples was the expected and we established two values, 600 and 300 miRNAs as reference. Regarding the number of miRNAs in our samples, we described that 24 out of 27 samples expressed approximately between 600 and 900 miRNAs; only 3 samples did not express more than 600 miRNAs **(Figure 11.A)**. Analysis of the percentage of mapped reads to the sequence of the most expressed miRNA in

each sample showed that 3 miRNAs were mainly expressed, hsa-miR10b-5p, hsa-miR10a-5p and Hsa-miR-486-5p **(Figure 11.B)**. In 21 samples of EF, the highest miRNA secreted was hsa-miR-10b-5p. In the remaining 6 samples, hsa-miR-10a-5p and hsa-miR-486-5p were the highest expressed, each one in 3 samples. In mammalian cells, miR-10a and miR-10b are located upstream of HoxB4 and HoxD4, respectively, and it was proposed that miR-10 cluster might play an important role in ovarian folliculogenesis by repressing proliferation and inducing apoptosis during granulosa cells development (161). Its importance is due to the same mechanism being required in the endometrium in order to achieve receptivity status. Also, in bovine specimens (162), it was demonstrated that miR-10b was 10-fold upregulated in the fetal bovine ovary compared with the somatic cells. Same authors using human samples, demonstrated that this miRNA is upregulated during follicle atresia. After the ovulation, the oocyte released from the dominant follicle becomes the *corpus luteum* and the remaining follicles undergo follicular atresia. On average, 94% of the luteal phase follicles are atretic (163); this could suggest the reason why during luteal phase this miRNAs was the highest expressed in almost all the samples.

To filter the data in the preliminary analysis, we considered miRNAs that did not express more than 1 CPM in at least 3 samples as not expressed and we removed them from the analysis. After, in order to detect the outliers in the study, Robust Principal Component Analysis (RPCA) with the Hubert algorithm was performed. It yields more accurate estimates with non-contaminated datasets and more robust estimates with contaminated datasets producing a diagnostic plot that displays and classifies the outliers (164). According to this method, 4 samples were considered outliers. Specifically, 2 LH +0 samples, 1 LH +3 sample and 1 LH +5 sample.

The 2 LH +0 samples and the LH +5 samples excluded, were those that showed less than 600 miRNAs per sample. The remaining outlier, belonging to the LH +3 group, differs in miRNAs expression from the rest of the samples from its same biological group. After normalization procedure, we performed the following analysis with the remaining 23 samples, in detail in LH +0 (n=7), LH +3 (n=8), LH +5 (n=6) and LH +7 (n=2). In the natural cycle, we performed several comparisons between the different phases. This enabled us to determine a temporal miRNAs characterization of the miRNA signature depending on their differential expression during the luteal phase. Since a 2-fold is typically considered

a useful cut-off (165), only those miRNAs having a FC value of 2 or more and with FDR <0.05 were considered for the analysis in order to reduce the false positive results. The number of significantly differentially expressed miRNAs from each comparison is showed in **Table 6**. Interestingly, the majority of differentially secreted miRNAs showed a downregulation during the early pre-receptive compared with late pre-receptive and receptive phases. This could indicate that the environment needed for the transition to endometrial receptivity status requires the upregulation of some miRNAs, which could affect the endometrial transcriptomic signature.

Table 6. Number of differential expressed miRNAs along natural cycle (FC>2; p-value <0.05)

Comparison	N. downregulated	N. upregulated
LH +0 vs. LH +3	2	9
LH +0 vs. LH +5	18	7
LH +0 vs. LH +7	11	6
LH +3 vs. LH +5	14	1
LH +3 vs. LH +7	5	0
LH +5 vs. LH +7	0	0

Specifically, we identified 17 differentially expressed miRNAs in LH +0 compared to LH +7 (11 downregulated and 6 upregulated), 5 miRNAs were downregulated in LH +3 compared with LH +7 and no miRNAs were found differentially expressed between LH +5 and LH +7 **(Figure 12.A).** This could be probably due to the temporary proximity between these two phases. Also, another possible explanation could be that the length of luteal phase varies among different women (166).

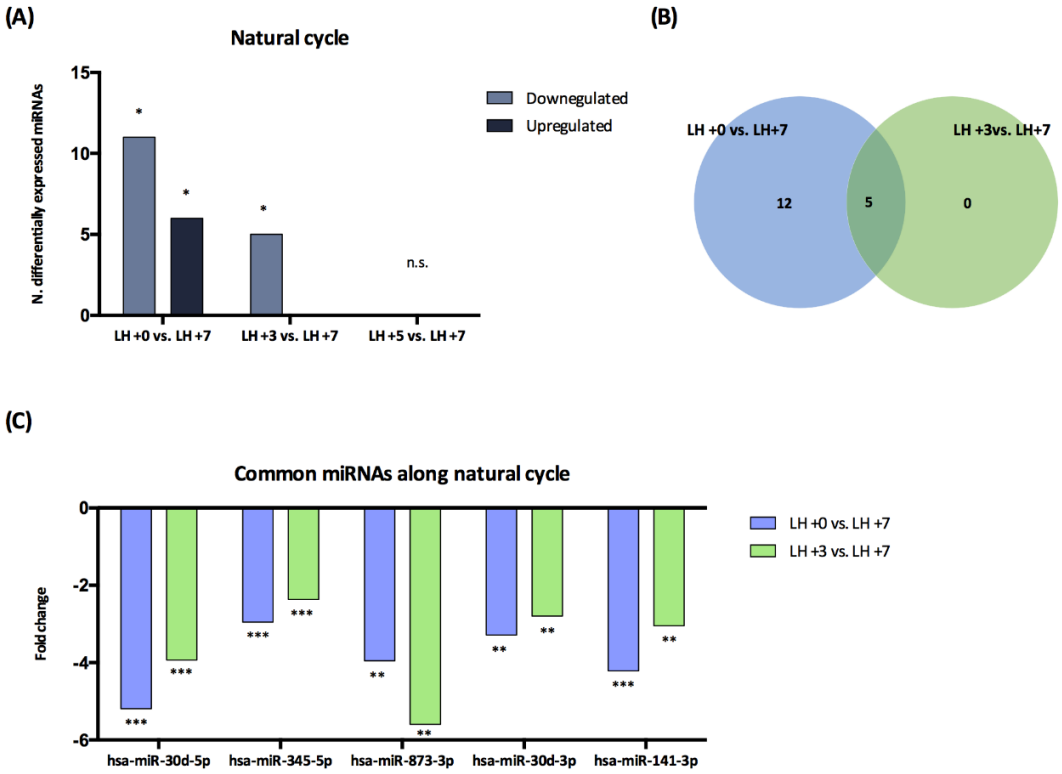

Figure 12. miRNAs behaviour in natural cycle. (A) Diagram represents the number of differentially expressed miRNAs detected in both EdgeR and DESeq2 packages. Differential expression analysis was performed comparing LH +7 profile with pre-receptive phases of the cycle, LH +0, LH +3 and LH +5. (B) Venn diagram shows common miRNAs differentially expressed in pre-receptive phases vs. LH +7. (C) FC representation of common miRNAs differentially expressed in LH +0, LH +3 vs. LH +7. (*) P<0.05; (**) P<0.01; (***) P<0.001, (n.s.) non-significant.

A Venn diagram was used to represent common pattern among the phases **(Figure 12.B)**. Thus, 5 miRNAs (hsa-miR-30d-5p, hsa-miR-345-5p, hsa-miR-873-3p, hsa-miR-30d-3p and hsa-miR-141-3p) were found differentially downregulated in LH +0 and LH +3, vs. LH +7; their fold change is represented in the (**Figure 12.C)**. The same miRNAs, were also considered as potential biomarkers of endometrial receptivity in natural cycle **(Figure 13).** Figure 13 shows that depending on their expression, these miRNAs can differentiate quite well between the two phases, in fact, samples from the same group cluster together.

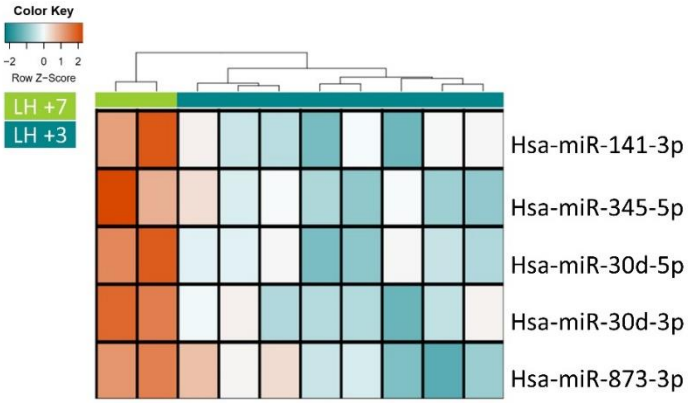

Figure 13. Potential biomarkers miRNAs in natural cycle. Heat map diagram and hierarchical clustering based on summarized intensity values of differentially expressed miRNA. Groups are differentiated by colours: LH +7 in light green and LH +3 in dark green. The colour scale shows the log2-fold change of a miRNA across all samples; blue coloured squares show low expression; red colour represents high level of miRNA expression and white squares indicate moderate expression.

The miRNAs, hsa-mir-30d-5p and hsa-miR-30d-3p, are members of the miR-30 family, they play important roles in regulating endometrial receptivity (167, 168). Hsa-mir-30d-5p has been previously described in the endometrium with an important role in implantation, its secretion from epithelial cells and its subsequently internalization by trophoblast cells has been demonstrated (121). Its role in gene reprogramming at the time of endometrial receptivity was also described (168). Hsa-miR-30d-5p and hsa-miR-873 displayed the highest fold change values in LH +3 compared with LH +7. Regarding hsa-miR-873, the importance of its upregulation during the receptive phase is supported by a study focused on the analysis of miRNAs in embryonic tissue which revealed a downregulation of this miRNA in women suffering from an ectopic vs. a healthy pregnancy (169).

Hsa-miR-141-3p belongs to the miR-200 family, which is highly expressed in epithelial cells. It has been described that miR-200 family members accumulate significantly during early phases of ovarian tumorigenesis (170). The fact that there are remarkable similarities between the behaviour of invasive trophoblast cells and that of invasive cancer cells, highlights its potential role during endometrial receptivity in preparing the endometrium for the embryo invasion. Indeed, a preliminary study proposed hsa-miR-141 as molecular marker for pregnancy monitoring and diagnosis, since it had been seen increased with gestational age (171). We hypothesize that its role in implantation could

start in the endometrial receptivity period and could be involved in favouring the establishment of pregnancy.

Also, hsa-miR-345-5p was found downregulated (FC=-2,37) comparing LH +3 with LH +7, its role in endometrial receptivity is not yet described, but we found a relation with endometrial receptivity in a recent study on Integrated Genomic Analysis of Idiopathic Pulmonary Fibrosis. This study notice the role of hsa-miR-345-5p in CAMs pathways (172). This pathway is implicated in endometrial epithelium in maintain the continuity and protectiveness of the luminal cell layer while permitting implantation of the embryo (173).

In **Table 7**, were described the respective fold changes and adjusted p-values for each of these miRNAs in LH +3 vs LH +7.

Table 7. Differential expressed miRNA in LH +3 vs. LH +7

LH +3 vs. LH +7	EdgeR		DeSeq2	
miRNA	***FDR***	***FC***	***padj***	***FC***
hsa-miR-30d-5p	1.06429E-05	-3.88	7.32E-05	-3.93
hsa-miR-345-5p	0.006122761	-2.39	0.004997	-2.37
hsa-miR-873-3p	0.158677581	-4.38	0.015405	-4.60
hsa-miR-30d-3p	0.011267006	-2.80	0.03996	-2.80
hsa-miR-141-3p	0.011267006	-3.01	0.042316	-3.05

The analysis of miRNA profiles in the current cycle, which is the physiological natural cycle, agrees with the idea that miRNAs are hormonally regulated during the cycle.

Sequencing validation results by RT-qPCR

Based on the miRNA abundance (CPM/total number of miRNA reads) we carried out the validation for those miRNAs showing the highest fold change values between the two phases. The expression of hsa-miR-30d-5p, hsa-miR-345-5p, hsa-miR-873-3p and hsa-miR-141-3p was validated in 2 different samples; in detail, LH +3 (n=1) and LH +7 (n=1). Results from RT-qPCR experiment showed that all the miRNAs were downregulated in LH +3 vs LH +7, thus confirming the sequencing results **(Figure 14).**

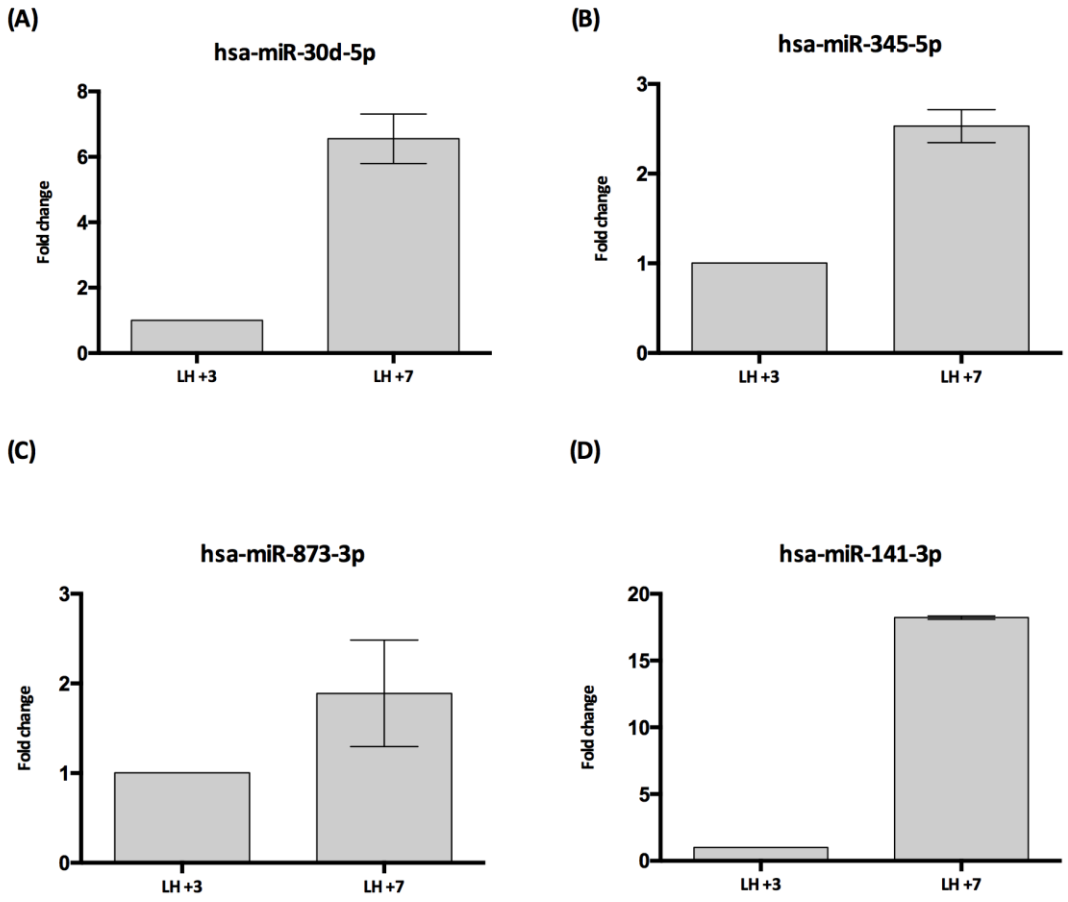

Figure 14. RT-qPCR validation of potential receptivity biomarkers in natural cycle. Four miRNAs were chosen to be validated using RT-qPCR in LH +3 and LH +7 samples. Fold changes were calculated using $2^{-\Delta\Delta Ct}$ formula. In detail (A) Hsa-miR-30d (FC: 6.55); (B) hsa-miR-345-5p (FC: 2.53); (C) hsa-miR-873-3p (FC: 1.89); (D) hsa-miR-141-3p (FC: 18.22). Differences between groups were non-significant (p>0.05).

5.2. miRNAs signature identified in EF in HRT cycles

In order to characterize the miRNAs secreted into the EF during the luteal phase of the HRT cycle, a total of 31 EF samples were analysed from 31 volunteers.

The number of miRNAs expressed per sample and the highest miRNAs per sample were described in a preliminary exploratory data analysis. What we have seen is that the big amount of the samples showed between 600 and more than 900 miRNAs, 1 sample did not reach the threshold of 600 miRNAs and 1 did not reach the threshold of 300 miRNAs **(Figure 15.A)**. Concerning the highest miRNAs expressed per sample, in HRT cycle as for the natural cycle, hsa-miR-10b-5p was the miRNA with the highest percentage of reads in 18 over 31 samples. In 9 samples, the miRNA with the highest percentage of reads

was hsa-miR-486-5p. In the remaining 4 samples, 3 showed hsa-miR10a-5p as the highest miRNA and 1 hsa-miR-223-3p **(Figure 15.B).** Curiously, hsa-miRNA-223-3p was the highest expressed in a sample from P +5 obtained during the expected WOI. Online sequence alignment showed that there is a putative binding site of miR-223-3p on the 3'UTR of *LIF*, which is considered to be an important marker of endometrial receptivity (174).

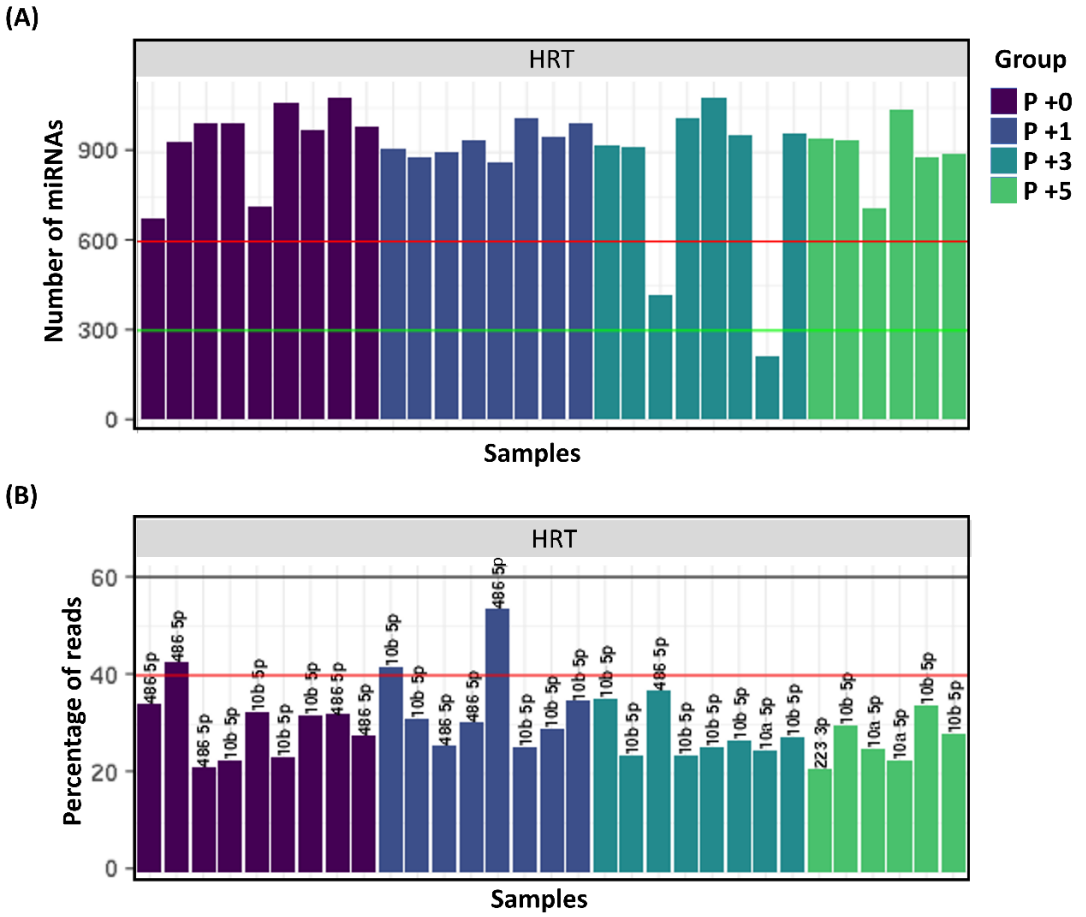

Figure 15. Pre-processing data in HRT cycle. (A) The numbers of miRNAs expressed per for the 31 HRT samples analysed. Each bar in the graph represents a different sample of natural cycle. In purple are represented P +0 samples, in blue P +1 samples, in dark green P +3 samples and in light green P +5 samples. The red and the green lines mark 600 and 300 miRNAs expressed respectively. (B) The graph shows the percentage of the highest miRNA per sample.

After the outlier's exclusions through Robust PCA methods, 23 samples remained for the following analysis: In each phase P +0 (n=6), P +1 (n=8), P +3 (n=5) and P +5 (n=4). Differential expression analysis was performed with the aim to identify the profile of the

miRNAs secreted in EF during the HRT cycle. A total of 154 miRNAs were found differentially expressed as result from all the comparisons of the cycle.

From each comparison, the number of differentially expressed miRNAs is showed in **Table 8.** We observed that the number of differentially expressed miRNAs decreased when comparing near temporal phases. Specifically, no miRNAs were found differentially expressed in P +0 vs. P +1 or in P +1 vs. P +3.

Interestingly, 15 miRNAs were found differentially expressed between P +3 vs. P +5. The fact that no differentially expressed miRNAs were found in the previous comparison, supposes a drastic change in miRNAs expression in the brief time in which the endometrium pass from a pre-receptive to a receptive phase **(Figure 16.A).**

Table 8. Differentially expressed miRNAs in HRT cycle (FC>2; p-value <0.05)

Comparison	N. downregulated	N. upregulated
P +0 vs. P +1	0	0
P +0 vs. P +3	1	2
P +0 vs. P +5	51	36
P +1 vs. P +3	0	0
P +1 vs. P +5	30	19
P +3 vs. P +5	12	3

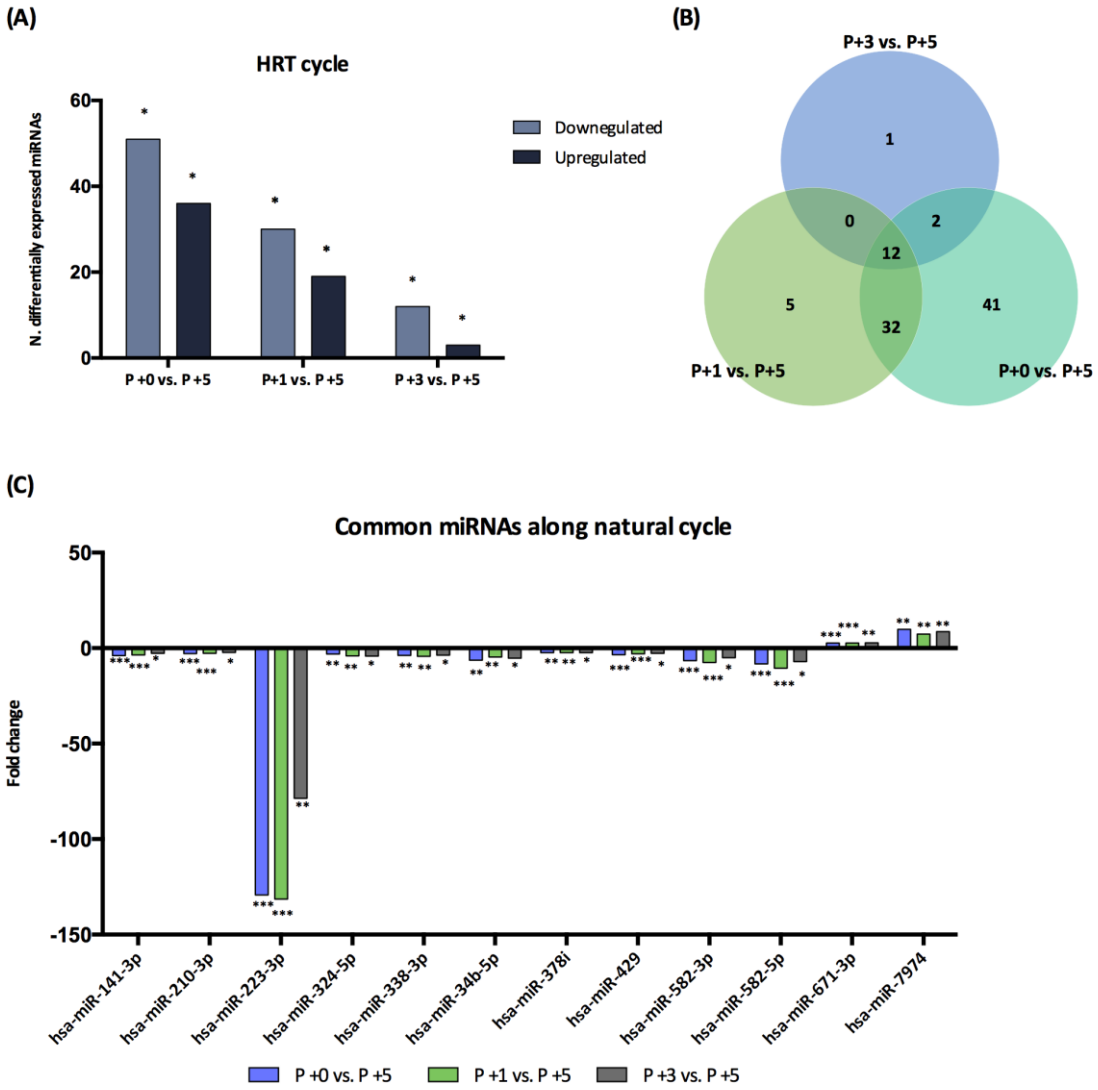

Figure 16. miRNAs behaviour in HRT cycle. (A) Graph representing the number of miRNAs differentially expressed between pre-receptive and receptive phases. (B) Venn diagram shows the number of common miRNA between the comparisons showed in panel A. (C) Graphical representation of fold change of the 12 differentially expressed miRNAs in common between pre-receptive vs. receptive phase of HRT cycle. (*) P<0.05; (**) P<0.01; (***) P<0.001.

We also investigated the trend of those miRNAs which were in common among P +0, P +1 and P +3 phases vs. P +5 **(Figure 16.B)**. Thereby, we identified 12 miRNAs (hsa-miR-141-3p, hsa-miR-210-3p, hsa-miR-223-3p, hsa-miR-324-5p, hsa-miR-338-3p, hsa-miR-34b-5p, hsa-miR378i, hsa-miR-429, hsa-miR-582-3p, hsa-miR-582-5p, hsa-miR-671-3p hsa-miR-7974) that were downregulated in P +0, P +1 and P +3 phases vs. P +5.

Among them, the most abundant miRNA was hsa-miR-223-3p. It reached its maximal difference in P +1 vs P +5 **(Figure 16.C).** miR-223-3p was described in mice where it was inversely expressed to LIF during implantation (2). Also, its expression was described in

dysregulated early embryonic tissues and in the fallopian tube of women with ectopic pregnancy (175). Also, hsa-miR-582-5p, was described by Kuokkanen et al., significantly upregulated in the mid-secretory phase (176).

In order to identify those miRNAs whose expression could help us to distinguish between a pre-receptive and a receptive endometrial status, and therefore identify possible biomarkers of endometrial receptivity, we put more interest on differentially expressed miRNAs between P +3 and P +5. They were represented in **Figure 17**. Based on the miRNAs expression, hierarchical cluster analysis shows that all P +5 samples cluster together and separated from P +3 samples, in agreement with their biological group.

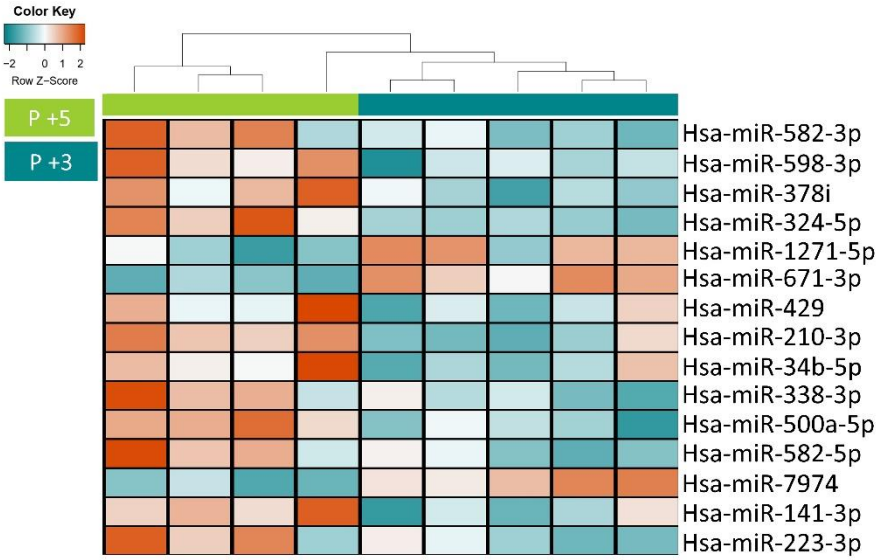

Figure 17. Potential receptivity miRNA biomarkers in HRT cycle. Heat map diagram and hierarchical clustering based on summarized intensity values of differentially expressed miRNA during P +5 vs P +3. The colour scale shows. The colour scale shows the log2-fold change of each miRNA across all samples; blue coloured squares show low expression; red colour represents high level of miRNA expression and white squares indicate moderate expression.

Sequencing results validation by RT-qPCR

In order to validate sequencing results, based on their abundance, those miRNAs with the higher fold change value were selected for the following validation experiments **(Table 9).**

Table 9. Differentially expressed miRNAs, between P +3 and P +5.

P +3 vs. P +5	edgeR		DeSeq2	
miRNAs	***FDR***	***FC***	***padj***	***FC***
hsa-miR-223-3p	0.021	-77.28	0.013	-78.56
hsa-miR-582-5p	0.025	-6.22	0.042	-7.08
hsa-miR-34b-5p	0.028	-5.22	0.036	-5.28
hsa-miR-582-3p	0.030	-4.91	0.039	-4.97
hsa-miR-324-5p	0.021	-4.04	0.027	-4.10
hsa-miR-338-3p	0.029	-3.49	0.040	-3.69
hsa-miR-500a-5p	0.028	-2.70	0.039	-2.87
hsa-miR-429	0.021	-2.70	0.021	-2.73
hsa-miR-141-3p	0.021	-2.67	0.026	-2.68
hsa-miR-378i	0.028	-2.35	0.032	-2.37
hsa-miR-210-3p	0.023	-2.19	0.032	-2.19
hsa-miR-598-3p	0.021	-2.14	0.014	-2.16
hsa-miR-671-3p	0.021	2.75	0.014	2.80
hsa-miR-1271-5p	0.038	4.21	0.039	4.22
hsa-miR-7974	0.023	7.12	0.014	8.62

The expression of hsa-miR-223-3p and hsa-miR-582-5p was validated in 5 samples **(Figure 18)**; in detail, P +3 sample (n=1) and P +5 samples (n=4). RT-qPCR confirmed the fold change direction of the sequencing results.

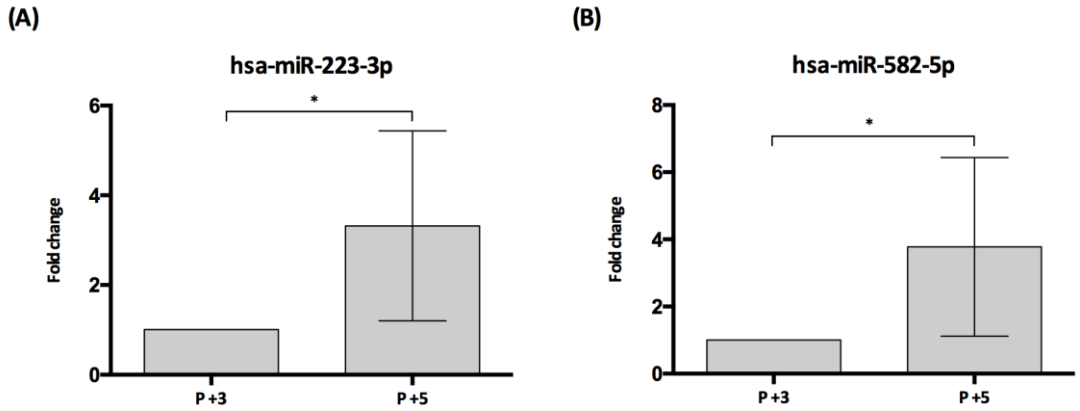

Figure 18. RT-qPCR validation of potential biomarker in HRT cycle. Two miRNAs (A) hsa-miR-223-3p and (B) hsa-miR-582-5p were chosen to be validated using RT-qPCR in 4 samples P +5 and one sample of P +3. Fold change were calculated using FC=$2^{-\Delta\Delta Ct}$ formula. (*) P<0.05.

5.3. miRNAs signature comparison between natural vs. HRT cycles

We performed a differential analysis between both types of cycles in order to investigate the manner in which the HRT might influence the secretion of miRNAs in EF. The differential expression analysis however did not show any differentially expressed miRNA when the same phases of both cycles were compared, except for LH +0 vs. P +0 in which only 2 miRNAs were differentially expressed **(Figure 19).**

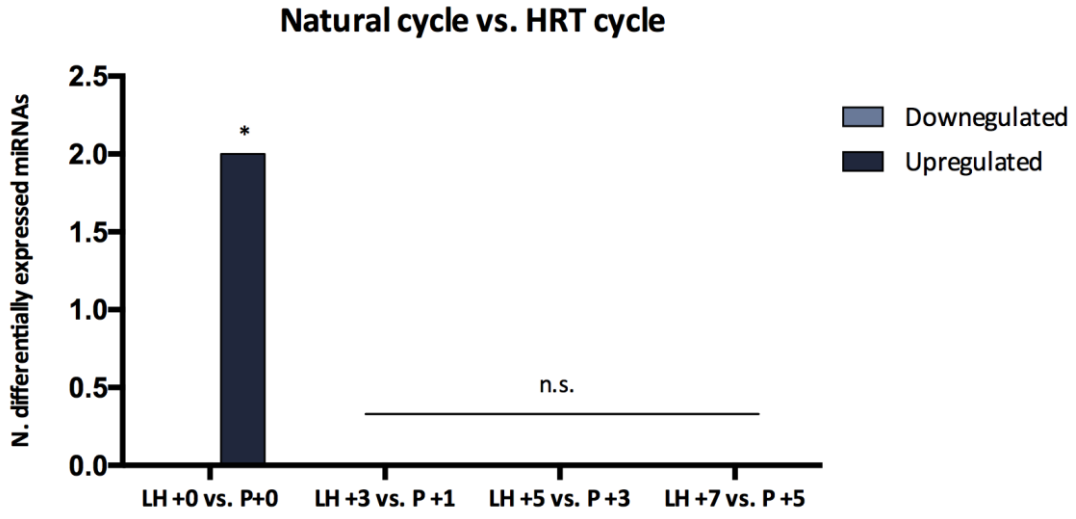

Figure 19. Differential expressed miRNAs between correspondent phases in natural and HRT cycle. (*) P<0.05; (n.s.) non-significant.

The literature shows that there is not a universal opinion on the better choice to perform endometrial preparation for ET. Some studies are in favour with the idea that natural cycle is associated with better outcomes compared to the use of HRT (177). In support, a retrospective work of Katharina Hancke, on 203 women, demonstrated that the pregnancy rates and live birth rates were superior in natural cycle compared with substituted cycle with a live birth rate of 20.9% and 12.7% respectively (178). Conversely, other studies affirm that there is no significant difference in live birth rates for FET in modified natural and HRT, in women using either own-egg derived embryos or donor-egg-derived embryos (179). No significant differences were described in the pregnancy and miscarriage rates in natural and HRT cycles (180). From a clinical perspective, a randomized study, conducted by Mounge et al., in 2012, which included a total of 159 women, demonstrated that clinical pregnancy and live birth rates were remarkably similar between the two groups of randomized patients (181). Another study from Gelbaya et al., with 417 women (212 women in natural cycle and 205 women in HRT cycle downregulated with GnRH agonist) demonstrated that there wasn't differences in implantation, pregnancy or live birth rates per cycle or per embryo transferred (182).

According to the studies that show no significantly differences among natural cycle and HRT cycle, our analysis of the miRNAs component secreted from endometrial cells into the EF during luteal phase, did not show significant differentially secreted miRNAs between both type of cycles.

Given that, no significant differences have been found between the two cycles, HRT is proposed as a better option since it allows to program in advance the day of embryo transfer (183). This option is not possible in natural cycle because the length of follicular phases varies among patients (183-185). Also, by performing HRT cycle the problem of spontaneous ovulation, commonly associated with the natural cycle, is avoided.

5.3.1. Integrated miRNAs and gene expression analysis based on ERA genes

Functional analysis of miRNAs is usually done using the Gene Ontology (186, 187) or via Kegg pathway annotations (188, 189) associated with the genes or gene products the miRNAs are predicted to regulate. Due to their property to target thousands of mRNAs,

the interpretation of functional analyses can be difficult and not representative for miRNAs (190).

The study of the gene targets of miRNAs that were differentially expressed in EF has been focused on finding the target genes that we know are expressed in the endometrium. Thus, functional analysis based on the genes included in the ERA test was performed. These genes are differentially expressed during luteal phase and depending on their up or downregulation, the predictor of the test is able to identify the period of endometrial receptivity. For this reason, we used the data obtained from ERA database from 60 women, from whose we had the detailed trend of the ERA genes during luteal phase of HRT cycle.

Differentially miRNAs obtained from all the comparisons of the HRT cycle were used to perform the functional analysis. Once the ERA target was identified for each miRNA **(Table 10),** the miRNA/mRNA opposite trend was investigated. This analysis is based on the idea that the predicted mRNAs targets are changing in the opposite direction of the miRNAs for which they are target (191). After this screening, we found 62 validated interactions reported in miRtarbase and 81 interactions predicted in mBstar. Due to the fact that a single gene could have more than one miRNA target, a final number of 97 ERA genes are involved in a total of 143 interactions **(Table 10)**.

Table 10. ERA genes target of differentially expressed miRNAs in HRT cycle.

Validated by mirTarbase		**Predicted by mbStar**	
miRNA	Gene Name	miRNA	Gene Name
hsa-miR-106b-5p	*ACADSB*	hsa-miR-3688-3p	*ACADSB*
hsa-miR-20b-5p	*ACADSB*	hsa-miR-3117-3p	*ANK3*
hsa-miR-335-3p	*ADAMTS8*	hsa-miR-582-5p	*ANK3*
hsa-miR-197-3p	*AGR2*	hsa-miR-508-3p	*ARID5B*
hsa-miR-185-5p	*AQP3*	hsa-miR-3117-3p	*ATP6V1A*
hsa-miR-193b-3p	*ASPM*	hsa-miR-106a-5p	*CAPN6*
hsa-miR-193b-3p	*BUB1B*	hsa-miR-20b-5p	*CAPN6*
hsa-miR-193b-3p	*CDC20*	hsa-miR-3688-3p	*CAPN6*
hsa-miR-197-3p	*CES1*	hsa-miR-222-5p	*CRISP3*
hsa-miR-20b-5p	*CYBRD1*	hsa-miR-18a-5p	*CTNNA2*
hsa-miR-185-5p	*EFNA1*	hsa-miR-29b-3p	*CYP3A5*
hsa-miR-326	*EPHB3*	hsa-miR-16-2-3p	*DDX52*
hsa-miR-15a-5p	*GABARAPL1*	hsa-miR-324-5p	*EMCN*
hsa-miR-504-5p	*GADD45A*	hsa-miR-199b-5p	*ENPEP*

hsa-miR-2115-3p	*GALNT4*	hsa-miR-335-3p	*ENPEP*
hsa-miR-200c-3p	*IGF2*	hsa-miR-106a-5p	*FGB*
hsa-miR-193b-3p	*KIF11*	hsa-miR-15a-5p	*FGB*
hsa-miR-144-3p	*LRRC1*	hsa-miR-20b-5p	*FGB*
hsa-miR-141-3p	*RASSF2*	hsa-miR-337-3p	*GALNT4*
hsa-miR-200c-3p	*RASSF2*	hsa-miR-2115-3p	*GALNT4*
hsa-miR-3688-3p	*SLC16A6*	hsa-miR-16-2-3p	*HEY1*
hsa-miR-758-3p	*SLC1A1*	hsa-miR-3688-3p	*HEY1*
hsa-miR-181c-5p	*SLC7A1*	hsa-miR-146a-5p	*HPGD*
hsa-miR-3150b-3p	*SLC7A1*	hsa-miR-20b-5p	*HPGD*
hsa-miR-3688-3p	*SLC7A1*	hsa-miR-3150b-3p	*HPGD*
hsa-miR-106a-5p	*SOD2*	hsa-let-7g-3p	*IGFBP1*
hsa-miR-185-5p	*SOD2*	hsa-miR-3688-3p	*KCNJ2*
hsa-miR-20b-5p	*SOD2*	hsa-miR-185-5p	*KMO*
hsa-miR-222-5p	*SOD2*	hsa-miR-190b	*KMO*
hsa-miR-200a-5p	*SOX17*	hsa-miR-3150b-3p	*KMO*
hsa-miR-376a-5p	*SYNE2*	hsa-miR-2115-3p	*LEPREL1*
hsa-miR-193b-3p	*TACC3*	hsa-miR-203b-3p	*LIF*
hsa-miR-203a-3p	*TOP2A*	hsa-miR-16-2-3p	*LRRC1*
hsa-miR-193b-3p	*TOP2A*	hsa-let-7g-3p	*LRRC17*
hsa-miR-126-3p	*VCAM1*	hsa-miR-335-3p	*MAOA*
hsa-miR-324-5p	*ASS1*	hsa-miR-185-5p	*OFD1*
hsa-miR-324-5p	*CKB*	hsa-miR-326	*PAQR4*
hsa-miR-193b-3p	*COTL1*	hsa-miR-16-2-3p	*PPARGC1A*
hsa-miR-365a-3p	*GALNT4*	hsa-miR-200a-5p	*PRC1*
hsa-miR-365b-3p	*GALNT4*	hsa-miR-363-3p	*PTPRR*
hsa-miR-324-5p	*KCNG1*	hsa-miR-376a-5p	*RPRM*
hsa-miR-30d-5p	*KIF11*	hsa-miR-508-3p	*SCGB2A2*
hsa-miR-223-3p	*LIF*	hsa-miR-582-5p	*SFRP4*
hsa-miR-200a-3p	*RASSF2*	hsa-miR-203b-3p	*SLC7A1*
hsa-miR-429	*RASSF2*	hsa-miR-335-3p	*SNX10*
hsa-miR-324-5p	*TACC3*	hsa-miR-16-2-3p	*SNX10*
hsa-miR-130b-5p	*THBS2*	hsa-miR-338-3p	*SOX17*
hsa-miR-204-5p	*SPDEF*	hsa-miR-30d-3p	*SOX17*
hsa-miR-204-5p	*STEAP4*	hsa-miR-16-2-3p	*STEAP4*
hsa-miR-204-5p	*ALPL*	hsa-miR-222-5p	*SYNE2*
hsa-miR-126-5p	*ARID5B*	hsa-miR-106a-5p	*THBS2*
hsa-miR-30d-3p	*ATP6V0E2*	hsa-miR-30d-3p	*XCL1*
hsa-miR-193b-3p	*BARD1*	hsa-miR-449a	*ANK3*
hsa-miR-106b-5p	*CYBRD1*	hsa-miR-34b-5p	*OPRK1*
hsa-miR-144-3p	*FGB*	hsa-miR-34c-5p	*POLD4*
hsa-miR-144-5p	*ID4*	hsa-miR-429	*PPARGC1A*
hsa-miR-106b-5p	*IER3*	hsa-miR-429	*RAD54B*
hsa-miR-197-3p	*LRP4*	hsa-miR-204-5p	*SLC7A1*
hsa-miR-335-3p	*SLC38A1*	hsa-miR-34c-5p	*XCL1*

hsa-miR-126-5p	*SNX10*	hsa-miR-584-5p	*BCL6*
hsa-miR-144-5p	*SOD2*	hsa-miR-873-3p	*CLDN10*
hsa-miR-106b-5p	*SOD2*	hsa-miR-130b-5p	*FGB*
		hsa-miR-130b-5p	*HAND2*
		hsa-miR-873-3p	*HPGD*
		hsa-miR-223-5p	*HPGD*
		hsa-miR-584-5p	*IL15*
		hsa-miR-584-5p	*IL2RB*
		hsa-miR-363-3p	*LRRC1*
		hsa-miR-223-5p	*PROM1*
		hsa-miR-20b-5p	*ENPEP*
		hsa-miR-205-5p	*EPHB3*
		hsa-miR-34c-5p	*GALNT4*
		hsa-miR-126-5p	*LMCD1*
		hsa-miR-126-5p	*MFAP5*
		hsa-miR-34b-3p	*OPRK1*
		hsa-miR-200c-3p	*PPARGC1A*
		hsa-miR-31-5p	*PPARGC1A*
		hsa-miR-223-5p	*PPARGC1A*
		hsa-miR-338-5p	*RAD54B*
		hsa-miR-205-5p	*SLC16A6*
		hsa-miR-106b-5p	*THBS2*

The most representative family in our analysis was the miR-200 family; It is composed of miR-200a, miR-200b, miR-200c, miR-141, and miR-429 and it has been reported to be highly expressed in epithelial tissues (192). We found 5 members of the miR-200 family which showed an opposite trend with the expression of ERA genes. Four of them, hsa-miR-200a-3p, hsa-miR-200c-3p, hsa-miR-429, and hsa-miR141-3p, showed opposite trend with *RASSF2* **(Figure 20)**. *RASSF2* has a potential role in inhibition of EMT regulating signalling processes through its interaction with Vimentin (193). Since the miRNAs targeting of *RASSF2* showed a downregulation in the first days of luteal phase and upregulation in P +5, it could represent one of the mechanisms which contribute to the preparation of the endometrium regulating the timing for embryo implantation. Members of hsa-miR-17 family were also found in our results, such as hsa-miR-20b-5p, hsa-miR-106a-5p and hsa-miR-106b-5p. All the three miRNAs showed an opposite trend with Superoxide dismutase 2 (*SOD2*). Their trends showed that they were upregulated during the first stages of the luteal phase and downregulated in receptive phase, moment in which *SOD2* is highly expressed. The lower expression of its miRNAs target is

coincident with the well-established idea that a decline of *SOD2* is involved in apoptotic process and cell death and its presence is fundamental in order to protect blastocyst from reactive oxygen species. Since, a good correlation has been observed between mRNA, proteins and enzyme activity level, suggesting that SOD is regulated at pre-translational level (194), we considered our results as an hypothetic regulatory mechanism.

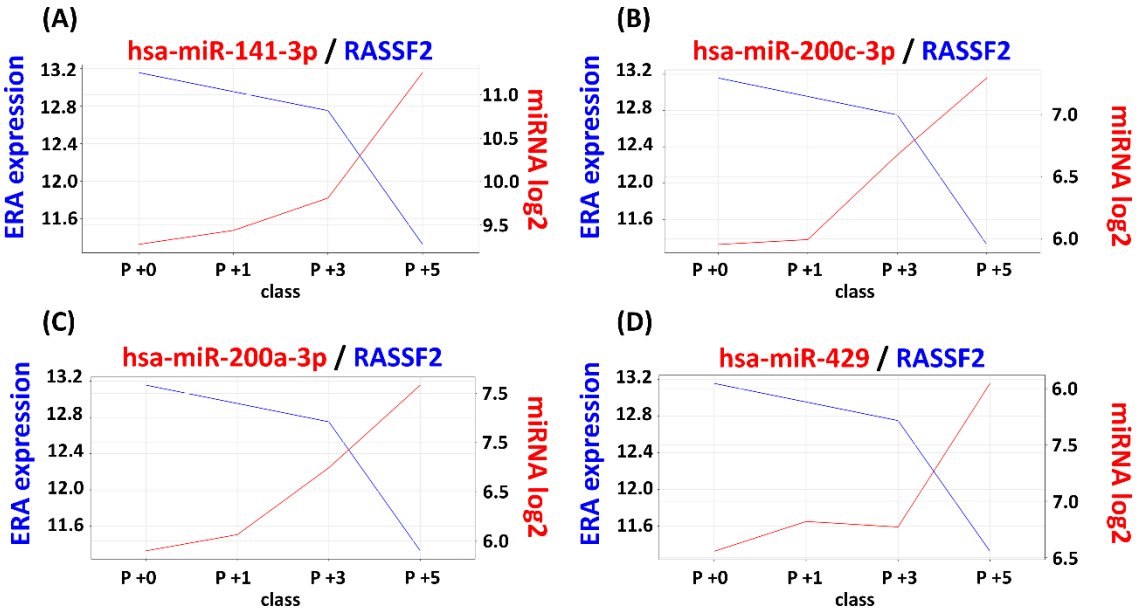

Figure 20. miR-200 family members and their target *RASSF2* trends. In the figure, miR-200 family members' trends were correlated with their ERA target, *RASSF2* (A) hsa-miR141-3p (B) hsa-miR-200c-3p (C) hsa-miR-200a-3p and (D) hsa-miR-429. The correlation miRNA/mRNA target showed opposite trend between the miRNAs and their target.

Another miRNA, identified *in vitro* and *in vivo* in a mouse animal model, during peri-implantation and the preimplantation period was hsa-miR-144 (195). In our analysis, hsa-miR-144-3p/5p showed opposite trend with 4 ERA genes, involved in pathways such as TGF-beta, FoxO and signalling pathways regulating the pluripotency of stem cells. The miRNA with the highest number of ERA genes target, 8 in total, was miR-193b-3p. It was described that it could regulate trophoblasts migration and invasion through binding onto the 3'UTR target site of TGF-β2 (196). To understand which functional pathway were involved based on our analysis, we used KEGG database for the 97 genes to carry out the pathway analysis of the integrated miRNA/mRNA network. The results showed 51 pathways, involved in endometrial receptivity **(Table 11)**. Several of them are regulated by at least two of the ERA genes target selected by the filtering method

described previously. One of those, is for example, the Cytokine-cytokine receptor interactions pathway. It is described that this receptor pathway has an important role in endometrial receptivity by modulating different physiological aspects of trophoblast invasion. This pathway was regulated by two ERA genes, *LIF* and *IL5*. *LIF*, was found to interact with hsa-miR-223-3p. The gene is present in the human endometrium at higher levels during the secretory vs. proliferative phase of the menstrual cycle and is also detected in the first-trimester decidua (197). Regarding *IL5*, it was predicted to be the target of hsa-miR-584-5p.

Other pathways in which at least 2 targets were found, were the cell adhesion molecules, FoxO signalling (198), and Leukoyte transendothelial migration, which presents an important role in the initiation of molecular interactions to capture the blastocyst or leukocyte, respectively (83). Also, pathways such as cell cycle, oocyte meiosis, longevity regulating pathway, signalling pathways regulating pluripotency of stem cells, Jack-Stat signalling pathway and GABAergic synapse. Moreover, pathways regulated by 3 genes are the most interesting. For instance, TNF signalling pathway (199).

Table 11. Kegg pathways associated with 28 ERA genes. Each pathway is showed with its KEGG identifier (134).

Kegg pathway		ERA genes
hsa00071	Fatty acid degradation	*ACADSB*
hsa00280	Valine, leucine and isoleucine degradation	*ACADSB*
hsa01100	Metabolic pathways	*ACADSB, CES1, CYP3A5, MAOA*
hsa01212	Fatty acid metabolism	*ACADSB*
hsa05205	Proteoglycans in cancer	*ANK3, IGF2*
hsa04110	Cell cycle	*CDC20, BUB1B*
hsa04114	Oocyte meiosis	*CDC20*
hsa04120	Ubiquitin mediated proteolysis	*CDC20*
hsa04514	Cell adhesion molecules (CAMs)	*CLDN10, VCAM1*
hsa04530	Tight junction	*CLDN10*
hsa04670	Leukocyte transendothelial migration	*CLDN10, VCAM1*
hsa00140	Steroid hormone biosynthesis	*CYP3A5*
hsa00830	Retinol metabolism	*CYP3A5*
hsa00980	Metabolism of xenobiotics by cytochrome P450	*CYP3A5*
hsa04068	FoxO signaling pathway	*GABARAPL1, SOD2*
hsa04140	Regulation of autophagy	*GABARAPL1*
hsa04727	GABAergic synapse	*GABARAPL1, SLC38A1*

hsa04350 TGF beta signaling pathway	*ID4*
hsa04550 Signaling pathways regulating pluripotency of stem cells	*ID4, LIF*
hsa04060 Cytokine cytokine receptor interaction	*IL15, LIF*
hsa04630 Jak STAT signaling pathway	*IL15, LIF*
hsa04668 TNF signaling pathway	*IL15, LIF, VCAM1*
hsa00260 Glycine, serine and threonine metabolism	*MAOA*
hsa00330 Arginine and proline metabolism	*MAOA*
hsa00340 Histidine metabolism	*MAOA*
hsa00350 Tyrosine metabolism	*MAOA*
hsa00360 Phenylalanine metabolism	*MAOA*
hsa00380 Tryptophan metabolism	*MAOA*
hsa04726 Serotonergic synapse	*MAOA*
hsa04728 Dopaminergic synapse	*MAOA*
hsa04152 AMPK signaling pathway	*PPARGC1A*
hsa04211 Longevity regulating pathway	*PPARGC1A, SOD2*
hsa04910 Insulin signaling pathway	*PPARGC1A*
hsa04920 Adipocytokine signaling pathway	*PPARGC1A*
hsa04922 Glucagon signaling pathway	*PPARGC1A*
hsa04931 Insulin resistance	*PPARGC1A*
hsa03440 Homologous recombination	*RAD54B*
hsa04310 Wnt signaling pathway	*SFRP4, SOX17*
hsa04724 Glutamatergic synapse	*SLC38A1*
hsa05206 MicroRNAs in cancer	*SLC7A1*
hsa04146 Peroxisome	*SOD2*
hsa03013 RNA transport	*TACC3*
hsa04145 Phagosome	*THBS2*
hsa04151 PI3K Akt signaling pathway	*THBS2*
hsa04510 Focal adhesion	*THBS2*
hsa04512 ECM receptor interaction	*THBS2*
hsa04064 NF kappa B signaling pathway	*VCAM1*
hsa04933 AGE RAGE signaling pathway in diabetic complications	*VCAM1*
hsa0496 Vasopressin regulated water reabsorption	*AQP3*
hsa04978 Mineral absorption	*CYBRD1*
hsa04360 Axon guidance	*EPHB3*

5.3.2. miRNA-mRNA interaction validation

Since we previously demonstrated the importance of hsa-miR-30d-5p during embryo implantation and its important role during the embryo-maternal communication, we moved up to validate *in vitro* the interaction with its ERA gene target, Kinesin Family Member 11 (*KIF11*).

In **Figure 21** we can appreciate the opposite trend between hsa-miR-30d-5p and *KIF11* during luteal phase.

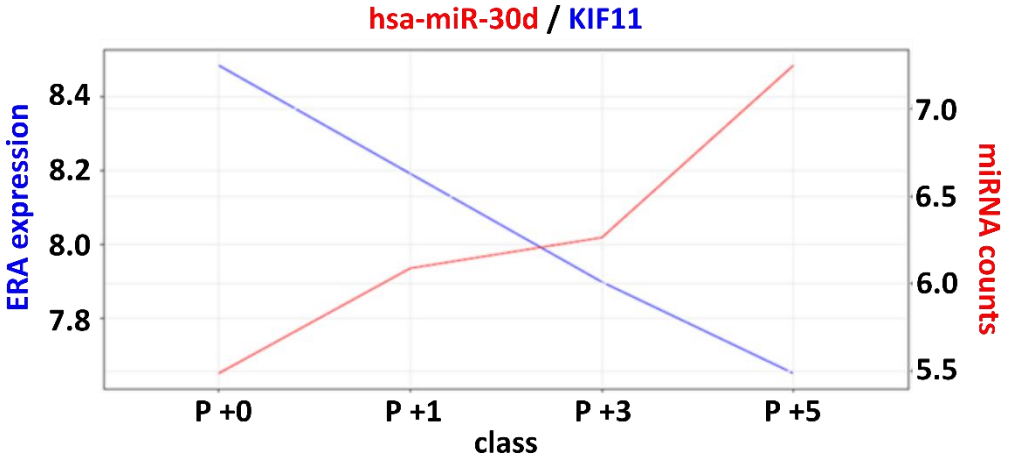

Figure 21. Expression profile of *KIF11* and has-mir-30d-5p during luteal phase

An *in vitro* experiment was performed using Ishikawa cells as model of endometrial layer. Ishikawa cells represent a well-differentiated human endometrial adenocarcinoma cell line. Mimic and inhibitor of has-miR-30d-5p were used to study *KIF11* expression in response. miRNA mimics are small, chemically modified double-stranded RNAs that mimic endogenous miRNAs. After 48h from Ishikawa cell line transfection with the hsa-miR-30d-5p mimic, total RNA was extracted to be measured by RT-qPCR. The expression level of KIF11 was compared among the different conditions. Non- transfected Ishikawa cells were used as control condition, allowing us to estimate the endogenous expression of KIF11 mRNA levels. In the condition treated with hsa-miR-30d-5p mimic, we observed a great reduction of KIF11 expression, supporting the idea of an interaction with the miRNA **(Figure 22).** In the third condition, an inhibitor of the endogenous hsa-miR-30d-5p was added to the cell culture. The inhibitor has the function to target endogenous miRNA, avoiding mRNA silencing or degradation, and therefore, our results agree with this hypothesis, since KIF11 is slightly overexpressed in this experimental condition **(Figure 22).**

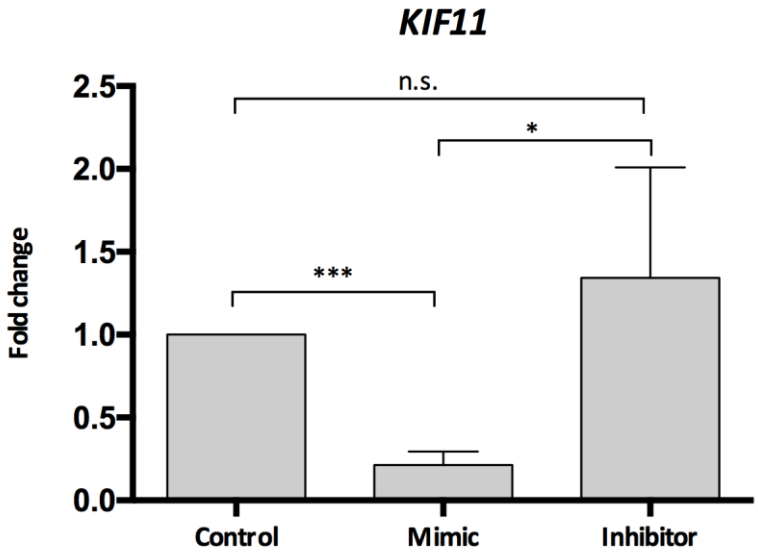

Figure 22. *KIF11* mRNA fold change after mimic and inhibitor transfection experiment. (*) P<0.05; (***) P<0.001; (n.s.) non-significant.

KIF11 belongs to the Kinesins family, a family of 45 proteins, and encodes the EG5 protein, which is essential for cell division (200). Murine Knsl1 (*Kif11*) null-embryos die prior to implantation between morula and blastocyst stage (201, 202). Angiogenesis is a key event during the embryo implantation, *KIF11* has been described as a potent inhibitor of VEGF-A, a major proangiogenic factor *in vivo*. We hypothesize that its elevated expression during the first stages of luteal phase promote the correct angiogenesis during the late stages of luteal phase. This could be considered as a regulation of the timing for the correct implantation. Also, we investigated if the protein expression was affected by this interaction, but we didn't find any variation between the control and the mimic condition. We know that protein abundance is regulated by several complex mechanisms, and that measuring the mRNA abundance, only permits to observe the first steps of a long regulatory events. A possible explanation for our results could be found in the fact that an important factor in the differences between mRNA and protein abundance is the distinct synthesis and decay rates. These, have different lifetimes, on the order of minutes for an mRNA, and hours to years for a protein (203), but the rates of synthesis or decay for mRNA and protein from a single gene are unrelated (204). It could be that particular mRNA are degraded while its protein has higher half life and remains in the cellular pool.

5.4. miRNAs signature identified in EF in COS +hCG cycles

Then, we characterized the miRNAs signature in COS cycle where final oocyte maturation was induced by hCG.

The number of miRNAs expressed per sample and the miRNA with the highest percentage of reads per sample was described. We have observed that for the majority of the samples more than 600 miRNAs were detected; only in 3 out of the total 26 samples the threshold of 300 miRNAs was not reached **(Figure 23.A).**

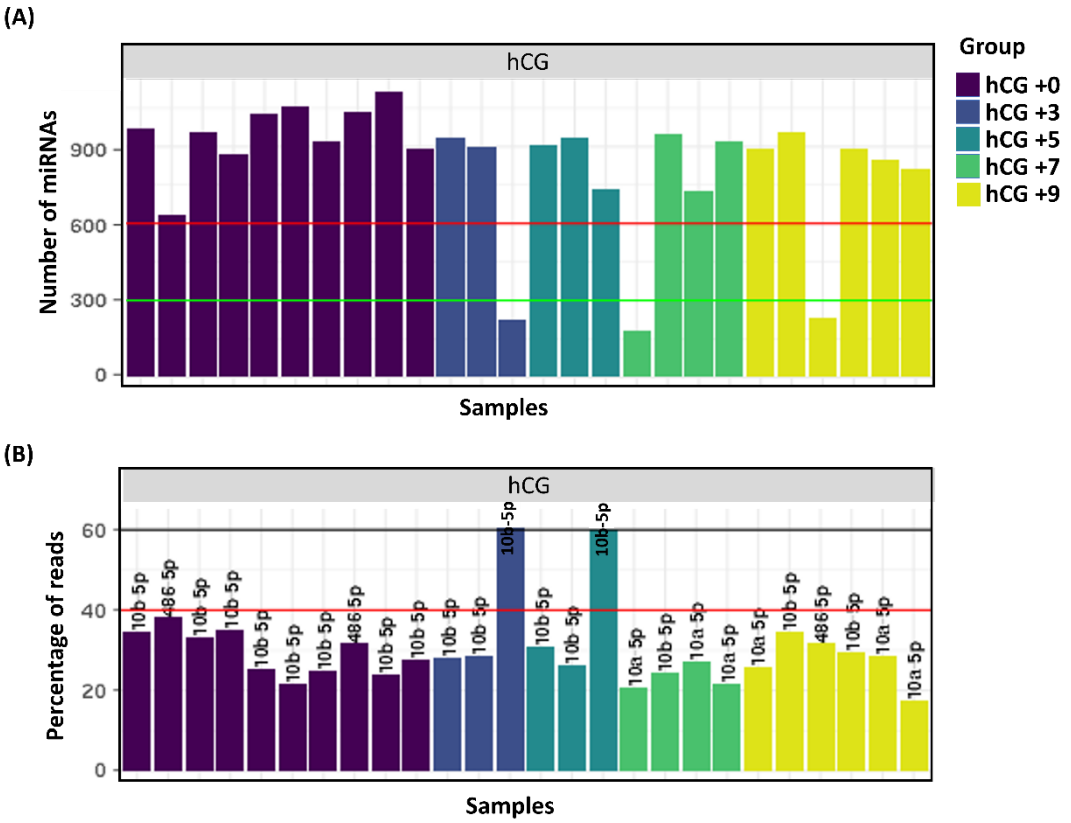

Figure 23. Pre-processing data in COS +hCG cycle. (A) The number of miRNAs expressed per samples is expressed for the 26 samples. Each bar in the graph represents a different sample of COS +hCG cycle. In purple are represented hCG +0 samples, in blue hCG +3 samples, in dark green hCG +5 samples, in light green hCG +7 samples and in yellow hCG +9. The red and the green lines mark 600 and 300 miRNAs expressed respectively. (B) The graph shows the percentage of the highest miRNA per sample. The red line represents the threshold of the 40% of aligned reads.

Also in this cycle, the most abundant miRNA in almost all the samples was hsa-miR-10b. In particular, in 2 of them (one hCG +3 sample and one hCG +5 sample) represented more than 40% of the reads **(Figure 23.B).** After normalization procedures, 18 samples remained for the subsequent analysis, in hCG +0 (n=8), in hCG +3 (n=2) in hCG +5 (n=2) in hCG +7 (n=3) and in hCG +9 (n=3).

We then compared miRNAs expression level between the different phases of the cycle. The number of differentially expressed miRNAs resulting from each comparison is showed in **table 12**.

Table 12. Differentially expressed miRNAs during the luteal phase of COS + hCG cycle (FC>2; p-value <0.05)

Comparison	N. Downregulated	N. Upregulated
hCG +0 vs. hCG +3	13	9
hCG +0 vs. hCG +5	30	15
hCG +0 vs. hCG +7	71	59
hCG +0 vs. hCG +9	68	54
hCG +3 vs. hCG +5	0	0
hCG +3 vs. hCG +7	4	3
hCG +3 vs. hCG +9	4	5
hCG +5 vs. hCG +7	0	3
hCG +5 vs. hCG +9	3	6
hCG +7 vs. hCG +9	3	1

We observed that after 3 days from the ovulation trigger, 22 miRNAs were differentially expressed from the day of the ovulation trigger. After 5 days from ovulation 45 miRNAs were differentially expressed compared with hCG +0. Seven days after the ovulation trigger, 130 miRNAs were differentially expressed compared with hCG +0 (**Figure 24.A**). These data indicate the big differences existing at miRNA level between a non-receptive and a receptive endometrium.

From our results, we have not found significant differences in miRNAs expression between hCG +3 and hCG +5, so considering their similarities, we could hypothesize the existence of a pre-receptive miRNA profile. The only miRNA, differentially upregulated in all the phases vs. hCG +7 was hsa-miR-410-3p **(Figure 24.B).** Its fold change value compared with hCG +7 is (FC: 3.24) in hCG +0, (FC: 2.21) in hCG +3 and (FC: 2.42) in hCG +5 (**Figure 24.C**). Focused on the differences between pre-receptive and receptive phase, it was more abundant in hCG +5. For this miRNA, predicted target genes involved in functional processes such as hypoxia, apoptosis and cytoskeleton reorganization have been described (205). The process of apoptosis is fundamental to allow the embryo to invade the endometrium. It was described that from day 19-20 of the luteal phase, there

is an increase of the number of apoptotic cells in glandular epithelium of the basalis and later in the functionalis layers of the endometrium (206).

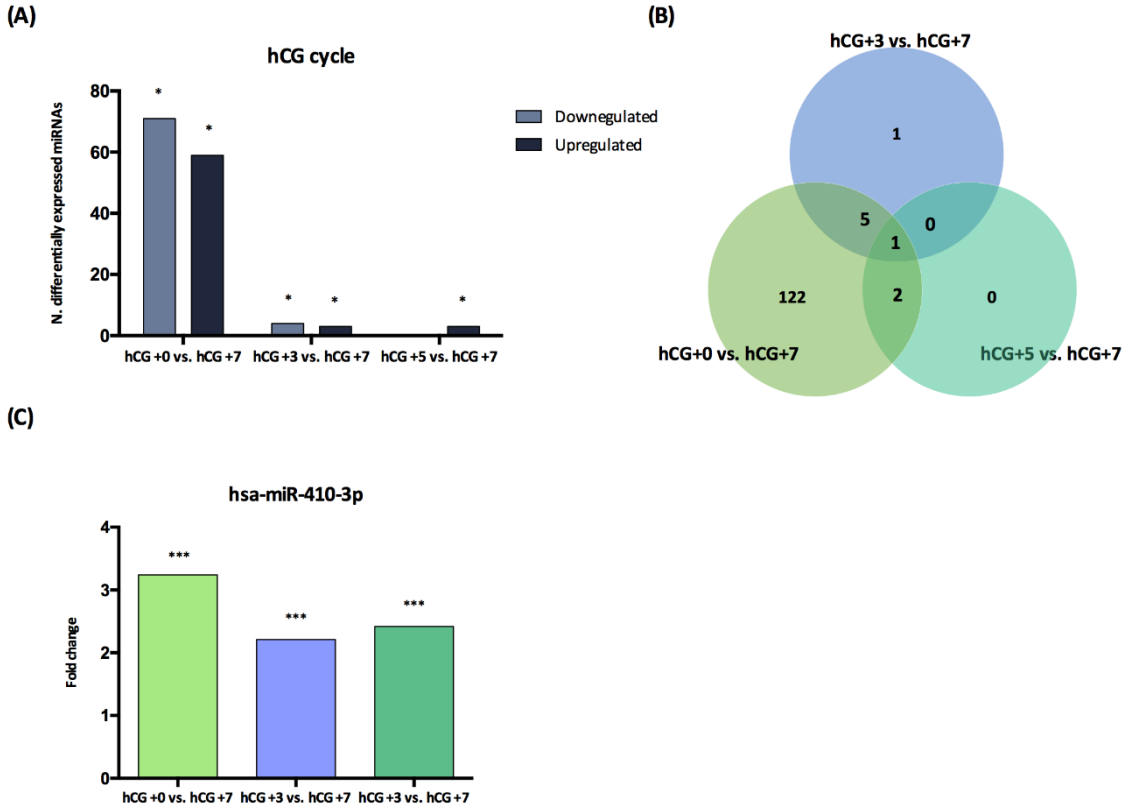

Figure 24. miRNAs behaviour in COS +hCG cycle. (A) Graph representing the number of miRNAs differentially expressed between pre-receptive and receptive phases. (B) Venn diagram represents common miRNAs pattern along hCG cycle. (C) Fold change representation of hsa-miR-410-3p. (*) P<0.05; (***) P<0.001.

We were indeed able to identify 4 miRNAs that were differentially expressed between hCG +7 and hCG +9. This could allow us to distinguish the receptive phase from the post-receptive phases. In order to investigate the potential biomarkers of the receptive status in hCG cycle, miRNAs differentially expressed between hCG +5 and hCG +7, hsa-miR-410-3p, hsa-miR-431-3p and hsa-miR-127-5p, showed in **Table 13** were all selected for the next validation experiment. Based on their expression, samples belonging to pre-receptive phase cluster together, as well as for the receptive samples (**Figure 25**).

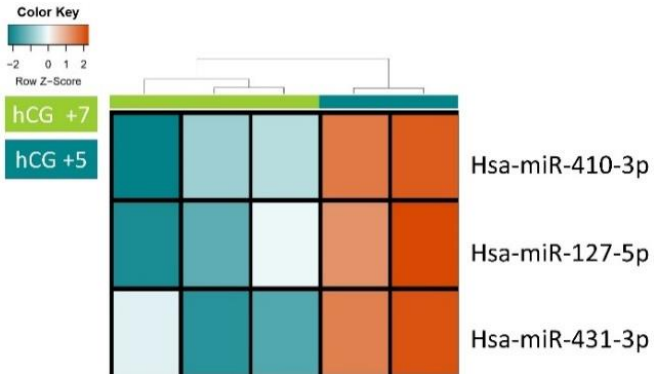

Figure 25. Potential biomarker in COS +hCG cycle. Heat map diagram and hierarchical clustering based on summarized intensity values of differentially expressed miRNA. Groups are differentiated by colours: hCG +7 in light green and hCG +5 in dark green. The colour scale shows the log2-fold change of each miRNA across all samples; blue coloured squares show low expression; red colour represents high level of miRNA expression and white squares indicate moderate expression.

Along with hsa-miR-410-5p, the role of these miRNAs in endometrial receptivity was previously described. In a study performed on goat, it was proposed that hsa-miR-431-3p could participate in the regulation of endometrial receptivity through the nervous system by silencing Kremen1, an antagonist of Wnt/beta-catenin signalling (207). In agreement with our results, another study, has been also seen that, hsa-miR-127-5p was differentially expressed during peri-implantation and in day 4, day 5, and day 6 pregnant uteri in mice (208).

Table 13. Potential biomarkers from COS + hCG cycle

hCG +5 vs. hCG +7				
	edgeR		DeSeq2	
miRNA	***FDR***	***FC***	***padj***	***FC***
hsa-miR-410-3p	0.002	2.51	0.0015	2.42
hsa-miR-431-3p	0.002	4.21	0.0027	4.42
hsa-miR-127-5p	0.038	2.46	0.035	2.42

Sequencing results validation by RT-qPCR

The expression of hsa-miR-410-3p, hsa-miR-431-3p, and hsa-miR-127-5p was validated in one sample of hCG +5 and one sample from hCG +7. The results of RT-qPCR confirmed the upregulation of all the 3 miRNAs in hCG +5 vs. hCG +7 **(Figure 26).**

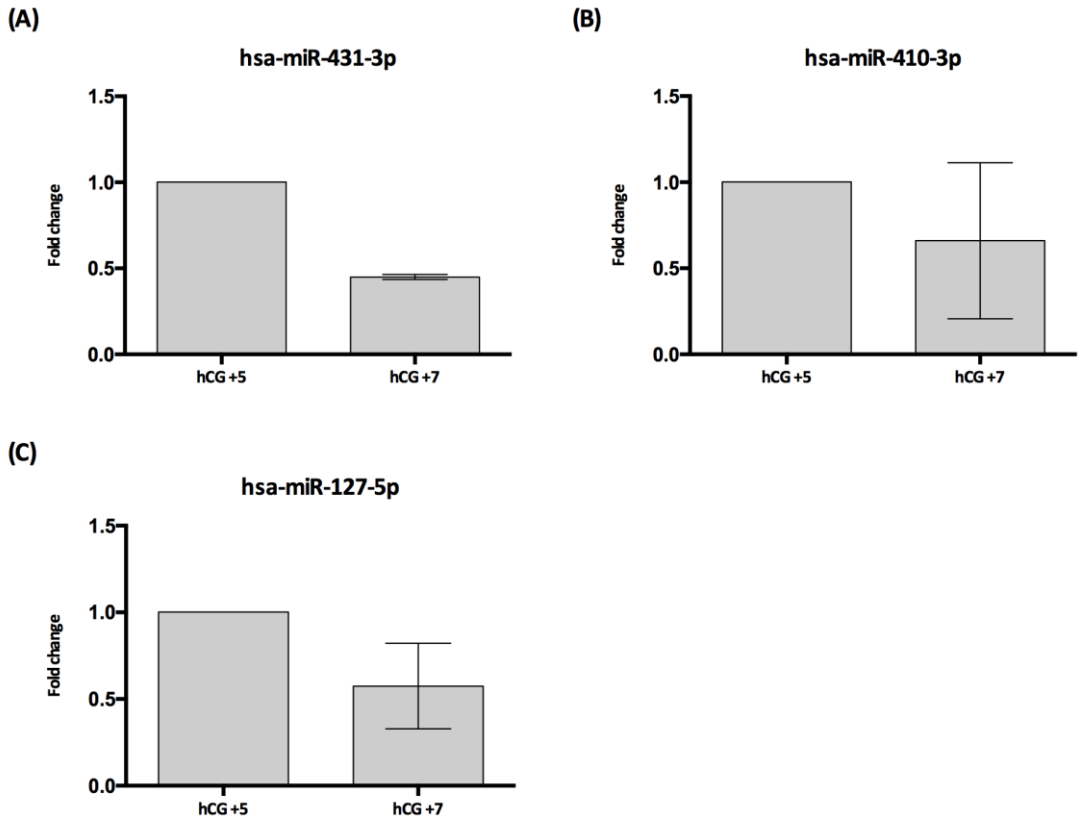

Figure 26. RT-qPCR validation of potential biomarker in COS +hCG samples. miRNAs (A) hsa-miR-431-3p, (B) hsa-miR-410-3p and (C) hsa-miR-127-5p were chosen to be validated using RT-qPCR in a hCG +5 and a hCG +7 samples. Fold change were calculated using $2^{-\Delta\Delta Ct}$ formula. Differences between groups were non-significant (p>0.05).

5.5. miRNAs signature identified in EF in COS +GnRH-a cycles

The effects of the GnRH-a trigger on the luteal phase leads to defects in the luteal phase resulting in a decrease of the implantation and clinical pregnancy rates and also an increase of abortion in fresh embryo transfer cycles compared to routine IVF cycle with hCG triggering (209, 210). Exploratory analysis of raw data for COS +GnRH-a cycle, allowed us to maximize insight into miRNAs secreted in EF in COS cycle in which ovulation has been triggered using GnRH-a. The number of the expressed miRNAs per samples demonstrated that almost all the samples overcome the threshold of 600 miRNAs, 1 sample expressed between 300 and 600 miRNAs and 1 sample did not reach the 300 miRNAs **(Figure 27.A)**. The analysis of the percentage of the reads confirmed in this cycle hsa-miR-10b-5p as the most abundant miRNA in most of the samples **(Figure 27.B)**.

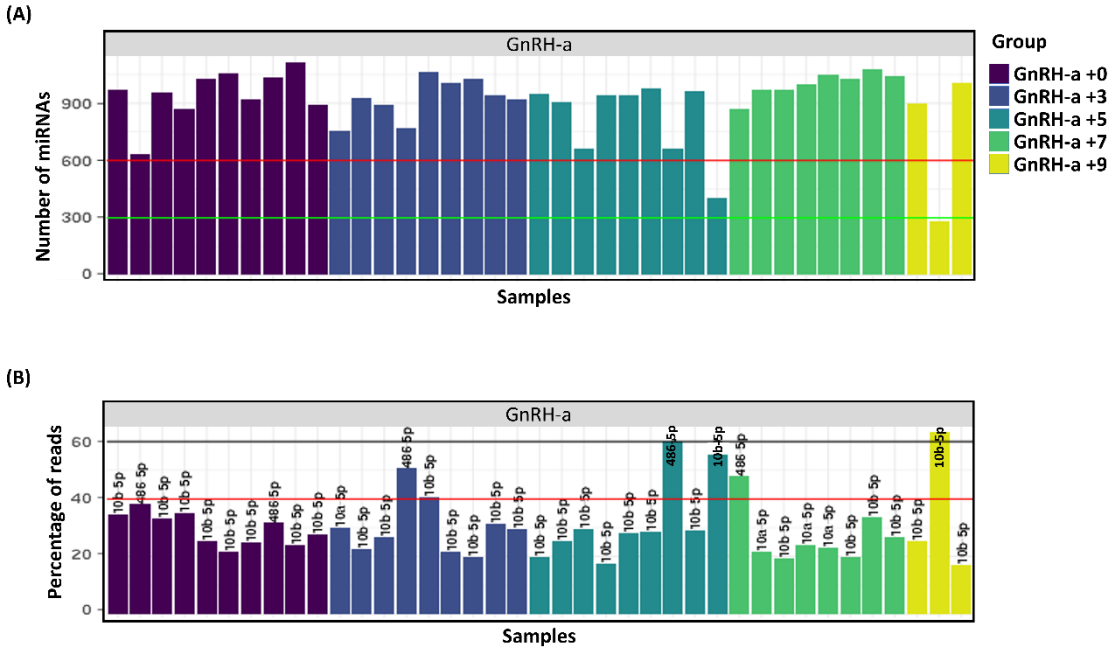

Figure 27. Pre-processing data in COS +GnRH-a cycle. (A) the number of miRNAs expressed per samples is expressed for the 39 samples. Each bar in the graph represents a different sample of COS +GnRH-a cycle. In purple are represented GnRH-a +0 samples, in blue GnRH-a +3 samples, in dark green GnRH-a +5 samples, in light green GnRH-a +7 samples and in yellow GnRH-a +9. The red and the green lines mark 600 and 300 miRNAs expressed respectively. (B) the graph shows the percentage of the highest miRNA per sample. The red line represents the threshold of the 40% of aligned reads.

Normalization procedures following the first descriptive analysis, showed a final population of 28 samples. The number of samples in each phase was: GnRH-a +0 (n=8), GnRH-a +3 (n=2), GnRH-a +5 (n=2), GnRH-a +7 (n=3) and finally in GnRH-a +9 (n=3)

A total of 322 miRNAs were found differentially expressed during COS +GnRH-a cycle **(Table 14).**

Table 14. Number of differentially expressed miRNAs between GnRH-a phases comparisons (FC>2; p-value <0.05)

Comparison	N. downregulated	N. upregulated
GnRH-a +0 vs. GnRH-a +3	13	13
GnRH-a +0 vs. GnRH-a +5	38	26
GnRH-a +0 vs. GnRH-a +7	54	34
GnRH-a +0 vs. GnRH-a +9	21	18
GnRH-a +3 vs. GnRH-a +5	1	0
GnRH-a +3 vs. GnRH-a +7	28	11
GnRH-a +3 vs. GnRH-a +9	15	5
GnRH-a +5 vs. GnRH-a +7	1	2
GnRH-a +5 vs. GnRH-a +9	19	9
GnRH-a +7 vs. GnRH-a +9	12	2

Compared with the receptive phase, GnRH-a +0 presents 88 differentially expressed miRNAs, GnRH-a +3 shows 39 differentially expressed miRNAs and GnRH-a +5 shows 3 miRNAs differentially expressed (**Figure 28.A**). Two miRNAs were differentially expressed in common between the three comparisons (**Figure 28.B**). Regarding hsa-miR-7974, it reached its maximum FC value in GnRH-a +3 vs. GnRH-a +7. It decreases just a little in GnRH-a +5 vs. GnRH-a +7 but still showing very high value. Concerning hsa-miR-224-5p, its expression was constant at a 3 FC in all the phases compared with GnRH-a +7.

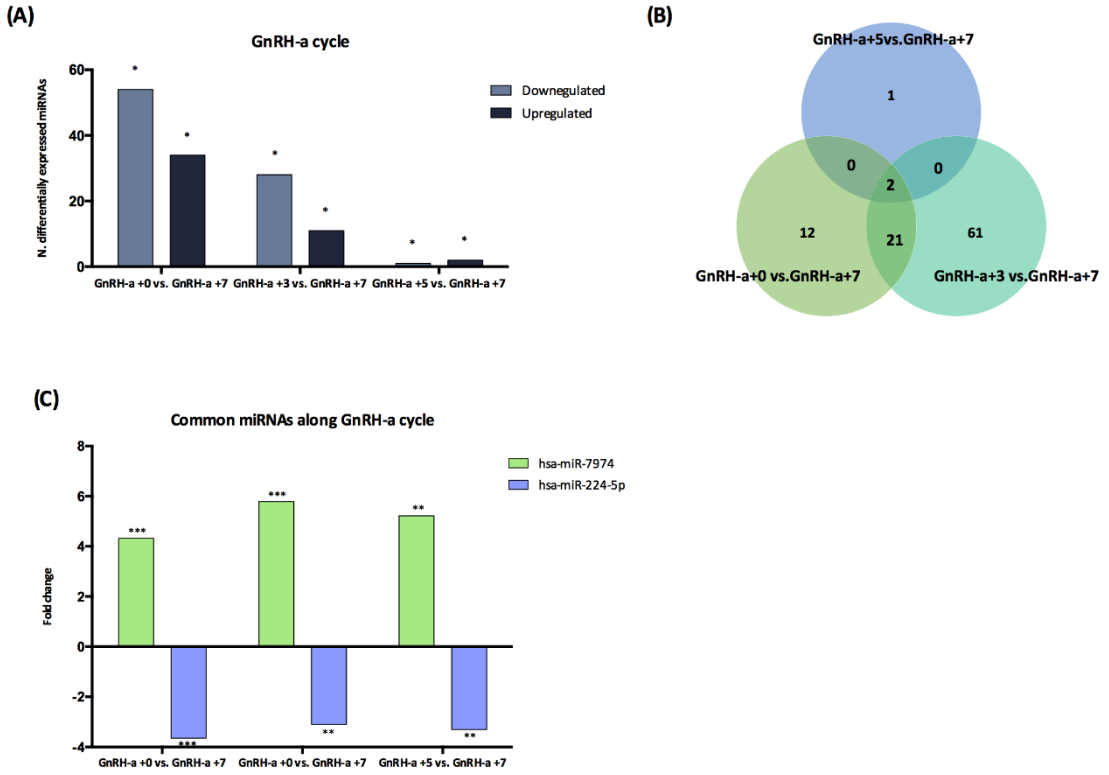

Figure 28. miRNAs behaviour in COS +GnRH-a cycle. (A) Graph represents differential miRNAs expression in pre-receptive compared to receptive phase. (B) Venn diagrams illustrate miRNAs in common among the three comparisons showed in A. (C) Graph represents the fold change of the two common miRNAs, in all the three comparisons considered. (*) P<0.05; (**) P<0.01; (***) P<0.001.

From our results, we observed that between the day GnRH-a +0 and GnRH-a +3, 22 differentially expressed miRNAs were found. This suggests that endometrium starts to secrete miRNAs in EF that might impact the mechanisms leading to endometrial receptivity. One miRNA was found differentially expressed between GnRH-a +3 and GnRH-a +5 and this was hsa-miR-223-3p. As we have previously seen in COS cycle with

hCG, we could say that, since their high similarity, GnRH-a +3 and GnRH-a +5 offer a unique miRNAs signature of the pre-receptive phase in this type of cycle.

Regarding the comparison between GnRH-a +5 and GnRH-a +7, we found 3 differentially expressed miRNAs (hsa-miR-181a-3p, hsa-miR-224-5p and hsa-miR-7974). hsa-miR-181a-3p and hsa-miR-7974 were upregulated in the pre-receptive phase vs. the receptive, and hsa-miR-224-5p is downregulated in the pre-receptive phase vs. the receptive phase.

About the predicted target of hsa-miR-181a-3p, is transforming growth factor beta (TGF-β) (211). Moreover, using miRpath tool we found that hsa-miR-224-5p is involved in the regulation of Prolactin signalling pathway. There, we found 3 predicted targets, such as MAPK8, which is also involved in TGF-β pathway, Integrin signalling, p53 signalling NF-kB signalling, among others (212). To understand the importance of miRNAs in endometrial receptivity preparation, we focused our attention in those miRNAs differential expressed between GnRH-a +5 and GnRH-a +7 (**Figure 29**). More information about the p-value and the fold change of these miRNAs proceeding from this comparison is showed in **Table 15**. Depending on the expression of the differentially expressed miRNA, the samples clustered only partially with the same of their biological group.

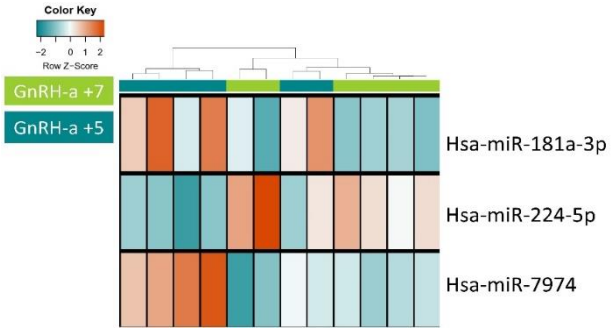

Figure 29. Potential biomarkers miRNAs in COS +GnRH-a cycle. Heat map diagram and hierarchical clustering based on summarized intensity values of differentially expressed miRNA ($p<0.05$) between GnRH-a +5 samples represented in light green and GnRH-a +7 represented in dark green. The colour scale shows the log2-fold change of each miRNA across all samples; blue coloured squares show low expression; red colour represents high level of miRNA expression and white squares indicate moderate expression.

Table 15. Differentially expressed miRNAs in pre-receptive vs. receptive phases of GnRH-a cycle

GnRH-a +5 vs. GnRH-a +7				
	EdgeR		deSeq2	
miRNA	***FDR***	***FC***	***padj***	***FC***
hsa-miR-181a-3p	0.00091	2	4.11E-05	2.03
hsa-miR-7974	0.0054	4.63	0.002894	5.21
hsa-miR-224-5p	0.013	-3.36	0.017199	-3.29

Sequencing results validation

In order to validate sequencing results, hsa-miR-181a-3p and hsa-miR-224-5p were chosen. Validation was performed in 3 GnRH-a samples: GnRH-a +5 (n=2) and GnRH-a +7 (n=1). RT-qPCR confirmed the same fold change direction as the sequencing results for both miRNAs. We validated the upregulation of hsa-miR-181a-3p in pre-receptive phase (GnRH-a +5) vs. receptive phase (GnRH-a +7), showing in a GnRH-a +5 sample a difference of 9 FC value (**Figure 30.A)**. Also, the downregulation of hsa-miR-224-5p was validated in GnRH-a +5 samples vs. GnRH-a +7 sample **(Figure 30.B)**.

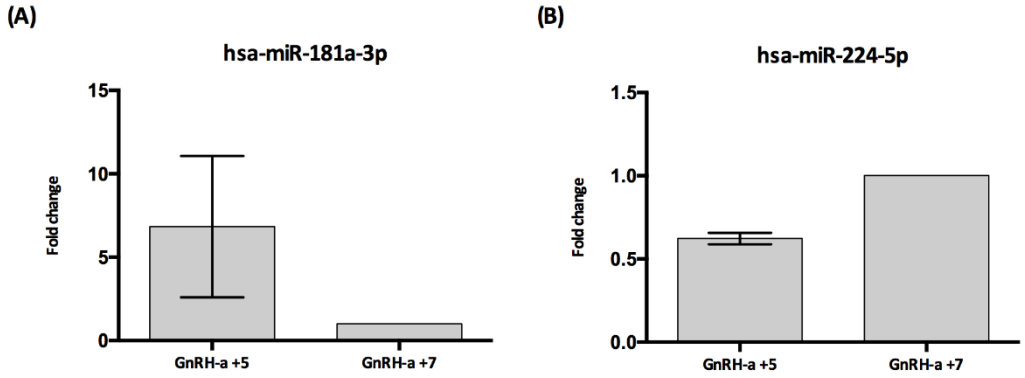

Figure 30. RT-qPCR validation of potential biomarkers in COS +GnRH-a samples. 2 miRNAs (A) hsa-miR-181a-3p and (B) hsa-miR-224-5p were chosen to be validated using RT-qPCR in 2 GnRH-a +5 samples and one sample of GnRH-a +7. Fold change were calculated using $2^{-\Delta\Delta Ct}$ formula. Differences between groups were non-significant (p>0.05).

5.6. Comparison of COS +hCG vs. COS +GnRH-a cycles.

The effects of GnRH-a triggering on the luteal phase is controversial. Some studies demonstrate that GnRH-a trigger leads to defects in the luteal phase resulting in a decrease of the implantation and clinical pregnancy rates and also increase abortion in fresh embryo transfer cycles compared to routine IVF cycle with hCG triggering (209).

Comparisons between corresponding phases of both types of cycles showed significant differences in miRNAs expression (**Figure 31)**.

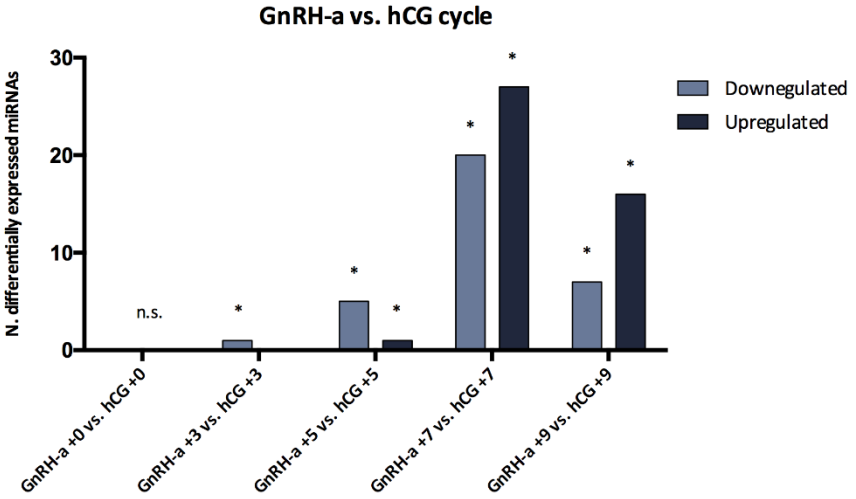

Figure 31. Number of miRNAs with a statistically significant differential expression between corresponding phases of the two COS cycles depending on triggering method. (*) P < 0.05; (n.s.) non-significant.

Interestingly, we found only 1 miRNA differential expressed between hCG +3 vs. GnRH-a +3 (hsa-miR-152-5p), 6 miRNAs between hCG +5 vs. GnRH-a +5 (hsa-miR-152-5p, hsa-miR-146b-5p, hsa-miR-184, hsa-miR-30d-5p, and hsa-miR-425-3p downregulated and hsa-miR-1260b upregulated) and 47 miRNAs differentially expressed in hCG +7 vs. GnRH-a +7 (Table 16).

Table 16. Differentially expressed miRNAs between receptive phases of the two COS cycles

GnRH-a +7 vs. hCG +7				
	DeSeq2		edgeR	
miRNAs	**padj**	**FC**	**FDR**	**FC**
hsa-miR-152-5p	1.56707E-05	-8.658	3.18485E-06	-7.881
hsa-miR-193a-5p	3.1057E-05	-6.916	2.40E-06	-6.183
hsa-miR-146b-5p	0.009	-4.298	0.0077	-4.183
hsa-miR-184	0.015	-4.029	0.0086	-3.876
hsa-miR-146a-5p	0.011	-3.826	0.0089	-3.683
hsa-miR-4446-3p	0.035	-3.640	0.020	-3.581
hsa-miR-204-5p	0.020	-3.357	0.010	-3.425
hsa-miR-375	0.024	-3.429	0.021	-3.299
hsa-miR-92b-5p	0.048	-3.370	0.034	-3.154
hsa-miR-365b-5p	0.022	-3.051	0.014	-2.978
hsa-miR-182-5p	1.56707E-05	-2.802	1.33669E-05	-2.758

hsa-miR-1266-5p	0.010	-2.747	0.0089	-2.681
hsa-miR-874-5p	0.025	-2.754	0.026	-2.599
hsa-miR-1180-3p	0.024	-2.502	0.026	-2.420
hsa-miR-30d-5p	0.0015	-2.388	0.0021	-2.384
hsa-let-7b-5p	0.00049	-2.383	0.0007	-2.331
hsa-miR-183-5p	0.22	-2.139	0.0021	-2.259
hsa-miR-345-5p	0.0057	-2.314	0.0073	-2.251
hsa-miR-425-3p	0.024	-2.332	0.027	-2.247
hsa-miR-135b-5p	0.048	-2.049	0.041	-2.009
hsa-miR-143-5p	0.048	2.077	0.049	2.046
hsa-miR-127-5p	0.0037	2.115	0.0072	2.112
hsa-miR-493-5p	0.0057	2.095	0.0089	2.126
hsa-miR-431-3p	0.024	2.439	0.026	2.300
hsa-miR-548k	0.024	2.354	0.02604	2.369
hsa-miR-299-3p	0.014	2.434	0.014	2.403
hsa-miR-101-3p	0.014	2.330	0.01	2.408
hsa-miR-19b-3p	0.043	2.390	0.034	2.445
hsa-miR-222-5p	0.035	2.495	0.049	2.471
hsa-miR-548o-3p	0.003	2.580	0.005	2.504
hsa-miR-136-3p	0.003	2.579	0.005	2.582
hsa-miR-136-5p	0.035	2.751	0.039	2.630
hsa-miR-149-5p	0.024	2.647	0.029	2.646
hsa-miR-590-3p	0.048	3.457	0.039	2.718
hsa-miR-376c-3p	0.004	2.791	0.006	2.726
hsa-miR-126-3p	0.0043	2.639	0.006	2.743
hsa-miR-101-5p	0.029	3.002	0.025	2.834
hsa-miR-548e-3p	0.011	3.041	0.011	2.912
hsa-miR-199b-5p	0.009	2.924	0.014	2.936
hsa-miR-589-3p	0.030	3.451	0.035	3.034
hsa-miR-494-3p	0.025	3.274	0.035	3.053
hsa-miR-450a-5p	0.00974	3.092	0.013	3.098
hsa-miR-450b-5p	0.014	3.137	0.021	3.140
hsa-miR-337-3p	0.022	4.856	0.029	4.346
hsa-miR-19a-3p	0.0024	4.580	0.005	4.617
hsa-miR-376a-5p	0.0032	17.671	0.002	8.807
hsa-miR-4772-5p	0.0022	39.143	0.002	18.361

In order to understand the role of the differentially expressed miRNAs between GnRH-a +7 vs hCG +7, we performed a functional analysis based on the differentially expressed miRNAs. Firstly, we selected the miRNAs having a fold change value greater or less than 4. The detection of differentially expressed miRNAs was based on those miRNAs with a minimum of 2 FC. For this reason, in order to filter the miRNAs we fixed the cut off to 4 FC. Then, we used Mir path Diana tool based on Kegg annotations in order to find which

functional pathways could be altered between these two cycles. After that, based on a bibliographic review, we filtered those pathways involved in endometrial receptivity. Thereby, we found that among the several pathways (34 in total) regulated by the selected downregulated miRNAs (hsa-miR-152-5p, hsa-miR-193a-5p, and hsa-miR-146b-5p) all of them are involved in regulation of the ErbB signalling pathway (hsa04012) as shown in **Table 17.** Besides, hsa-miR-152-5p and hsa-miR-146b-5p are involved in the regulation of the actin cytoskeleton (hsa04810). hsa-miR-152-5p is involved in the regulation of 15 pathways with an important function in the establishment of the endometrial receptiveness. For instance, focal adhesion pathway was controlled by a miRNA downregulated in the receptive phase of GnRH-a +7 vs. hCG +7. This could be a possible hypothesis for the better prognosis of hCG in implantation. Same hypothesis could be done in other cases such as the regulation of the Notch signalling family pathway by hsa-miR-146b-5p. These pathways regulate proliferation, apoptosis, differentiation, invasion and adhesion.

Table 17. Kegg pathway regulated by downregulated miRNAs in GnRH-a +7 vs. hCG +7. Each pathway is showed with its KID.

Pathway	p-value	miRNA
Circadian rhythm (hsa04710)	0.005	hsa-miR-152
Dorso-ventral axis formation (hsa04320)	0.01	hsa-miR-152
Endometrial cancer (hsa05213)	0.003	hsa-miR-152
ErbB signaling pathway (hsa04012)	0.0002	hsa-miR-152, hsa-miR-193a-5p,hsa-miR-146b-5p
Focal adhesion (hsa04510)	0.0009	hsa-miR-152
Neurotrophin signaling pathway (hsa04722)	0.03	hsa-miR-146b-5p
Notch signaling pathway (hsa04330)	0.03	hsa-miR-146b-5p
p53 signaling pathway (hsa04115)	0.005	hsa-miR-152
Pathways in cancer (hsa05200)	0.001	hsa-miR-152
PI3K-Akt signaling pathway (hsa04151)	0.005	hsa-miR-152
Regulation of actin cytoskeleton (hsa04810)	0.001	hsa-miR-152, hsa-miR-146b-5p
RNA degradation (hsa03018)	0.03	hsa-miR-152
TGF-beta signaling pathway (hsa04350)	0.001	hsa-miR-152
Ubiquitin mediated proteolysis (hsa04120)	0.01	hsa-miR-152
Wnt signaling pathway (hsa04310)	0.02	hsa-miR-152

Otherwise, regarding to the selected upregulated miRNAs (hsa-miR-337-3p, hsa-miR-19a-3p, hsa-miR-376a-5p and hsa-miR-4772-5p), we were able to identify 22 functional pathways showed in **Table 18**. Among that, 7 pathways are regulated by two of the selected miRNAs. We also found that hsa-miR19-a3p is upregulated in GnRH-a +7 vs. hCG +7. It regulates Hedgehog signalling, which is detrimental in the dialogue between the blastocyst and uterus. The higher expression of this miRNA in comparison with hCG could affect the establishment of correct communication between endometrium and blastocyst.

Table 18. Kegg pathway regulated by upregulated miRNAs in GnRH-a +7 vs. hCG +7. Each pathway is showed with its KID.

Pathway	p-value	miRNA
mTOR signaling pathway (hsa04150)	5.99E-11	hsa-miR-19a-3p, hsa-miR-337-3p
D-Glutamine and D-glutamate metabolism (hsa00471)	8.80E-06	hsa-miR-4772-5p, hsa-miR-376a-5p
Progesterone-mediated oocyte maturation (hsa04914)	2.34E-05	hsa-miR-19a-3p, hsa-miR-337-3p
Biosynthesis of unsaturated fatty acids (hsa01040)	6.28E-05	hsa-miR-376a-5p
Glutamatergic synapse (hsa04724)	0.0001	hsa-miR-19a-3p
Long-term potentiation (hsa04720)	0.0002	hsa-miR-19a-3p
ErbB signaling pathway (hsa04012)	0.0002	hsa-miR-337-3p
Gap junction (hsa04540)	0.0004	hsa-miR-19a-3p
p53 signaling pathway (hsa04115)	0.0007	hsa-miR-19a-3p, hsa-miR-4772-5p
GnRH signaling pathway (hsa04912)	0.001	hsa-miR-19a-3p
Insulin signaling pathway (hsa04910)	0.001	hsa-miR-19a-3p, hsa-miR-337-3p
Aldosterone-regulated sodium reabsorption (hsa04960)	0.003	hsa-miR-19a-3p, hsa-miR-337-3p
Arginine and proline metabolism (hsa00330)	0.004	hsa-miR-4772-5p, hsa-miR-376a-5p
Endometrial cancer (hsa05213)	0.008	hsa-miR-19a-3p, hsa-miR-337-3p
MAPK signaling pathway (hsa04010)	0.01	hsa-miR-376a-5p
ABC transporters (hsa02010)	0.01	hsa-miR-19a-3p, hsa-miR-4772-5p
PI3K-Akt signaling pathway (hsa04151)	0.01	hsa-miR-337-3p
Phosphatidylinositol signaling system (hsa04070)	0.02	hsa-miR-19a-3p
Pathways in cancer (hsa05200)	0.02	hsa-miR-337-3p
Cholinergic synapse (hsa04725)	0.02	hsa-miR-19a-3p

Transcriptional misregulation in cancer (hsa05202)	0.04	hsa-miR-337-3p
Focal adhesion (hsa04510)	0.04	hsa-miR-19a-3p

Sequencing results validation

Based on the miRNA abundance (normalized read frequency/total number of miRNA reads) we carried out the validation for those miRNAs showing the highest fold change values between the two phases. In order to avoid false positives generated from sequencing. The expression of hsa-4772-5p, hsa-miR-450b-5p, hsa-miR-193a-5p, hsa-miR-146b-5p and hsa-miR-184 was validated in 2 samples.

We found that the 5 miRNAs agreed with the sequencing results **(Figure 32).**

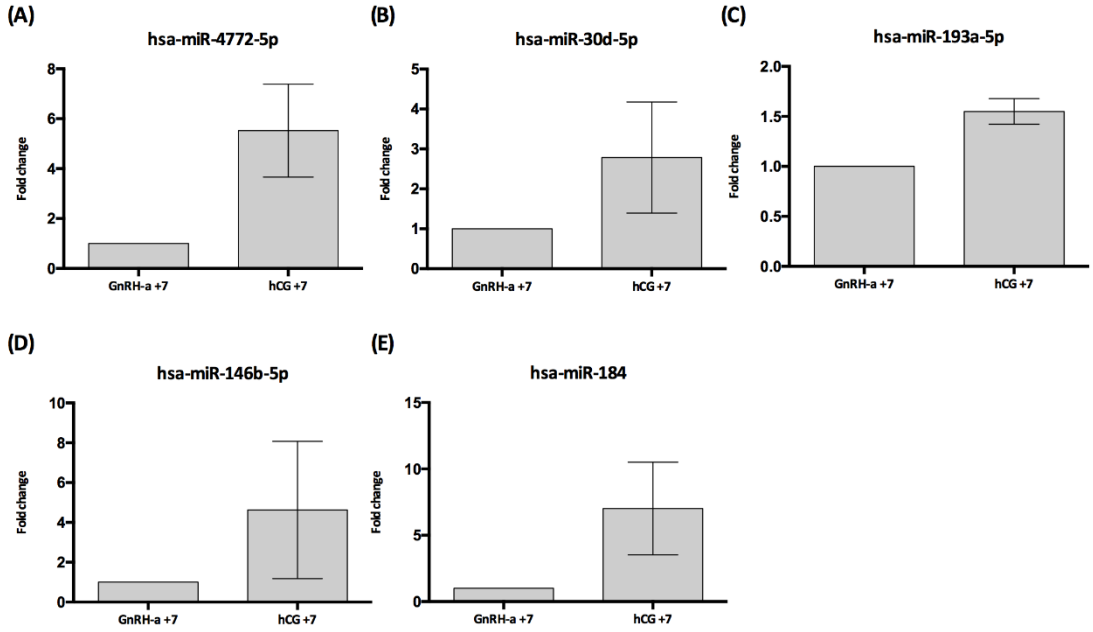

Figure 32. RT-qPCR validation in hGC+7 vs. GnRH-a +7 samples. Bar graph represents the resulting fold change obtained by RT-qPCR comparing GNRH-a +5 with GnRH-a +7 samples for the 5 miRNAs chosen for their validation: (A) hsa-miR-4772-5p, (B) hsa-miR-193a-5p, (C) hsa-miR-30d-5p, (D) hsa-miR-184, and (E) hsa-miR-146b-5p. Differences between groups were non-significant (p>0.05).

Due to the correlation between uterine function and its secretory profile, EF is considered a helpful source of biomarkers. The glandular epithelium secretes substances into the EF, whose molecular content varies during the menstrual cycle. Thanks to the analysis of the differential secretion of those molecules, we can estimate the endometrial state (93). The importance of uterine fluid lies in the fact that it represents the medium where early embryonic development takes place. No less important is the fact that the aspiration of EF method does not affect pregnancy rate in the same cycle (99). During the last decades several molecules have been studied in EF, proteins (213, 214), lipids such PGE2 and PGF2α (215), and miRNA component (216, 217). Nowadays, a personalized diagnosis of endometrial receptivity is allowed by the ERA test using an endometrial biopsy. This study offers the basis to understand how the endometrium prepare itself for embryo implantation. At the same time, the timing of global miRNAs expression patterns could be considered for the construction of a non-invasive test which could predict the receptive status of endometrium in endometrial fluid.

6. Conclusions

6. Conclusions

1. Endometrial fluid aspiration represents a minimally invasive procedure for the study of miRNAs during the luteal phase of the menstrual cycle and for the development of diagnostic tools to assess endometrial function.

2. Considering differentially expressed miRNAs obtained along luteal phase within natural cycles, controlled ovarian stimulation cycles and hormonal replacement therapy, we confirm that hormonal treatments influence the secretion of the miRNAs in the endometrial fluid.

3. In each type of cycle, we were able to find potential biomarkers of endometrial receptivity. In natural cycles, in LH +3 vs. LH +7 (hsa-miR-30d-5p, hsa-miR-345-5p, hsa-miR-873-3p, and hsa-miR-141-3p). In HRT cycles, in P +3 vs. P +5 (hsa-miR-223-3p y hsa-miR-582-5p). In COS/hCG cycles in hCG +5 vs. hCG +7 (hsa-miR-410-3p, hsa-miR-431-3p and hsa-miR-127-5p), and finally in COS/GnRH-a +5 vs. GnRH-a +7 (hsa-miR-181a-3p y hsa-miR-224-5p).

4. No significant differences in miRNAs expression were found between natural and HRT cycle. This finding supports the similar endometrial status in both type of cycles.

5. We identified 62 validated and 81 predicted interactions of miRNAs differentially expressed in the HRT cycle with the ERA genes.

6. Based on miRNAs expression profile we can conclude that the endometrium reaches the receptivity differently in natural/HRT cycles and stimulated cycles.

7. In the comparison between the receptive phases of both types of COS cycles, the differences found in miRNAs expression suggest a further research on the topic to understand the deleterious effect of GnRH-a on the endometrium. This is supported by the evidence that miRNAs such as hsa-miR-30d, considered fundamental in WOI were less secreted in COS +GnRH–a.

7. References

7. References

1. Zegers-Hochschild F, Adamson GD, de Mouzon J, Ishihara O, Mansour R, Nygren K, et al. International Committee for Monitoring Assisted Reproductive Technology (ICMART) and the World Health Organization (WHO) revised glossary of ART terminology, 2009. Fertil Steril. 2009;92(5):1520-4.

2. Macaluso M, Wright-Schnapp TJ, Chandra A, Johnson R, Satterwhite CL, Pulver A, et al. A public health focus on infertility prevention, detection, and management. Fertil Steril. 2010;93(1):16 e1-0.

3. Practice Committee of American Society for Reproductive M. Definitions of infertility and recurrent pregnancy loss: a committee opinion. Fertil Steril. 2013;99(1):63.

4. Mascarenhas MN, Flaxman SR, Boerma T, Vanderpoel S, Stevens GA. National, regional, and global trends in infertility prevalence since 1990: a systematic analysis of 277 health surveys. PLoS Med. 2012;9(12):e1001356.

5. Mosher WD, Pratt WF. Fecundity and infertility in the United States: incidence and trends. Fertil Steril. 1991;56(2):192-3.

6. Azziz R, Carmina E, Chen Z, Dunaif A, Laven JS, Legro RS, et al. Polycystic ovary syndrome. Nat Rev Dis Primers. 2016;2:16057.

7. Dag ZO, Dilbaz B. Impact of obesity on infertility in women. J Turk Ger Gynecol Assoc. 2015;16(2):111-7.

8. Priya DM, Akhtar N, Ahmad J. Prevalence of hypothyroidism in infertile women and evaluation of response of treatment for hypothyroidism on infertility. Indian J Endocrinol Metab. 2015;19(4):504-6.

9. Simon A, Laufer N. Assessment and treatment of repeated implantation failure (RIF). J Assist Reprod Genet. 2012;29(11):1227-39.

10. Jarvis GE. Estimating limits for natural human embryo mortality. F1000Res. 2016;5:2083.

11. Salker M, Teklenburg G, Molokhia M, Lavery S, Trew G, Aojanepong T, et al. Natural selection of human embryos: impaired decidualization of endometrium disables embryo-maternal interactions and causes recurrent pregnancy loss. PLoS One. 2010;5(4):e10287.

12. Glujovsky D, Pesce R, Fiszbajn G, Sueldo C, Hart RJ, Ciapponi A. Endometrial preparation for women undergoing embryo transfer with frozen embryos or embryos derived from donor oocytes. Cochrane Database Syst Rev. 2010(1):CD006359.

13. Zeilmaker GH, Alberda AT, van Gent I, Rijkmans CM, Drogendijk AC. Two pregnancies following transfer of intact frozen-thawed embryos. Fertil Steril. 1984;42(2):293-6.

14. Roque M, Valle M, Kostolias A, Sampaio M, Geber S. Freeze-all cycle in reproductive medicine: current perspectives. JBRA Assist Reprod. 2017;21(1):49-53.

15. Ghobara T, Gelbaya TA, Ayeleke RO. Cycle regimens for frozen-thawed embryo transfer. Cochrane Database Syst Rev. 2017;7:CD003414.

16. Casper RF, Yanushpolsky EH. Optimal endometrial preparation for frozen embryo transfer cycles: window of implantation and progesterone support. Fertil Steril. 2016;105(4):867-72.

17. Groenewoud ER, Macklon NS, Cohlen BJ, group Ats. Cryo-thawed embryo transfer: natural versus artificial cycle. A non-inferiority trial. (ANTARCTICA trial). BMC Womens Health. 2012;12:27.

18. Groenewoud ER, Cohlen BJ, Al-Oraiby A, Brinkhuis EA, Broekmans FJ, de Bruin JP, et al. A randomized controlled, non-inferiority trial of modified natural versus artificial cycle for cryo-thawed embryo transfer. Hum Reprod. 2016;31(7):1483-92.

19. van de Vijver A, Polyzos NP, Van Landuyt L, Mackens S, Stoop D, Camus M, et al. What is the optimal duration of progesterone administration before transferring a vitrified-warmed cleavage stage embryo? A randomized controlled trial. Hum Reprod. 2016;31(5):1097-104.

20. Haahr T, Roque M, Esteves SC, Humaidan P. GnRH Agonist Trigger and LH Activity Luteal Phase Support versus hCG Trigger and Conventional Luteal Phase Support in Fresh Embryo Transfer IVF/ICSI Cycles-A Systematic PRISMA Review and Meta-analysis. Front Endocrinol (Lausanne). 2017;8:116.

21. Depalo R, Jayakrishan K, Garruti G, Totaro I, Panzarino M, Giorgino F, et al. GnRH agonist versus GnRH antagonist in in vitro fertilization and embryo transfer (IVF/ET). Reprod Biol Endocrinol. 2012;10:26.

22. Tannus S, Burke Y, McCartney CR, Kol S. GnRH-agonist triggering for final oocyte maturation in GnRH-antagonist IVF cycles induces decreased LH pulse rate and

amplitude in early luteal phase: a possible luteolysis mechanism. Gynecol Endocrinol. 2017:1-5.

23. Engmann L, DiLuigi A, Schmidt D, Nulsen J, Maier D, Benadiva C. The use of gonadotropin-releasing hormone (GnRH) agonist to induce oocyte maturation after cotreatment with GnRH antagonist in high-risk patients undergoing in vitro fertilization prevents the risk of ovarian hyperstimulation syndrome: a prospective randomized controlled study. Fertil Steril. 2008;89(1):84-91.

24. Andersen CY, Humaidan P, Ejdrup HB, Bungum L, Grondahl ML, Westergaard LG. Hormonal characteristics of follicular fluid from women receiving either GnRH agonist or hCG for ovulation induction. Hum Reprod. 2006;21(8):2126-30.

25. Kolibianakis EM, Schultze-Mosgau A, Schroer A, van Steirteghem A, Devroey P, Diedrich K, et al. A lower ongoing pregnancy rate can be expected when GnRH agonist is used for triggering final oocyte maturation instead of HCG in patients undergoing IVF with GnRH antagonists. Hum Reprod. 2005;20(10):2887-92.

26. Hill MJ, Miller KA, Frattarelli JL. A GnRH agonist and exogenous hormone stimulation protocol has a higher live-birth rate than a natural endogenous hormone protocol for frozen-thawed blastocyst-stage embryo transfer cycles: an analysis of 1391 cycles. Fertil Steril. 2010;93(2):416-22.

27. Diedrich K, Fauser BC, Devroey P, Griesinger G, Evian Annual Reproduction Workshop G. The role of the endometrium and embryo in human implantation. Hum Reprod Update. 2007;13(4):365-77.

28. Gargett CE, Nguyen HP, Ye L. Endometrial regeneration and endometrial stem/progenitor cells. Rev Endocr Metab Disord. 2012;13(4):235-51.

29. Cha J, Sun X, Dey SK. Mechanisms of implantation: strategies for successful pregnancy. Nat Med. 2012;18(12):1754-67.

30. Demir R, Kayisli UA, Celik-Ozenci C, Korgun ET, Demir-Weusten AY, Arici A. Structural differentiation of human uterine luminal and glandular epithelium during early pregnancy: an ultrastructural and immunohistochemical study. Placenta. 2002;23(8-9):672-84.

31. Cooke PS, Spencer TE, Bartol FF, Hayashi K. Uterine glands: development, function and experimental model systems. Mol Hum Reprod. 2013;19(9):547-58.

32. Filant J, Spencer TE. Uterine glands: biological roles in conceptus implantation, uterine receptivity and decidualization. Int J Dev Biol. 2014;58(2-4):107-16.

33. Burton GJ, Jauniaux E, Charnock-Jones DS. Human early placental development: potential roles of the endometrial glands. Placenta. 2007;28 Suppl A:S64-9.

34. Kelleher AM, Burns GW, Behura S, Wu G, Spencer TE. Uterine glands impact uterine receptivity, luminal fluid homeostasis and blastocyst implantation. Sci Rep. 2016;6:38078.

35. Kelleher AM, Peng W, Pru JK, Pru CA, DeMayo FJ, Spencer TE. Forkhead box a2 (FOXA2) is essential for uterine function and fertility. Proc Natl Acad Sci U S A. 2017;114(6):E1018-E26.

36. Vinketova K, Mourdjeva M, Oreshkova T. Human Decidual Stromal Cells as a Component of the Implantation Niche and a Modulator of Maternal Immunity. J Pregnancy. 2016;2016:8689436.

37. Peter Durairaj RR, Aberkane A, Polanski L, Maruyama Y, Baumgarten M, Lucas ES, et al. Deregulation of the endometrial stromal cell secretome precedes embryo implantation failure. Mol Hum Reprod. 2017;23(8):582.

38. Zhu H, Hou CC, Luo LF, Hu YJ, Yang WX. Endometrial stromal cells and decidualized stromal cells: origins, transformation and functions. Gene. 2014;551(1):1-14.

39. Gellersen B, Brosens JJ. Cyclic decidualization of the human endometrium in reproductive health and failure. Endocr Rev. 2014;35(6):851-905.

40. Macklon NS, Brosens JJ. The human endometrium as a sensor of embryo quality. Biol Reprod. 2014;91(4):98.

41. Ancelin M, Buteau-Lozano H, Meduri G, Osborne-Pellegrin M, Sordello S, Plouet J, et al. A dynamic shift of VEGF isoforms with a transient and selective progesterone-induced expression of VEGF189 regulates angiogenesis and vascular permeability in human uterus. Proc Natl Acad Sci U S A. 2002;99(9):6023-8.

42. Kim M, Park HJ, Seol JW, Jang JY, Cho YS, Kim KR, et al. VEGF-A regulated by progesterone governs uterine angiogenesis and vascular remodelling during pregnancy. EMBO Mol Med. 2013;5(9):1415-30.

43. Staun-Ram E, Shalev E. Human trophoblast function during the implantation process. Reprod Biol Endocrinol. 2005;3:56.

44. Matsuo H, Baba Y, Nair RM, Arimura A, Schally AV. Structure of the porcine LH- and FSH-releasing hormone. I. The proposed amino acid sequence. 1991. J Urol. 2002;167(2 Pt 2):1011-4; discussion 5.

45. Mais V, Kazer RR, Cetel NS, Rivier J, Vale W, Yen SS. The dependency of folliculogenesis and corpus luteum function on pulsatile gonadotropin secretion in cycling women using a gonadotropin-releasing hormone antagonist as a probe. J Clin Endocrinol Metab. 1986;62(6):1250-5.

46. Tsutsumi R, Webster NJ. GnRH pulsatility, the pituitary response and reproductive dysfunction. Endocr J. 2009;56(6):729-37.

47. Son WY, Das M, Shalom-Paz E, Holzer H. Mechanisms of follicle selection and development. Minerva Ginecol. 2011;63(2):89-102.

48. Reed BG, Carr BR. The Normal Menstrual Cycle and the Control of Ovulation. In: De Groot LJ, Chrousos G, Dungan K, Feingold KR, Grossman A, Hershman JM, et al., editors. Endotext. South Dartmouth (MA)2000.

49. Motola S, Popliker M, Tsafriri A. Response of follicle cells to ovulatory stimuli within the follicle and in primary culture. Mol Cell Endocrinol. 2008;282(1-2):26-31.

50. Maybin JA, Critchley HO. Menstrual physiology: implications for endometrial pathology and beyond. Hum Reprod Update. 2015;21(6):748-61.

51. Aplin JD. Embryo implantation: the molecular mechanism remains elusive. Reprod Biomed Online. 2006;13(6):833-9.

52. Aghajanova L, Hamilton AE, Giudice LC. Uterine receptivity to human embryonic implantation: histology, biomarkers, and transcriptomics. Semin Cell Dev Biol. 2008;19(2):204-11.

53. Uchida H, Maruyama T, Masuda H, Uchida S, Miki F, Hihara H, et al. How to Create an Embryo Penetration Route. Am J Reprod Immunol. 2016;75(3):326-32.

54. Singh M, Chaudhry P, Asselin E. Bridging endometrial receptivity and implantation: network of hormones, cytokines, and growth factors. J Endocrinol. 2011;210(1):5-14.

55. Brosens JJ, Salker MS, Teklenburg G, Nautiyal J, Salter S, Lucas ES, et al. Uterine selection of human embryos at implantation. Sci Rep. 2014;4:3894.

56. Zhang S, Lin H, Kong S, Wang S, Wang H, Wang H, et al. Physiological and molecular determinants of embryo implantation. Mol Aspects Med. 2013;34(5):939-80.

57. Kamijo T, Rajabi MR, Mizunuma H, Ibuki Y. Biochemical evidence for autocrine/paracrine regulation of apoptosis in cultured uterine epithelial cells during mouse embryo implantation in vitro. Mol Hum Reprod. 1998;4(10):990-8.

58. Cavassani KA, Ishii M, Wen H, Schaller MA, Lincoln PM, Lukacs NW, et al. TLR3 is an endogenous sensor of tissue necrosis during acute inflammatory events. J Exp Med. 2008;205(11):2609-21.

59. Cha J VF, Dey SK, Simón C. Sanders S. Molecular interplay in successful implantation, Ten Critical Topics in Reproductive Medicine. Science. 2013:44-8.

60. Noyes RW, Hertig AT, Rock J. Dating the endometrial biopsy. Am J Obstet Gynecol. 1975;122(2):262-3.

61. Li TC, Dockery P, Rogers AW, Cooke ID. How precise is histologic dating of endometrium using the standard dating criteria? Fertil Steril. 1989;51(5):759-63.

62. Murray MJ, Meyer WR, Zaino RJ, Lessey BA, Novotny DB, Ireland K, et al. A critical analysis of the accuracy, reproducibility, and clinical utility of histologic endometrial dating in fertile women. Fertil Steril. 2004;81(5):1333-43.

63. Papanikolaou EG, Tournaye H, Verpoest W, Camus M, Vernaeve V, Van Steirteghem A, et al. Early and late ovarian hyperstimulation syndrome: early pregnancy outcome and profile. Hum Reprod. 2005;20(3):636-41.

64. Usadi RS, Murray MJ, Bagnell RC, Fritz MA, Kowalik AI, Meyer WR, et al. Temporal and morphologic characteristics of pinopod expression across the secretory phase of the endometrial cycle in normally cycling women with proven fertility. Fertil Steril. 2003;79(4):970-4.

65. Stavreus-Evers A, Nikas G, Sahlin L, Eriksson H, Landgren BM. Formation of pinopodes in human endometrium is associated with the concentrations of progesterone and progesterone receptors. Fertil Steril. 2001;76(4):782-91.

66. Kabir-Salmani M, Nikzad H, Shiokawa S, Akimoto Y, Iwashita M. Secretory role for human uterodomes (pinopods): secretion of LIF. Mol Hum Reprod. 2005;11(8):553-9.

67. Aghajanova L, Stavreus-Evers A, Nikas Y, Hovatta O, Landgren BM. Coexpression of pinopodes and leukemia inhibitory factor, as well as its receptor, in human endometrium. Fertil Steril. 2003;79 Suppl 1:808-14.

68. Bentin-Ley U, Sjogren A, Nilsson L, Hamberger L, Larsen JF, Horn T. Presence of uterine pinopodes at the embryo-endometrial interface during human implantation in vitro. Hum Reprod. 1999;14(2):515-20.

69. Cavagna M, Mantese JC. Biomarkers of endometrial receptivity--a review. Placenta. 2003;24 Suppl B:S39-47.

70. Altmae S, Esteban FJ, Stavreus-Evers A, Simon C, Giudice L, Lessey BA, et al. Guidelines for the design, analysis and interpretation of 'omics' data: focus on human endometrium. Hum Reprod Update. 2014;20(1):12-28.

71. Riesewijk A, Martin J, van Os R, Horcajadas JA, Polman J, Pellicer A, et al. Gene expression profiling of human endometrial receptivity on days LH+2 versus LH+7 by microarray technology. Mol Hum Reprod. 2003;9(5):253-64.

72. Mirkin S, Arslan M, Churikov D, Corica A, Diaz JI, Williams S, et al. In search of candidate genes critically expressed in the human endometrium during the window of implantation. Hum Reprod. 2005;20(8):2104-17.

73. Talbi S, Hamilton AE, Vo KC, Tulac S, Overgaard MT, Dosiou C, et al. Molecular phenotyping of human endometrium distinguishes menstrual cycle phases and underlying biological processes in normo-ovulatory women. Endocrinology. 2006;147(3):1097-121.

74. Gomez E, Ruiz-Alonso M, Miravet J, Simon C. Human Endometrial Transcriptomics: Implications for Embryonic Implantation. Cold Spring Harb Perspect Med. 2015;5(7):a022996.

75. Koot YE, van Hooff SR, Boomsma CM, van Leenen D, Groot Koerkamp MJ, Goddijn M, et al. An endometrial gene expression signature accurately predicts recurrent implantation failure after IVF. Sci Rep. 2016;6:19411.

76. Boggavarapu NR, Lalitkumar S, Joshua V, Kasvandik S, Salumets A, Lalitkumar PG, et al. Compartmentalized gene expression profiling of receptive endometrium reveals progesterone regulated ENPP3 is differentially expressed and secreted in glycosylated form. Sci Rep. 2016;6:33811.

77. Diaz-Gimeno P, Horcajadas JA, Martinez-Conejero JA, Esteban FJ, Alama P, Pellicer A, et al. A genomic diagnostic tool for human endometrial receptivity based on the transcriptomic signature. Fertil Steril. 2011;95(1):50-60, e1-15.

78. Garrido-Gomez T, Ruiz-Alonso M, Blesa D, Diaz-Gimeno P, Vilella F, Simon C. Profiling the gene signature of endometrial receptivity: clinical results. Fertil Steril. 2013;99(4):1078-85.

79. Ruiz-Alonso M, Blesa D, Diaz-Gimeno P, Gomez E, Fernandez-Sanchez M, Carranza F, et al. The endometrial receptivity array for diagnosis and personalized embryo transfer as a treatment for patients with repeated implantation failure. Fertil Steril. 2013;100(3):818-24.

80. Lessey BA, Castelbaum AJ, Wolf L, Greene W, Paulson M, Meyer WR, et al. Use of integrins to date the endometrium. Fertil Steril. 2000;73(4):779-87.

81. Thomas K, Thomson A, Wood S, Kingsland C, Vince G, Lewis-Jones I. Endometrial integrin expression in women undergoing in vitro fertilization and the association with subsequent treatment outcome. Fertil Steril. 2003;80(3):502-7.

82. Alon R, Feigelson S. From rolling to arrest on blood vessels: leukocyte tap dancing on endothelial integrin ligands and chemokines at sub-second contacts. Semin Immunol. 2002;14(2):93-104.

83. Dominguez F, Yanez-Mo M, Sanchez-Madrid F, Simon C. Embryonic implantation and leukocyte transendothelial migration: different processes with similar players? FASEB J. 2005;19(9):1056-60.

84. Chen G, Xin A, Liu Y, Shi C, Chen J, Tang X, et al. Integrins beta1 and beta3 are biomarkers of uterine condition for embryo transfer. J Transl Med. 2016;14(1):303.

85. Knofler M, Pollheimer J. Human placental trophoblast invasion and differentiation: a particular focus on Wnt signaling. Front Genet. 2013;4:190.

86. Garrido-Gomez T, Quinonero A, Antunez O, Diaz-Gimeno P, Bellver J, Simon C, et al. Deciphering the proteomic signature of human endometrial receptivity. Hum Reprod. 2014;29(9):1957-67.

87. Boomsma CM, Kavelaars A, Eijkemans MJ, Lentjes EG, Fauser BC, Heijnen CJ, et al. Endometrial secretion analysis identifies a cytokine profile predictive of pregnancy in IVF. Hum Reprod. 2009;24(6):1427-35.

88. Li J, Tan Z, Li M, Xia T, Liu P, Yu W. Proteomic analysis of endometrium in fertile women during the prereceptive and receptive phases after luteinizing hormone surge. Fertil Steril. 2011;95(3):1161-3.

89. Alcazar JL. Three-dimensional ultrasound assessment of endometrial receptivity: a review. Reprod Biol Endocrinol. 2006;4:56.

90. Evans GE, Martinez-Conejero JA, Phillipson GT, Sykes PH, Sin IL, Lam EY, et al. In the secretory endometria of women, luminal epithelia exhibit gene and protein expressions that differ from those of glandular epithelia. Fertil Steril. 2014;102(1):307-17 e7.

91. Heger A, Sator M, Pietrowski D. Endometrial Receptivity and its Predictive Value for IVF/ICSI-Outcome. Geburtshilfe Frauenheilkd. 2012;72(8):710-5.

92. Miravet-Valenciano JA, Rincon-Bertolin A, Vilella F, Simon C. Understanding and improving endometrial receptivity. Curr Opin Obstet Gynecol. 2015;27(3):187-92.

93. Bhusane K, Bhutada S, Chaudhari U, Savardekar L, Katkam R, Sachdeva G. Secrets of Endometrial Receptivity: Some Are Hidden in Uterine Secretome. Am J Reprod Immunol. 2016;75(3):226-36.

94. Berlanga O, Bradshaw HB, Vilella-Mitjana F, Garrido-Gomez T, Simon C. How endometrial secretomics can help in predicting implantation. Placenta. 2011;32 Suppl 3:S271-5.

95. Salamonsen LA, Edgell T, Rombauts LJ, Stephens AN, Robertson DM, Rainczuk A, et al. Proteomics of the human endometrium and uterine fluid: a pathway to biomarker discovery. Fertil Steril. 2013;99(4):1086-92.

96. Salamonsen LA, Evans J, Nguyen HP, Edgell TA. The Microenvironment of Human Implantation: Determinant of Reproductive Success. Am J Reprod Immunol. 2016;75(3):218-25.

97. Casado-Vela J, Rodriguez-Suarez E, Iloro I, Ametzazurra A, Alkorta N, Garcia-Velasco JA, et al. Comprehensive proteomic analysis of human endometrial fluid aspirate. J Proteome Res. 2009;8(10):4622-32.

98. Ametzazurra A, Matorras R, Garcia-Velasco JA, Prieto B, Simon L, Martinez A, et al. Endometrial fluid is a specific and non-invasive biological sample for protein biomarker identification in endometriosis. Hum Reprod. 2009;24(4):954-65.

99. van der Gaast MH, Beier-Hellwig K, Fauser BC, Beier HM, Macklon NS. Endometrial secretion aspiration prior to embryo transfer does not reduce implantation rates. Reprod Biomed Online. 2003;7(1):105-9.

100. Beier HM, Beier-Hellwig K. Molecular and cellular aspects of endometrial receptivity. Hum Reprod Update. 1998;4(5):448-58.

101. Boomsma CM, Kavelaars A, Eijkemans MJ, Amarouchi K, Teklenburg G, Gutknecht D, et al. Cytokine profiling in endometrial secretions: a non-invasive window on endometrial receptivity. Reprod Biomed Online. 2009;18(1):85-94.

102. Hannan NJ, Jones RL, White CA, Salamonsen LA. The chemokines, CX3CL1, CCL14, and CCL4, promote human trophoblast migration at the feto-maternal interface. Biol Reprod. 2006;74(5):896-904.

103. Hannan NJ, Stephens AN, Rainczuk A, Hincks C, Rombauts LJ, Salamonsen LA. 2D-DiGE analysis of the human endometrial secretome reveals differences between receptive and nonreceptive states in fertile and infertile women. J Proteome Res. 2010;9(12):6256-64.

104. Scotchie JG, Fritz MA, Mocanu M, Lessey BA, Young SL. Proteomic analysis of the luteal endometrial secretome. Reprod Sci. 2009;16(9):883-93.

105. Hannan NJ, Paiva P, Meehan KL, Rombauts LJ, Gardner DK, Salamonsen LA. Analysis of fertility-related soluble mediators in human uterine fluid identifies VEGF as a key regulator of embryo implantation. Endocrinology. 2011;152(12):4948-56.

106. Binder NK, Evans J, Salamonsen LA, Gardner DK, Kaitu'u-Lino TJ, Hannan NJ. Placental Growth Factor Is Secreted by the Human Endometrium and Has Potential Important Functions during Embryo Development and Implantation. PLoS One. 2016;11(10):e0163096.

107. Boomsma CM, Kavelaars A, Eijkemans MJ, Fauser BC, Heijnen CJ, Macklon NS. Ovarian stimulation for in vitro fertilization alters the intrauterine cytokine, chemokine, and growth factor milieu encountered by the embryo. Fertil Steril. 2010;94(5):1764-8.

108. Dominguez F, Ferrando M, Diaz-Gimeno P, Quintana F, Fernandez G, Castells I, et al. Lipidomic profiling of endometrial fluid in women with ovarian endometriosisdagger. Biol Reprod. 2017;96(4):772-9.

109. Rapino C, Battista N, Bari M, Maccarrone M. Endocannabinoids as biomarkers of human reproduction. Hum Reprod Update. 2014;20(4):501-16.

110. Sordelli MS, Beltrame JS, Cella M, Gervasi MG, Perez Martinez S, Burdet J, et al. Interaction between lysophosphatidic acid, prostaglandins and the endocannabinoid

system during the window of implantation in the rat uterus. PLoS One. 2012;7(9):e46059.

111. Achache H, Tsafrir A, Prus D, Reich R, Revel A. Defective endometrial prostaglandin synthesis identified in patients with repeated implantation failure undergoing in vitro fertilization. Fertil Steril. 2010;94(4):1271-8.

112. Vilella F, Ramirez LB, Simon C. Lipidomics as an emerging tool to predict endometrial receptivity. Fertil Steril. 2013;99(4):1100-6.

113. Faruq O, Vecchione A. microRNA: Diagnostic Perspective. Front Med (Lausanne). 2015;2:51.

114. Hull ML, Nisenblat V. Tissue and circulating microRNA influence reproductive function in endometrial disease. Reprod Biomed Online. 2013;27(5):515-29.

115. Schee K, Lorenz S, Worren MM, Gunther CC, Holden M, Hovig E, et al. Deep Sequencing the MicroRNA Transcriptome in Colorectal Cancer. PLoS One. 2013;8(6):e66165.

116. Pritchard CC, Cheng HH, Tewari M. MicroRNA profiling: approaches and considerations. Nat Rev Genet. 2012;13(5):358-69.

117. Tetreault N, De Guire V. miRNAs: their discovery, biogenesis and mechanism of action. Clin Biochem. 2013;46(10-11):842-5.

118. Bidarimath M, Khalaj K, Wessels JM, Tayade C. MicroRNAs, immune cells and pregnancy. Cell Mol Immunol. 2014;11(6):538-47.

119. Sharkey AM, Macklon NS. The science of implantation emerges blinking into the light. Reprod Biomed Online. 2013;27(5):453-60.

120. Winter J, Jung S, Keller S, Gregory RI, Diederichs S. Many roads to maturity: microRNA biogenesis pathways and their regulation. Nat Cell Biol. 2009;11(3):228-34.

121. Vilella F, Moreno-Moya JM, Balaguer N, Grasso A, Herrero M, Martinez S, et al. Hsa-miR-30d, secreted by the human endometrium, is taken up by the pre-implantation embryo and might modify its transcriptome. Development. 2015;142(18):3210-21.

122. Dmitriev P, Barat A, Polesskaya A, O'Connell MJ, Robert T, Dessen P, et al. Simultaneous miRNA and mRNA transcriptome profiling of human myoblasts reveals a novel set of myogenic differentiation-associated miRNAs and their target genes. BMC Genomics. 2013;14:265.

123. Liu H, Brannon AR, Reddy AR, Alexe G, Seiler MW, Arreola A, et al. Identifying mRNA targets of microRNA dysregulated in cancer: with application to clear cell Renal Cell Carcinoma. BMC Syst Biol. 2010;4:51.

124. Wilczynska A, Bushell M. The complexity of miRNA-mediated repression. Cell Death Differ. 2015;22(1):22-33.

125. Ambs S, Prueitt RL, Yi M, Hudson RS, Howe TM, Petrocca F, et al. Genomic profiling of microRNA and messenger RNA reveals deregulated microRNA expression in prostate cancer. Cancer Res. 2008;68(15):6162-70.

126. Bagga S, Bracht J, Hunter S, Massirer K, Holtz J, Eachus R, et al. Regulation by let-7 and lin-4 miRNAs results in target mRNA degradation. Cell. 2005;122(4):553-63.

127. Giraldez AJ, Mishima Y, Rihel J, Grocock RJ, Van Dongen S, Inoue K, et al. Zebrafish MiR-430 promotes deadenylation and clearance of maternal mRNAs. Science. 2006;312(5770):75-9.

128. Guo H, Ingolia NT, Weissman JS, Bartel DP. Mammalian microRNAs predominantly act to decrease target mRNA levels. Nature. 2010;466(7308):835-40.

129. Larsson O, Nadon R. Re-analysis of genome wide data on mammalian microRNA-mediated suppression of gene expression. Translation (Austin). 2013;1(1):e24557.

130. Sanger F, Nicklen S, Coulson AR. DNA sequencing with chain-terminating inhibitors. Proc Natl Acad Sci U S A. 1977;74(12):5463-7.

131. Maxam AM, Gilbert W. A new method for sequencing DNA. Proc Natl Acad Sci U S A. 1977;74(2):560-4.

132. International Human Genome Sequencing C. Finishing the euchromatic sequence of the human genome. Nature. 2004;431(7011):931-45.

133. Goodwin S, McPherson JD, McCombie WR. Coming of age: ten years of next-generation sequencing technologies. Nat Rev Genet. 2016;17(6):333-51.

134. Sudmant PH, Rausch T, Gardner EJ, Handsaker RE, Abyzov A, Huddleston J, et al. An integrated map of structural variation in 2,504 human genomes. Nature. 2015;526(7571):75-81.

135. Tam S, de Borja R, Tsao MS, McPherson JD. Robust global microRNA expression profiling using next-generation sequencing technologies. Lab Invest. 2014;94(3):350-8.

136. Tam S, Tsao MS, McPherson JD. Optimization of miRNA-seq data preprocessing. Brief Bioinform. 2015;16(6):950-63.

137. Hu S, Yao G, Wang Y, Xu H, Ji X, He Y, et al. Transcriptomic changes during the pre-receptive to receptive transition in human endometrium detected by RNA-Seq. J Clin Endocrinol Metab. 2014;99(12):E2744-53.

138. Krjutskov K, Katayama S, Saare M, Vera-Rodriguez M, Lubenets D, Samuel K, et al. Single-cell transcriptome analysis of endometrial tissue. Hum Reprod. 2016;31(4):844-53.

139. Georgieva B, Milev I, Minkov I, Dimitrova I, Bradford AP, Baev V. Characterization of the uterine leiomyoma microRNAome by deep sequencing. Genomics. 2012;99(5):275-81.

140. van Dijk EL, Auger H, Jaszczyszyn Y, Thermes C. Ten years of next-generation sequencing technology. Trends Genet. 2014;30(9):418-26.

141. Motameny S, Wolters S, Nurnberg P, Schumacher B. Next Generation Sequencing of miRNAs - Strategies, Resources and Methods. Genes (Basel). 2010;1(1):70-84.

142. Alon S, Vigneault F, Eminaga S, Christodoulou DC, Seidman JG, Church GM, et al. Barcoding bias in high-throughput multiplex sequencing of miRNA. Genome Res. 2011;21(9):1506-11.

143. Ziemann M, Kaspi A, El-Osta A. Evaluation of microRNA alignment techniques. RNA. 2016;22(8):1120-38.

144. Wagner GP, Kin K, Lynch VJ. Measurement of mRNA abundance using RNA-seq data: RPKM measure is inconsistent among samples. Theory Biosci. 2012;131(4):281-5.

145. Garmire LX, Subramaniam S. Evaluation of normalization methods in mammalian microRNA-Seq data. RNA. 2012;18(6):1279-88.

146. Love MI, Huber W, Anders S. Moderated estimation of fold change and dispersion for RNA-seq data with DESeq2. Genome Biol. 2014;15(12):550.

147. Chambers CR, Patrick WM. Archaeal Nucleic Acid Ligases and Their Potential in Biotechnology. Archaea. 2015;2015:170571.

148. Friedlander MR, Mackowiak SD, Li N, Chen W, Rajewsky N. miRDeep2 accurately identifies known and hundreds of novel microRNA genes in seven animal clades. Nucleic Acids Res. 2012;40(1):37-52.

149. Kozomara A, Griffiths-Jones S. miRBase: annotating high confidence microRNAs using deep sequencing data. Nucleic Acids Res. 2014;42(Database issue):D68-73.

150. Robinson MD, Oshlack A. A scaling normalization method for differential expression analysis of RNA-seq data. Genome Biol. 2010;11(3):R25.

151. Todorov V, Filzmoser P. An object-oriented framework for robust multivariate analysis: na; 2009.

152. Chou CH, Chang NW, Shrestha S, Hsu SD, Lin YL, Lee WH, et al. miRTarBase 2016: updates to the experimentally validated miRNA-target interactions database. Nucleic Acids Res. 2016;44(D1):D239-47.

153. Bandyopadhyay S, Ghosh D, Mitra R, Zhao Z. MBSTAR: multiple instance learning for predicting specific functional binding sites in microRNA targets. Sci Rep. 2015;5:8004.

154. Kanehisa M, Sato Y, Kawashima M, Furumichi M, Tanabe M. KEGG as a reference resource for gene and protein annotation. Nucleic Acids Res. 2016;44(D1):D457-62.

155. Nishida M, Kasahara K, Kaneko M, Iwasaki H, Hayashi K. Establishment of a new human endometrial adenocarcinoma cell line, Ishikawa cells, containing estrogen and progesterone receptors. Nihon Sanka Fujinka Gakkai Zasshi. 1985;37(7):1103-11.

156. Bradford MM. A rapid and sensitive method for the quantitation of microgram quantities of protein utilizing the principle of protein-dye binding. Anal Biochem. 1976;72:248-54.

157. Schmieder R, Edwards R. Fast identification and removal of sequence contamination from genomic and metagenomic datasets. PLoS One. 2011;6(3):e17288.

158. Tonge DP, Gant TW. What is normal? Next generation sequencing-driven analysis of the human circulating miRNAOme. BMC Mol Biol. 2016;17:4.

159. Burgos KL, Javaherian A, Bomprezzi R, Ghaffari L, Rhodes S, Courtright A, et al. Identification of extracellular miRNA in human cerebrospinal fluid by next-generation sequencing. RNA. 2013;19(5):712-22.

160. Navakanitworakul R, Hung WT, Gunewardena S, Davis JS, Chotigeat W, Christenson LK. Characterization and Small RNA Content of Extracellular Vesicles in Follicular Fluid of Developing Bovine Antral Follicles. Sci Rep. 2016;6:25486.

161. Jiajie T, Yanzhou Y, Hoi-Hung AC, Zi-Jiang C, Wai-Yee C. Conserved miR-10 family represses proliferation and induces apoptosis in ovarian granulosa cells. Sci Rep. 2017;7:41304.

162. Li Y, Fang Y, Liu Y, Yang X. MicroRNAs in ovarian function and disorders. J Ovarian Res. 2015;8:51.

163. McNatty KP, Hillier SG, van den Boogaard AM, Trimbos-Kemper TC, Reichert LE, Jr., van Hall EV. Follicular development during the luteal phase of the human menstrual cycle. J Clin Endocrinol Metab. 1983;56(5):1022-31.

164. Hubert M, Rousseeuw PJ, Vanden Branden K. ROBPCA: A New Approach to Robust Principal Component Analysis. Technometrics. 2005;47(1):64-79.

165. McCarthy DJ, Smyth GK. Testing significance relative to a fold-change threshold is a TREAT. Bioinformatics. 2009;25(6):765-71.

166. Crawford NM, Pritchard DA, Herring AH, Steiner AZ. Prospective evaluation of luteal phase length and natural fertility. Fertil Steril. 2017;107(3):749-55.

167. Moreno-Moya JM, Vilella F, Martinez S, Pellicer A, Simon C. The transcriptomic and proteomic effects of ectopic overexpression of miR-30d in human endometrial epithelial cells. Mol Hum Reprod. 2014;20(6):550-66.

168. Altmae S, Martinez-Conejero JA, Esteban FJ, Ruiz-Alonso M, Stavreus-Evers A, Horcajadas JA, et al. MicroRNAs miR-30b, miR-30d, and miR-494 regulate human endometrial receptivity. Reprod Sci. 2013;20(3):308-17.

169. Dominguez F, Moreno-Moya JM, Lozoya T, Romero A, Martinez S, Monterde M, et al. Embryonic miRNA profiles of normal and ectopic pregnancies. PLoS One. 2014;9(7):e102185.

170. Kan CW, Hahn MA, Gard GB, Maidens J, Huh JY, Marsh DJ, et al. Elevated levels of circulating microRNA-200 family members correlate with serous epithelial ovarian cancer. BMC Cancer. 2012;12:627.

171. Chim SS, Shing TK, Hung EC, Leung TY, Lau TK, Chiu RW, et al. Detection and characterization of placental microRNAs in maternal plasma. Clin Chem. 2008;54(3):482-90.

172. Gangwar I, Kumar Sharma N, Panzade G, Awasthi S, Agrawal A, Shankar R. Detecting the Molecular System Signatures of Idiopathic Pulmonary Fibrosis through Integrated Genomic Analysis. Sci Rep. 2017;7(1):1554.

173. Singh H, Aplin JD. Adhesion molecules in endometrial epithelium: tissue integrity and embryo implantation. J Anat. 2009;215(1):3-13.

174. Dong X, Sui C, Huang K, Wang L, Hu D, Xiong T, et al. MicroRNA-223-3p suppresses leukemia inhibitory factor expression and pinopodes formation during embryo implantation in mice. Am J Transl Res. 2016;8(2):1155-63.

175. Feng Y, Zou S, Weijdegard B, Chen J, Cong Q, Fernandez-Rodriguez J, et al. The onset of human ectopic pregnancy demonstrates a differential expression of miRNAs and their cognate targets in the Fallopian tube. Int J Clin Exp Pathol. 2014;7(1):64-79.

176. Kuokkanen S, Chen B, Ojalvo L, Benard L, Santoro N, Pollard JW. Genomic profiling of microRNAs and messenger RNAs reveals hormonal regulation in microRNA expression in human endometrium. Biol Reprod. 2010;82(4):791-801.

177. Chang EM, Han JE, Kim YS, Lyu SW, Lee WS, Yoon TK. Use of the natural cycle and vitrification thawed blastocyst transfer results in better in-vitro fertilization outcomes : cycle regimens of vitrification thawed blastocyst transfer. J Assist Reprod Genet. 2011;28(4):369-74.

178. Hancke K, More S, Kreienberg R, Weiss JM. Patients undergoing frozen-thawed embryo transfer have similar live birth rates in spontaneous and artificial cycles. J Assist Reprod Genet. 2012;29(5):403-7.

179. Givens CR, Markun LC, Ryan IP, Chenette PE, Herbert CM, Schriock ED. Outcomes of natural cycles versus programmed cycles for 1677 frozen-thawed embryo transfers. Reprod Biomed Online. 2009;19(3):380-4.

180. Kalem Z, Kalem MN, Gurgan T. Methods for endometrial preparation in frozen-thawed embryo transfer cycles. J Turk Ger Gynecol Assoc. 2016;17(3):168-72.

181. Mounce G, McVeigh E, Turner K, Child TJ. Randomized, controlled pilot trial of natural versus hormone replacement therapy cycles in frozen embryo replacement in vitro fertilization. Fertil Steril. 2015;104(4):915-20 e1.

182. Gelbaya TA, Nardo LG, Hunter HR, Fitzgerald CT, Horne G, Pease EE, et al. Cryopreserved-thawed embryo transfer in natural or down-regulated hormonally controlled cycles: a retrospective study. Fertil Steril. 2006;85(3):603-9.

183. Zheng Y, Li Z, Xiong M, Luo T, Dong X, Huang B, et al. Hormonal replacement treatment improves clinical pregnancy in frozen-thawed embryos transfer cycles: a retrospective cohort study. Am J Transl Res. 2013;6(1):85-90.

184. Direito A, Bailly S, Mariani A, Ecochard R. Relationships between the luteinizing hormone surge and other characteristics of the menstrual cycle in normally ovulating women. Fertil Steril. 2013;99(1):279-85.

185. Ecochard R, Bouchard T, Leiva R, Abdulla S, Dupuis O, Duterque O, et al. Characterization of hormonal profiles during the luteal phase in regularly menstruating women. Fertil Steril. 2017;108(1):175-82 e1.

186. Lan C, Chen Q, Li J. Grouping miRNAs of similar functions via weighted information content of gene ontology. BMC Bioinformatics. 2016;17(Suppl 19):507.

187. Guo L, Zhao Y, Zhang H, Yang S, Chen F. Integrated evolutionary analysis of human miRNA gene clusters and families implicates evolutionary relationships. Gene. 2014;534(1):24-32.

188. Kanehisa M, Goto S. KEGG: kyoto encyclopedia of genes and genomes. Nucleic Acids Res. 2000;28(1):27-30.

189. Hamzeiy H, Suluyayla R, Brinkrolf C, Janowski SJ, Hofestaedt R, Allmer J. Visualization and Analysis of MicroRNAs within KEGG Pathways using VANESA. J Integr Bioinform. 2017;14(1).

190. Huntley RP, Sitnikov D, Orlic-Milacic M, Balakrishnan R, D'Eustachio P, Gillespie ME, et al. Guidelines for the functional annotation of microRNAs using the Gene Ontology. RNA. 2016;22(5):667-76.

191. Lu X, Ji C, Tong W, Lian X, Wu Y, Fan X, et al. Integrated analysis of microRNA and mRNA expression profiles highlights the complex and dynamic behavior of toosendanin-induced liver injury in mice. Sci Rep. 2016;6:34225.

192. Lu J, Getz G, Miska EA, Alvarez-Saavedra E, Lamb J, Peck D, et al. MicroRNA expression profiles classify human cancers. Nature. 2005;435(7043):834-8.

193. Barnoud T, Wilkey DW, Merchant ML, Clark JA, Donninger H. Proteomics Analysis Reveals Novel RASSF2 Interaction Partners. Cancers (Basel). 2016;8(3).

194. Guerin P, El Mouatassim S, Menezo Y. Oxidative stress and protection against reactive oxygen species in the pre-implantation embryo and its surroundings. Hum Reprod Update. 2001;7(2):175-89.

195. Chakrabarty A, Tranguch S, Daikoku T, Jensen K, Furneaux H, Dey SK. MicroRNA regulation of cyclooxygenase-2 during embryo implantation. Proc Natl Acad Sci U S A. 2007;104(38):15144-9.

196. Zhou X, Li Q, Xu J, Zhang X, Zhang H, Xiang Y, et al. The aberrantly expressed miR-193b-3p contributes to preeclampsia through regulating transforming growth factor-beta signaling. Sci Rep. 2016;6:19910.

197. White CA, Zhang JG, Salamonsen LA, Baca M, Fairlie WD, Metcalf D, et al. Blocking LIF action in the uterus by using a PEGylated antagonist prevents implantation: a nonhormonal contraceptive strategy. Proc Natl Acad Sci U S A. 2007;104(49):19357-62.

198. Kajihara T, Brosens JJ, Ishihara O. The role of FOXO1 in the decidual transformation of the endometrium and early pregnancy. Med Mol Morphol. 2013;46(2):61-8.

199. Achache H, Revel A. Endometrial receptivity markers, the journey to successful embryo implantation. Hum Reprod Update. 2006;12(6):731-46.

200. Castillo A, Morse HC, 3rd, Godfrey VL, Naeem R, Justice MJ. Overexpression of Eg5 causes genomic instability and tumor formation in mice. Cancer Res. 2007;67(21):10138-47.

201. Chauviere M, Kress C, Kress M. Disruption of the mitotic kinesin Eg5 gene (Knsl1) results in early embryonic lethality. Biochem Biophys Res Commun. 2008;372(4):513-9.

202. Kittler R, Putz G, Pelletier L, Poser I, Heninger AK, Drechsel D, et al. An endoribonuclease-prepared siRNA screen in human cells identifies genes essential for cell division. Nature. 2004;432(7020):1036-40.

203. Payne SH. The utility of protein and mRNA correlation. Trends Biochem Sci. 2015;40(1):1-3.

204. Baek D, Villen J, Shin C, Camargo FD, Gygi SP, Bartel DP. The impact of microRNAs on protein output. Nature. 2008;455(7209):64-71.

205. Lindoso RS, Collino F, Bruno S, Araujo DS, Sant'Anna JF, Tetta C, et al. Extracellular vesicles released from mesenchymal stromal cells modulate miRNA in renal tubular cells and inhibit ATP depletion injury. Stem Cells Dev. 2014;23(15):1809-19.

206. von Rango U, Classen-Linke I, Krusche CA, Beier HM. The receptive endometrium is characterized by apoptosis in the glands. Hum Reprod. 1998;13(11):3177-89.

207. Song Y, An X, Zhang L, Fu M, Peng J, Han P, et al. Identification and profiling of microRNAs in goat endometrium during embryo implantation. PLoS One. 2015;10(4):e0122202.

208. Pan Q, Chegini N. MicroRNA signature and regulatory functions in the endometrium during normal and disease states. Semin Reprod Med. 2008;26(6):479-93.

209. Alyasin A, Mehdinejadiani S, Ghasemi M. GnRH agonist trigger versus hCG trigger in GnRH antagonist in IVF/ICSI cycles: A review article. Int J Reprod Biomed (Yazd). 2016;14(9):557-66.

210. Youssef MA, Van der Veen F, Al-Inany HG, Mochtar MH, Griesinger G, Nagi Mohesen M, et al. Gonadotropin-releasing hormone agonist versus HCG for oocyte triggering in antagonist-assisted reproductive technology. Cochrane Database Syst Rev. 2014(10):CD008046.

211. Chegini N. Uterine microRNA signature and consequence of their dysregulation in uterine disorders. Anim Reprod. 2010;7(3):117-28.

212. Humaidan P, Van Vaerenbergh I, Bourgain C, Alsbjerg B, Blockeel C, Schuit F, et al. Endometrial gene expression in the early luteal phase is impacted by mode of triggering final oocyte maturation in recFSH stimulated and GnRH antagonist co-treated IVF cycles. Hum Reprod. 2012;27(11):3259-72.

213. Bhutada S, Basak T, Savardekar L, Katkam RR, Jadhav G, Metkari SM, et al. High mobility group box 1 (HMGB1) protein in human uterine fluid and its relevance in implantation. Hum Reprod. 2014;29(4):763-80.

214. Wolf DP, Mastroianni L, Jr. Protein composition of human uterine fluid. Fertil Steril. 1975;26(3):240-7.

215. Vilella F, Ramirez L, Berlanga O, Martinez S, Alama P, Meseguer M, et al. PGE2 and PGF2alpha concentrations in human endometrial fluid as biomarkers for embryonic implantation. J Clin Endocrinol Metab. 2013;98(10):4123-32.

216. Chan C, Virtanen C, Winegarden NA, Colgan TJ, Brown TJ, Greenblatt EM. Discovery of biomarkers of endometrial receptivity through a minimally invasive approach: a validation study with implications for assisted reproduction. Fertil Steril. 2013;100(3):810-7.

217. Ng YH, Rome S, Jalabert A, Forterre A, Singh H, Hincks CL, et al. Endometrial exosomes/microvesicles in the uterine microenvironment: a new paradigm for embryo-endometrial cross talk at implantation. PLoS One. 2013;8(3):e58502.